CAPITAL UNIVERSITY OF SCIENCE AND TECHNOLOGY, ISLAMABAD

Development and Evaluation of Nanostructured Lipid Carrier-Based Gel for Enhanced Wound Healing

by

Muhammad Yasir Ghaffar

A thesis submitted in partial fulfillment for the degree of Master of Philosophy

in the

Faculty of Pharmacy
Department of Pharmaceutics

2026

CERTIFICATE OF APPROVAL

Development and Evaluation of Nanostructured Lipid Carrier-Based Gel for Enhanced Wound Healing

by

Muhammad Yasir Ghaffar

(Registration No: MPH243003)

THESIS EXAMINING COMMITTEE

S. No.	Examiner	Name	Organization
(a)	External Examiner	Dr. M. Iqbal Nasiri	Hamdard, Islamabad
(b)	Internal Examiner	Dr Fazlullah Khan	CUST, Islamabad

Dr. Nadia Shamshad Malik
Thesis Supervisor
August, 2026

Dr. Nadia Shamshad Malik
Head
Dept. of Pharmaceutics
August, 2026

Dr. Muzaffar Abbas
Dean
Faculty of Pharmacy
August, 2026

Author's Declaration

I, **Muhammad Yasir Ghaffar** hereby state that my MPhil thesis titled "**Development and Evaluation of Nanostructured Lipid Carrier-Based Gel for Enhanced Wound Healing**" is my own work and has not been submitted previously by me for taking any degree from Capital University of Science and Technology, Islamabad or anywhere else in the country/abroad.

At any time if my statement is found to be incorrect even after my graduation, the University has the right to withdraw my MPhil Degree.

(Muhammad Yasir Ghaffar)

Registration No: MPH243003

Plagiarism Undertaking

I solemnly declare that research work presented in this thesis titled "**Development and Evaluation of Nanostructured Lipid Carrier-Based Gel for Enhanced Wound Healing**" is solely my research work with no significant contribution from any other person. Small contribution/help wherever taken has been duly acknowledged and that complete thesis has been written by me.

I understand the zero tolerance policy of the HEC and Capital University of Science and Technology towards plagiarism. Therefore, I as an author of the above titled thesis declare that no portion of my thesis has been plagiarized and any material used as reference is properly referred/cited.

I undertake that if I am found guilty of any formal plagiarism in the above titled thesis even after award of MPhil Degree, the University reserves the right to withdraw/revoke my MPhil degree and that HEC and the University have the right to publish my name on the HEC/University website on which names of students are placed who submitted plagiarized work.

(Muhammad Yasir Ghaffar)

Registration No: MPH243003

Acknowledgement

First and foremost, I am profoundly grateful to Allah, the Most Gracious and the Most Merciful, for granting me the strength, perseverance, and wisdom to complete this academic endeavor. His divine guidance has been a constant source of support throughout this journey.

I would like to express my sincere appreciation to Dr. Nadia Shamshad Malik, my research supervisor, for her invaluable guidance, continuous encouragement, and constructive feedback throughout the course of this study. Her expertise, insightful suggestions, and unwavering support were critical to the successful completion of this thesis. Her dedication to academic excellence and mentorship influenced the quality and direction of my research.

I extend my heartfelt thanks to my family, whose unwavering support, encouragement, and belief in my potential have been a constant source of motivation. Their patience and understanding provided me with the emotional strength needed to navigate this journey.

My sincere gratitude also goes to my research group colleagues and peers, whose collaboration, thoughtful discussions, and shared commitment to academic growth created a stimulating and supportive research environment.

I am also thankful to my friends, whose encouragement, positivity, and timely support brought balance and joy throughout this academic pursuit. I am thankful to PAFDA, LUMS, AMSON and Sargodha University for helping me in the research.

Lastly, I gratefully acknowledge my institute for providing the academic platform, resources, and conducive research environment that made this work possible. The infrastructure and administrative support played a significant role in facilitating various aspects of my research.

(Muhammad Yasir Ghaffar)

Abstract

Wound infections, particularly those caused by multidrug-resistant pathogens like MRSA and *Pseudomonas aeruginosa*, remain a critical clinical challenge due to the poor aqueous solubility and inadequate skin permeation of BCS Class IV fluoroquinolones such as norfloxacin. To overcome these multi-faceted barriers, we developed an optimized norfloxacin-loaded nanostructured lipid carrier (NLC) integrated into a Carbopol 940 hydrogel via hot homogenization-ultrasonication. The lead formulation (5% total lipid; Precirol ATO5: Labrafac WL1349 at 70:30; 1.5% Tween 80; 30% Transcutol P) exhibited a particle size of 102 nm, a polydispersity index of 0.267, a zeta potential of -37.7 mV, and an encapsulation efficiency of 94.95 ± 0.13%. Solid-state characterization (DSC and XRD) confirmed complete amorphization of norfloxacin within the lipid matrix, eliminating the crystalline solubility barrier, while rheological analysis confirmed pseudoplastic, wound-compatible gel characteristics. The hydrogel demonstrated pH-dependent sustained release via anomalous non-Fickian transport (Korsmeyer-Peppas R^2 = 0.999). Importantly, while the formulation showed higher release at acidic skin surface pH (5.5), it maintained substantial therapeutic release under the physiologically challenging alkaline wound pH (7.4), critically achieving a 1.60-fold higher *ex vivo* skin flux than the plain drug gel at its optimal acidic pH, thereby confirming effective circumvention of norfloxacin's intrinsic pH-dependent solubility limitation. Dermal safety was validated by a non-irritant classification (Primary Irritation Index = 0.00, OECD 404), and 3-month ICH-compliant stability studies confirmed physicochemical integrity under accelerated conditions. Remarkably, the NLC-gel demonstrated significantly superior antibacterial activity against *S. aureus, MRSA, E. coli, and P. aeruginosa* compared to the plain norfloxacin gel, effectively restoring therapeutic activity against multidrug-resistant wound isolates. Collectively, this NLC-hydrogel platform provides a safe, stable, and efficacious topical strategy that successfully overcomes the solubility, permeation, and resistance limitations of conventional norfloxacin formulations, offering a promising advanced therapeutic option for challenging multidrug-resistant wound infections, with potential for once-daily application and improved patient compliance.

Keywords Nanostructured lipid carriers, norfloxacin, topical drug delivery, wound infection, Carbopol 940, antibacterial activity, BCS Class IV

Contents

List of Figures

List of Tables

Abbreviations

%EE	Percent Entrapment Efficiency
α-SMA	Alpha-Smooth Muscle Actin
ATCC	American Type Culture Collection
bFGF	Basic Fibroblast Growth Factor
CA-MRSA	Community-Acquired Methicillin-Resistant *Staphylococcus aureus*
ClfA/ClfB	Clumping Factors A and B
CLSI	Clinical and Laboratory Standards Institute
CNA	Collagen-Binding Protein (*Staphylococcal*)
CYP1A2	Cytochrome P450 1A2
DALY	Disability-Adjusted Life Year
DGME	Diethylene Glycol Monoethyl Ether
EGF	Epidermal Growth Factor
EPS	Extracellular Polymeric Substance
ER	Enhancement Ratio
ESBL	Extended-Spectrum Beta-Lactamase
FnBPA/B	Fibronectin-Binding Proteins A and B
GRAS	Generally Recognised as Safe
GyrA	DNA Gyrase Subunit A
GyrB	DNA Gyrase Subunit B
HA-MRSA	Healthcare-Associated Methicillin-Resistant *Staphylococcus aureus*
HAI	Healthcare-Associated Infection
HLB	Hydrophile-Lipophile Balance

HPMC	Hydroxypropyl Methylcellulose
ica	Intercellular Adhesin Operon (*Staphylococcal* biofilm)
ICU	Intensive Care Unit
IDF	International Diabetes Federation
IGF-1	Insulin-like Growth Factor-1
IL-1β	Interleukin-1 Beta
IL-6	Interleukin-6
IL-8	Interleukin-8
MBIC	Minimum Biofilm Inhibitory Concentration
MCT	Medium-Chain Triglycerides
MDR	Multidrug-Resistant
mecA	Methicillin Resistance Gene (encodes PBP2a)
MexAB-OprM	Multidrug Efflux Pump System of *Pseudomonas aeruginosa* (RND family)
MFS	Major Facilitator Superfamily (efflux transporter class)
MMP	Matrix Metalloproteinase
MWCO	Molecular Weight Cut-Off
NADPH	Nicotinamide Adenine Dinucleotide Phosphate (Reduced form)
NF-κB	Nuclear Factor Kappa B
NFX	Norfloxacin
NFX-NLC	Norfloxacin-Loaded Nanostructured Lipid Carrier
NHS	National Health Service (United Kingdom)
NLC	Nanostructured Lipid Carrier
NorA	Norfloxacin Efflux Pump A (Major Facilitator Superfamily; *S. aureus*)
OECD	Organisation for Economic Co-operation and Development
OprD	Outer Membrane Porin D (*Pseudomonas aeruginosa*)
P_{app}	Apparent Permeability Coefficient (Caco-2 assay; cm/s)
ParC	Topoisomerase IV Subunit C
ParE	Topoisomerase IV Subunit E

PBP	Penicillin-Binding Protein
PBP2a	Penicillin-Binding Protein 2a (encoded by *mecA*; low β-lactam affinity)
PDGF	Platelet-Derived Growth Factor
PEO	Polyethylene Oxide (hydrophilic block of Poloxamer)
PIA	Polysaccharide Intercellular Adhesin (staphylococcal biofilm matrix)
PII	Primary Irritation Index (Draize scoring)
PLA	Polylactic Acid
PLGA	Poly(lactic-co-glycolic acid)
PVL	Panton-Valentine Leukocidin
Q_{24}	Cumulative Drug Permeated per Unit Area at 24 Hours ($\mu g/cm^2$)
QRDR	Quinolone Resistance-Determining Region
R	Resistant
RAGE	Receptor for Advanced Glycation End Products
RH	Relative Humidity
RND	Resistance-Nodulation-Division (efflux pump superfamily)
SCCmec	Staphylococcal Cassette Chromosome *mec* (mobile genetic element)
SEDDS	Self-Emulsifying Drug Delivery Systems
SLS	Sodium Lauryl Sulphate
SSI	Surgical Site Infection
SSTI	Skin and Soft Tissue Infection
TGF-β	Transforming Growth Factor-Beta
TGF-β_1	Transforming Growth Factor-Beta 1
TIMP	Tissue Inhibitor of Metalloproteinase
T_{lag}	Lag Time (skin permeation parameter)
VEGF	Vascular Endothelial Growth Factor
WHO	World Health Organization

ZOI	Zone of Inhibition
ZP	Zeta Potential

Chapter 1

Introduction

1.1 Wound Healing and the Global Burden of Wound Infections

The skin constitutes the body's primary physical and immunological barrier against environmental insults, microbial invasion, and transepidermal water loss.

When this barrier is disrupted, through surgical incision, traumatic injury, thermal burns, or progressive tissue breakdown, a tightly regulated biological cascade is initiated to restore structural and functional integrity [1, 2].

This restorative process, collectively termed wound healing, proceeds through four overlapping and interdependent phases: haemostasis, characterised by platelet activation and fibrin clot formation within seconds of injury; inflammation, driven by neutrophil and macrophage infiltration over the first 72–96 hours; proliferation, encompassing granulation tissue deposition, angiogenesis, and re-epithelialisation between days 4 and 21; and remodelling, involving the progressive maturation of collagen architecture over months to years [2]. Under normal physiological conditions, these phases progress in an orderly temporal sequence. When disrupted, most critically by microbial infection, healing is arrested at the inflammatory phase, giving rise to the chronic, non-healing wound phenotype [3].

The global burden of wound-related morbidity is both substantial and escalating. Chronic wounds affect an estimated 1–2% of populations in developed nations and considerably higher proportions in low- and middle-income countries, where uncontrolled comorbidities and limited access to specialised wound care substantially amplify risk [3]. The global wound care market is projected to surpass USD 25 billion by 2026, reflecting the enormous clinical demand for innovative therapeutic solutions [4]. In the context of Pakistan specifically, the burden is compounded by a diabetes prevalence that ranks the country first globally according to International Diabetes Federation estimates, widespread unregulated antibiotic use that accelerates resistance development, and environmental conditions that increase wound contamination risk. The four principal categories of chronic wounds, diabetic foot ulcers, venous leg ulcers, pressure injuries, and non-healing surgical wounds, all share a defining clinical vulnerability: the propensity for secondary microbial infection. In the diabetic foot alone, a lower limb amputation occurs every 30 seconds globally as a direct consequence of infection-driven complications, underscoring the critical importance of effective, sustained antimicrobial delivery to the wound bed. Infection is, unequivocally, the primary biological and clinical barrier to wound healing [5, 6].

1.2 Current Therapeutic Approaches and their Limitations

Contemporary wound infection management relies principally on two therapeutic modalities: systemic antibiotic therapy and conventional topical antimicrobial formulations. Both approaches are constrained by well-characterised pharmacokinetic and physicochemical limitations that fundamentally restrict their effectiveness against the wound pathogens of greatest clinical concern.

Systemic antibiotic therapy, administered orally or parenterally, is the standard of care for wound infections with systemic features, yet its pharmacokinetic basis is inherently unfavourable in the wound context. Drug penetration into wound

tissue depends upon tissue perfusion, precisely the parameter most profoundly compromised in the high-risk wound populations most susceptible to infection.

Peripheral arterial disease in diabetic patients may reduce foot tissue perfusion to 10–20% of normal values, generating a pharmacokinetic dead zone in which systemic antibiotics fail to achieve effective wound-bed concentrations despite therapeutic plasma levels [7, 8].

Even in adequately perfused wounds, interstitial drug concentrations rarely exceed 40–60% of plasma values. Repeated systemic antibiotic courses additionally impose selective pressure across the entire body microbiome, accelerating the emergence of methicillin-resistant *Staphylococcus aureus* (MRSA) and multidrug-resistant *Pseudomonas aeruginosa* the two most clinically recalcitrant wound pathogens while generating systemic adverse effects including nephrotoxicity, Clostridioides difficile-associated colitis, and fluoroquinolone-associated tendinopathy that are particularly consequential in the elderly, immunocompromised patients who constitute the majority of the chronic wound population [9, 10].

Conventional topical formulations, creams, ointments, and aqueous gels, offer the theoretical advantage of direct wound-site drug delivery without systemic distribution. However, these formulations are limited by rapid displacement from the wound surface by exudate flow, a lack of sustained drug release mechanisms, and the formidable physicochemical barrier presented by the stratum corneum.

This 15–20 μm layer of highly ordered lamellar lipid bilayers restricts transcutaneous permeation to molecules satisfying stringent criteria: molecular weight below 500 Da, moderate lipophilicity (logP 1–3), and low melting point [11]. Most wound-relevant antibiotics and norfloxacin specifically , satisfy none of these criteria in crystalline form, rendering conventional topical delivery pharmacokinetically inadequate.

Advanced first-generation systems including chitosan-based nanofibers, liposomal formulations, and electrospun constructs represent incremental improvements but uniformly fail to integrate controlled sustained release, wound bioadhesion, and

broad-spectrum efficacy against resistant pathogens into a single, practically translatable formulation [12, 13]. A fundamental and clinically consequential gap in the therapeutic arsenal therefore remains.

1.3 Norfloxacin: Pharmacological Rationale and Physicochemical Challenge

Norfloxacin ($C_{16}H_{18}FN_3O_3$; MW 319.33 g/mol) is a first-generation fluoroquinolone antibiotic that exerts concentration-dependent bactericidal activity through the dual inhibition of DNA gyrase (GyrA/GyrB subunits) and topoisomerase IV (ParC/ParE subunits) [14, 15].

By stabilising enzyme-DNA cleavage complexes and stabilizing enzyme-DNA cleavage complexes that stall replication forks; subsequent fork processing generates double-strand breaks that exceed cellular repair capacity, triggering SOS-mediated cell death at above-MIC concentrations, norfloxacin achieves broad-spectrum bactericidal activity encompassing precisely the four principal wound-colonising pathogens targeted in this study.

Against *S. aureus* ATCC 6538, minimum inhibitory concentrations (MICs) range from 0.5 to 4 μg/mL via topoisomerase IV inhibition; against *E. coli* ATCC 25922, MICs of 0.06–0.25 μg/mL reflect the dominant sensitivity of gram-negative DNA gyrase to fluoroquinolone poisoning.

Against MRSA ATCC 43300, elevated MICs are attributable to NorA major facilitator superfamily efflux pump activity; against *P. aeruginosa* ATCC 27853, constitutive MexAB-OprM efflux elevates the intrinsic MIC to 1–8 μg/mL [14, 16].

Beyond direct bactericidal action, norfloxacin at sub-MIC concentrations suppresses NF-κB-mediated pro-inflammatory cytokine production and facilitates fibroblast proliferation, contributing indirectly to the restoration of the wound healing microenvironment [7]. Four decades of clinical pharmacological data and an

established safety profile further support its selection as the model antibacterial agent for topical NLC formulation development.

Despite these compelling pharmacological attributes, norfloxacin is classified as a Biopharmaceutics Classification System (BCS) Class IV agent , characterised by simultaneously low aqueous solubility and low membrane permeability [17]. This dual limitation is not merely a practical inconvenience but a fundamental physicochemical constraint on its conventional topical delivery.

The amphoteric ionisation profile of norfloxacin ($pK_{a1} = 6.35$ for the piperazinyl nitrogen; $pK_{a2} = 8.80$ for the carboxylic acid) generates a pH-dependent solubility profile in which minimum aqueous solubility of approximately 0.32-0.39mg/mL occurs at the isoelectric point near pH 7.4-7.5, the very pH prevailing at infected wound beds [18]. This creates a fundamental therapeutic paradox: the dissolved drug concentration available for antibacterial activity is lowest precisely at the site and pH where maximum therapeutic need exists. The calculated LogP of -1.03 for the zwitterionic species further precludes productive interaction with the lipophilic lamellar structure of the stratum corneum. Conventional norfloxacin Carbopol gel formulations fail primarily because this crystalline solubility barrier limits dissolved drug concentrations at wound-bed pH to values far below the MIC of target organisms, generating subtherapeutic exposure that represents an optimal selective environment for fluoroquinolone resistance development rather than an effective therapeutic intervention.

Norfloxacin (NFX), a second-generation fluoroquinolone antibacterial agent, exerts broad-spectrum bactericidal action by inhibiting bacterial DNA gyrase and topoisomerase IV, thereby disrupting DNA replication in a wide array of Gram-negative organisms such as *Pseudomonas aeruginosa* and *Escherichia coli*, as well as several Gram-positive pathogens including *Staphylococcus aureus*, the most common bacterial species implicated in delayed or infected wound healing [19]. This broad antibacterial coverage has made norfloxacin a preferred antibiotic candidate for topical wound-care formulations: norfloxacin-loaded lipid-polymer hybrid nanoparticles have been shown to retain full antibacterial potency against both

Gram-positive and Gram-negative wound pathogens while achieving nearly 90% cumulative drug release within 24 hours, confirming its suitability for site-targeted topical delivery [19].

Similarly, norfloxacin-loaded chitosan-based nanofiber and sponge dressings have demonstrated accelerated healing in burn and excisional wound models, with antibacterial efficacy directly proportional to the sustained release rate of the drug from the polymeric matrix [20]. Considering its well-documented broad-spectrum antibacterial efficacy, favorable safety profile, and proven track record in topical and wound-healing drug delivery systems, norfloxacin is a rational drug of choice for incorporation into a Nanostructured Lipid Carrier (NLC)-based gel; the NLC platform can compensate for norfloxacin's poor aqueous solubility and limited skin permeability while enhancing entrapment efficiency, ensuring sustained and controlled release, improving skin retention, and maintaining a moist wound-healing environment, ultimately promoting faster bacterial clearance and accelerated re-epithelialization compared to conventional topical formulations.

1.4 Nanostructured Lipid Carriers and Carbopol 940 Gel: Proposed Solution

Pharmaceutical nanotechnology provides a mechanistically rational and evidence-supported solution to the dual challenge posed by norfloxacin's BCS Class IV profile. Among the diverse nanocarrier platforms investigated for topical drug delivery, nanostructured lipid carriers (NLCs) represent the most advanced lipid-based system currently available [21, 22]. NLCs are formulated by blending structurally incompatible solid and liquid lipid components, in the present study, Precirol® ATO 5 (glyceryl palmitostearate) and Labrafac® WL 1349 (medium-chain triglycerides), stabilised in aqueous dispersion by surfactants including Tween® 80, Poloxamer 188, and co surfactant Transcutol® P. The deliberate structural incompatibility between the lipid components prevents complete crystallisation of the matrix, generating a disordered, amorphous or nanostructured lipid phase

in which norfloxacin is maintained in a molecularly dispersed state, effectively eliminating the crystalline lattice energy barrier responsible for its poor aqueous solubility and thereby markedly enhancing its apparent solubility and dissolution rate at wound-bed pH [21, 23].

NLCs are selected over their first-generation predecessors, solid lipid nanoparticles (SLNs), because SLNs are plagued by polymorphic crystallisation of the lipid matrix during storage, progressively expelling the encapsulated drug and generating uncontrolled burst release [24, 25].

They are preferred over liposomes on account of superior physical stability, substantially higher drug loading for BCS Class IV molecules, intrinsic biocompatibility of physiological glyceride lipid components with the wound healing environment, and scalable manufacture. The nanosized lipid particles additionally enhance stratum corneum permeation through productive lipid exchange interactions with the ordered ceramide-rich lamellae of the stratum corneum, and exploit the follicular shunt pathway for direct delivery to the dermal compartment [11]. To extend wound contact time and prevent NLC aggregation during storage, the optimised NFX-NLC dispersion is incorporated into a Carbopol 940 gel matrix. Carbopol 940, a crosslinked polyacrylic acid polymer (MW∼4,000 kDa), forms pseudoplastic, optically transparent gels at pH 5.5–6.5 that adhere to wound surfaces through hydrogen-bonding interactions with wound glycoproteins, resisting displacement by wound exudate and maintaining the drug in sustained contact with the wound bed [26, 27]. The dual NLC-gel system generates a biphasic release profile: an initial rapid component from NLC surface drug, followed by sustained matrix diffusion-controlled release that maintains above-MIC concentrations over clinically relevant periods [28].

1.5 Problem Statement and Literature Gap

Despite norfloxacin's well-documented broad-spectrum bactericidal efficacy against the principal wound-colonising pathogens, its clinical potential in topical

wound infection management remains fundamentally constrained by the limitations of currently available delivery systems. The NorA efflux pump in MRSA and the MexAB-OprM system in *P. aeruginosa* actively export fluoroquinolones from the bacterial cytoplasm, necessitating sustained supratherapeutic local drug concentrations for bactericidal efficacy , concentrations that are not achievable through the transient, low-level drug release provided by conventional topical formulations or by first-generation advanced delivery systems. Existing approaches, chitosan nanofibers, liposomes, SLNs, and self-emulsifying systems, have individually addressed limited aspects of this challenge but have not successfully integrated controlled sustained release, wound bioadhesion, adequate stratum corneum penetration, and broad-spectrum bactericidal activity against both MRSA and *P. aeruginosa* into a single, clinically practical formulation.

Critically, no published study to date has developed, characterised, or evaluated a norfloxacin-loaded nanostructured lipid carrier incorporated into a Carbopol 940 gel matrix for topical wound infection management. No prior study has evaluated norfloxacin NLC gel permeation at both the acidic skin surface pH (5.5) and the wound-bed pH (7.4), nor demonstrated susceptible-range antibacterial activity against both MRSA (ATCC 43300) and *P. aeruginosa* (ATCC 27853) from a norfloxacin topical formulation at dose levels achievable in clinical practice. No stability data exist under ICH Q1A(R2) accelerated conditions (40°C/75% RH) for this formulation class, a regulatory prerequisite for products intended for clinical use in Pakistan (Zone IVb) ((30°C/75% RH)). The present study uniquely and comprehensively addresses each of these gaps.

1.6 Research Aim and Objectives

1.6.1 Aim

To develop, characterise, optimise, and evaluate a Carbopol 940-based norfloxacin-loaded nanostructured lipid carrier (NFX-NLC) gel for topical wound infection

management, targeting enhanced drug solubilisation, superior skin permeation, controlled sustained drug release, and broad-spectrum bactericidal efficacy against principal wound pathogens including MRSA and *Pseudomonas aeruginosa*.

1.6.2 Objectives

i. To prepare norfloxacin-loaded NLCs by hot homogenisation followed by ultrasonication, systematically optimising the solid-liquid lipid ratio, surfactant concentration, and drug loading to achieve particle size < 300 nm, PDI < 0.3, zeta potential ≥ 30 mV, and encapsulation efficiency $> 80\%$.

ii. To characterise prepared NLC formulations for particle size, PDI, zeta potential, surface morphology (SEM), drug encapsulation efficiency, thermal behaviour (DSC), drug-excipient compatibility (FTIR), crystallographic state (XRD), and *in vitro* drug release kinetics.

iii. To incorporate the optimised NFX-NLC dispersion into Carbopol 940 gel matrices at 0.3%, 0.6%, and 0.9% w/w and select the optimal gel formulation based on comprehensive physicochemical characterisation.

iv. To evaluate physicochemical properties of the NFX-NLC gel including visual appearance, pH, viscosity, rheological behaviour, spreadability, and extrudability.

v. To assess *ex vivo* skin permeation using Franz static diffusion cells at pH 5.5 and pH 7.4, determining steady-state flux (Jss), permeability coefficient (Kp), lag time, cumulative permeation (Q_{24}), and enhancement ratio.

vi. To evaluate the antibacterial activity of the NFX-NLC gel by agar well diffusion method against *Staphylococcus aureus* (ATCC 6538), MRSA (ATCC 43300), *Escherichia coli* (ATCC 25922), and *Pseudomonas aeruginosa* (ATCC 27853) at three dose levels (2.5 mg, 5 mg, and 10 mg), with zone of inhibition (ZOI) interpreted against published norfloxacin susceptibility thresholds and compared against the plain norfloxacin Carbopol gel as a control formulation.

vii. To conduct ICH Q1A(R2)-compliant accelerated stability studies at 4°C, 25°C/60% RH, and 40°C/75% RH over defined time points, assessing particle size, drug content, pH, and physical appearance.

1.7 Research Hypothesis

It is hypothesised that the incorporation of norfloxacin within an optimised nanostructured lipid carrier matrix, subsequently integrated into a bioadhesive Carbopol 940 gel, will overcome the solubility and permeability limitations imposed by the drug's BCS Class IV classification and will deliver statistically superior antibacterial activity, skin permeation, and controlled sustained drug release compared with a plain norfloxacin Carbopol 940 gel of equivalent drug concentration. Specifically:

i. The NLC lipid matrix (Precirol ATO 5 / Labrafac WL 1349) will maintain norfloxacin in an amorphous or molecularly dispersed state , confirmed by absence of the crystalline melting endotherm in DSC and disappearance of characteristic diffraction peaks in XRD , thereby eliminating the crystalline solubility barrier at wound-bed pH and enhancing dissolution rate and apparent aqueous solubility.

ii. Nanosized lipid particles will enhance transcutaneous norfloxacin permeation through lipid exchange interactions with stratum corneum lamellar bilayers and preferential follicular shunt accumulation, producing a statistically significant enhancement ratio (ER $\geq$ 2) relative to plain norfloxacin Carbopol gel at pH 5.5, the primary topical delivery condition.

iii. The dual NLC-Carbopol gel matrix will generate a sustained biphasic release profile , initial rapid antibacterial coverage from surface-associated drug followed by sustained diffusion-controlled release from the lipid core , maintaining norfloxacin concentrations above the MIC of all four target wound pathogens over a clinically relevant 24-hour period.

iv. It is hypothesized that the NFX-NLC gel will achieve susceptible-range zones of inhibition against all four target wound pathogens including MRSA (ATCC 43300)

and *P. aeruginosa* (ATCC 27853) at all evaluated dose levels, and will demonstrate statistically superior antibacterial performance compared to the plain norfloxacin Carbopol gel, attributable to the enhanced membrane permeability and sustained drug release conferred by the nanostructured lipid carrier system.

Chapter 2

Literature Review

2.1 Wound Healing: Biology Phases and Clinical Significance

2.1.1 Definition and Classification of Wounds

A wound is defined as any disruption of the normal anatomy and physiological function of the skin and underlying tissues, arising from physical, chemical, thermal, electrical, or biological insult [1].

Wounds are broadly classified as acute or chronic based on their temporal healing behaviour, with further subdivision according to wound depth, mechanism of injury, and the physiological context in which they arise [2, 3].

Table 2.1 provides a structured classification of the principal wound categories encountered in clinical practice, together with their etiological basis, expected healing trajectory, principal complication risks, and predominant infecting microorganisms.

Acute wounds arise from defined traumatic events and, in the absence of complicating factors, heal within a predictable period through the orderly progression of the four canonical wound healing phases [1, 2].

TABLE 2.1: Classification of Wound Types, Clinical Characteristics, and Principal Infecting Pathogens

Wound Category	**Etiology**	**Clinical Examples**	**Expected Healing**	**Complication Risk**	**Pathogens of Concern**
Acute Surgical	Surgical incision	Post-operative incision	Primary intention (7–14 days)	Surgical site infection	*S. aureus*, MRSA
Acute Traumatic	Mechanical trauma	Lacerations, abrasions, bites	Secondary intention (2–4 weeks)	Contamination, sepsis	*S. aureus*, *E. coli*
Burn Wounds	Thermal chemical electrical	Partial/full-thickness burns	Variable, depth-dependent	MRSA, *P. aeruginosa*	*P. aeruginosa*, MRSA, *A. baumannii*
Diabetic Foot Ulcer	Neuropathy + ischaemia + hyperglycaemia	Plantar ulcer, heel ulcer	Chronic (months–years)	Amputation, osteomyelitis	Polymicrobial, MRSA
Venous Leg Ulcer	Chronic venous hypertension	Gaiter area ulceration	Chronic, high recurrence	Biofilm, cellulitis	*S. aureus*, *P. aeruginosa*
Pressure Injury	Sustained ischaemic compression	Sacral, heel, trochanteric	Chronic, grade dependent	Deep tissue infection	*S. aureus*, *E. coli*, anaerobes

Note. MRSA = methicillin-resistant *Staphylococcus aureus*; SSTIs = skin and soft tissue infections; SSIs = surgical site infections.

Surgically incised wounds, characterised by sharp wound margins and favourable conditions for primary intention healing, represent the most straightforward category. Traumatic acute wounds, including lacerations, abrasions, puncture wounds, and bite injuries, present with greater tissue contamination and bioburden and may necessitate secondary intention healing.

Burn wounds represent a therapeutically distinct and uniquely challenging category: the destruction of the full-thickness skin barrier creates a vast protein-rich wound surface immediately accessible to environmental and endogenous microorganisms, the avascular eschar precludes systemic antibiotic delivery to the wound site, and the combination of impaired innate immunity and frequent empirical antibiotic exposure creates a selective environment for multidrug-resistant organisms, particularly MRSA and *P. aeruginosa* [8, 9].

Chronic wounds are defined by their failure to progress through the normal healing continuum within three months despite appropriate clinical management, reflecting pathological arrest at the inflammatory phase [3, 29]. Common to all chronic wound categories is a dysregulated inflammatory microenvironment characterised by elevated pro-inflammatory cytokines (TNF-α, IL-1β, IL-6), excessive matrix metalloproteinase (MMP) activity that degrades growth factors and extracellular matrix components, impaired growth factor bioavailability, and high bacterial bioburden, the combination of which perpetuates the inflammatory state and prevents progression to the regenerative events of the proliferative phase [3, 30].

2.1.2 Epidemiology and Global Burden of Wound Infections

The global epidemiology of wound infections is characterised by high and rising prevalence, substantial economic burden, and marked disparities between high-income and low-to-middle-income countries. In the United States, skin and soft tissue infections account for approximately 14 million outpatient visits annually [7]. Surgical site infections (SSIs) constitute the most common healthcare-associated

infection and are associated with two-fold increases in hospital mortality and average additional costs of USD 10,000–25,000 per case [6]. Point-prevalence studies across European hospital settings document wound infection rates of 15–25% of all healthcare-associated infections, with gram-positive organisms, particularly *S. aureus*, accounting for 40–50% of isolates [8, 9]. National Health Service data from England estimate the annual cost of managing all wound types at over £8.3 billion, with wound infection representing the single largest driver of cost variability.

In Pakistan, the burden of wound infection is compounded by several structural and epidemiological factors. The country bears the fourth highest global burden of diabetes mellitus (International Diabetes Federation data), generating an extensive population at risk for diabetic foot ulcers, the most common and clinically consequential chronic wound category. The prevalence of MRSA among *S. aureus* wound isolates in tertiary care hospitals in Pakistan has been reported at 30–60% in recent surveys, substantially exceeding rates observed in many Western healthcare systems, reflecting the compounding effects of overcrowded hospital facilities, limited infection control infrastructure, and unregulated antibiotic dispensing that allows over-the-counter access to fluoroquinolones and cephalosporins without prescription. These epidemiological features substantially amplify the clinical relevance and potential public health impact of developing topical delivery systems capable of achieving and sustaining therapeutic concentrations against drug-resistant wound pathogens.

2.1.3 Phases of Normal Wound Healing

Haemostasis, the first phase of wound healing, is initiated within seconds of vascular disruption through platelet activation at the wound site. Exposure of subendothelial collagen and tissue factor triggers the sequential activation of primary haemostasis, platelet adhesion, activation, and aggregation mediated by von Willebrand factor-collagen binding and ADP/thromboxane A_2-dependent platelet activation, and secondary haemostasis, culminating in thrombin-mediated fibrinogen cleavage and fibrin polymerisation. The resulting platelet-fibrin clot performs

the dual function of haemostatic plug and provisional extracellular matrix scaffold, into which growth factors stored within platelet α-granules (PDGF, TGF-β, VEGF, EGF) are released upon platelet activation, initiating the chemoattraction of inflammatory cells that defines the next phase [1].

The inflammatory phase, beginning within minutes of injury and extending for 4–6 days in normally healing acute wounds, is dominated sequentially by neutrophil and macrophage activity. Neutrophils, attracted by PDGF, complement activation products (C3a, C5a), and formylated bacterial peptides, arrive within 2–4 hours and serve the critical dual function of pathogen elimination through oxidative burst and non-oxidative mechanisms, and cytokine-mediated amplification of the inflammatory response.

Monocyte-derived macrophages arriving at 48–96 hours represent the pivotal transitional cell population bridging inflammation and proliferation: M1-polarised macrophages continue pathogen clearance; M2-polarised macrophages secrete pro-reparative growth factors (PDGF, VEGF, TGF-β_1, IGF-1) that drive the subsequent proliferative response.

Critically, the persistence of M1 macrophage polarization, sustained by continued bacterial infection and pathogen-associated molecular patterns, is the central cellular mechanism underlying the arrest of healing at the inflammatory phase in infected chronic wounds [2, 29].

The proliferative phase (days 4–21) encompasses angiogenesis, fibroplasia, and re-epithelialisation [1, 2]. Angiogenesis, driven by VEGF, bFGF, and angiopoietins secreted by activated macrophages and endothelial cells, establishes the oxygen and nutrient supply required for fibroblast proliferation and collagen synthesis. Fibroblasts synthesise type III collagen, fibronectin, and hyaluronic acid, forming the granulation tissue matrix; a proportion undergo TGF-β_1-mediated differentiation into α-smooth muscle actin-expressing myofibroblasts that mediate wound contraction. Re-epithelialisation, the migration of keratinocytes from wound margins and surviving hair follicle units across the granulation tissue surface, constitutes the defining event of wound closure. The remodelling phase, extending for

months to years, involves progressive replacement of disorganised type III collagen with mechanically superior type I collagen, cross-linked by lysyl oxidase to achieve a maximum tensile strength of 70–80% of unwounded skin at 12–18 months [2].

2.1.4 Factors Disrupting Normal Wound Healing

Microbial biofilm formation represents the most critical and clinically prevalent factor disrupting wound healing [8]. Biofilms, structured microbial communities enclosed within a self-produced extracellular polymeric matrix (EPS), confer antimicrobial resistance 100–1,000-fold greater than planktonic counterparts through multiple concurrent mechanisms: the EPS matrix retards antibiotic diffusion; metabolically quiescent bacteria at the biofilm core are intrinsically tolerant to antibiotics requiring active replication for efficacy; quorum sensing coordinates virulence factor expression and efflux pump upregulation; and a persister cell subpopulation provides the reservoir for biofilm re-establishment after treatment cessation [10, 30]. Molecular microbiological studies indicate that biofilms are present in up to 60–80% of chronic wound beds versus fewer than 6% of acute wound specimens, strongly implicating biofilm establishment as a causal driver of wound chronicity rather than merely its consequence.

Diabetes mellitus impairs wound healing through peripheral sensorimotor neuropathy (permitting unrecognised repetitive microtrauma), peripheral arterial disease (reducing tissue perfusion and antibiotic delivery), and direct hyperglycaemia-mediated cellular dysfunction [3, 5]. Non-enzymatic glycation of collagen and growth factors reduces biological activity; advanced glycation end products activate NF-κB via receptor for advanced glycation end products (RAGE), perpetuating chronic inflammation; and hyperglycaemia-induced reactive oxygen species trigger fibroblast and keratinocyte apoptosis. Immune dysfunction, manifesting as impaired neutrophil chemotaxis, defective macrophage polarisation, and diminished complement activity, substantially increases wound infection susceptibility and severity in diabetic patients. Poor vascularity, tissue hypoxia, nutritional deficiencies, and pharmacological immunosuppression represent additional disrupting

factors that collectively define the hostile wound microenvironment targeted by the NFX-NLC Carbopol 940 gel [29].

2.2 Wound Infections: Pathogenesis and Microbiology

2.2.1 Pathogenesis of Wound Infection

Wound infection is defined as the invasion of viable wound tissue by microorganisms replicating to sufficient densities to elicit a pathological host inflammatory response, clinically manifested as localised erythema, warmth, oedema, pain, and purulent exudate, with quantitative microbial culture demonstrating pathogens exceeding 10^5 colony-forming units per gram of wound tissue [30, 31].

The pathogenesis involves sequential bacterial adherence, colonisation, proliferation, invasion through the wound bed, and immune evasion, a continuum in which progression is determined by the balance between microbial virulence and the integrity of the local wound immune microenvironment [8].

The ability to interrupt this progression through sustained local delivery of bactericidal concentrations of norfloxacin constitutes the primary pharmacological objective of the NFX-NLC gel.

The clinically important distinction between wound contamination, colonisation, and infection reflects progressive increases in microbial biomass, metabolic activity, and immunological impact. Contamination, the transient presence of organisms without multiplication, is ubiquitous in all wounds. Colonisation , sustained replication without host tissue damage, is present in virtually all chronic wounds and does not in itself impair healing.

Critical colonisation and infection represent the pathological states in which microbial activity begins to impair cellular healing programmes through virulence

factor secretion, biofilm formation, and immune activation, warranting antimicrobial intervention [12, 30].

2.2.2 Principal Wound Pathogens and their Clinical Significance

Staphylococcus aureus is the dominant pathogen in wound infections globally, isolated from 40–80% of culture-positive wound specimens across epidemiological studies encompassing acute traumatic wounds, surgical site infections, chronic diabetic ulcers, and venous leg ulcers [8, 9].

Its exceptional clinical ubiquity reflects a versatile virulence armamentarium: surface adhesins including fibronectin-binding proteins (FnBPA/FnBPB), collagen-binding protein (CNA), and clumping factors (ClfA/ClfB) mediate adhesion to wound matrix proteins; secreted factors including α-haemolysin, Panton-Valentine leukocidin (PVL), and toxic shock syndrome toxin-1 amplify local tissue destruction and systemic inflammatory responses; and coagulase converts fibrinogen to a protective pseudocapsule around bacterial colonies, shielding them from phagocytic clearance. The biofilm-forming capacity of *S. aureus* , driven by the ica operon-encoded polysaccharide intercellular adhesin (PIA) , further compounds treatment difficulty.

Methicillin-resistant *S. aureus* (MRSA), defined by the mecA gene encoding penicillin-binding protein 2a (PBP2a) with negligible β-lactam affinity, represents a critically important subset of wound-colonising staphylococci. PBP2a retains transpeptidase activity in the presence of β-lactam concentrations that saturate all native *S. aureus* PBPs, rendering MRSA resistant to all penicillins, cephalosporins, and carbapenems and substantially narrowing therapeutic options [9]. Fluoroquinolone resistance in MRSA is mediated primarily through NorA , a major facilitator superfamily (MFS) efflux transporter that exports norfloxacin and other hydrophilic fluoroquinolones from the bacterial cytoplasm via proton antiport, reducing intracellular drug concentrations below the topoisomerase IV

Table 2.2: Principal Wound Pathogens: Virulence Factors, Resistance Mechanisms, and Clinical Significance

Pathogen	**Classification**	**Key Virulence Factors**	**Principal Resistance Mechanisms**	**Wound Infection Significance**
S. aureus ATCC 6538	Gram-positive coccus	Fibronectin adhesins (FnBPA/B), α-haemolysin, Panton-Valentine leukocidin, coagulase, biofilm (PIA)	Methicillin-susceptible; NorA efflux pump may reduce fluoroquinolone accumulation	Leading cause of acute SSTIs and SSIs; isolated from 30–60% of wound cultures
MRSA ATCC 43300	Gram-positive coccus	All *S. aureus* virulence factors; PVL; enhanced biofilm; TSST-1	mecA-encoded PBP2a (β-lactam resistance); NorA efflux (fluoroquinolones); broad multidrug resistance	Dominant in chronic wounds, burns, and HAIs; associated with treatment failure and limb amputation
E. coli ATCC 25922	Gram-negative rod	Type 1 and P fimbriae, α-haemolysin, iron-acquisition systems (aerobactin), capsular polysaccharides	ESBL production (CTX-M variants); intrinsic ampicillin resistance; emerging fluoroquinolone resistance	Important in diabetic foot ulcers, perineal wounds; ESBL-producing strains increasingly prevalent
P. aeruginosa ATCC 27853	Gram-negative rod	Alginate biofilm, pyocyanin, exotoxin A, elastase (LasB), rhamnolipids, quorum sensing (las/rhl/pqs systems)	MexAB-OprM constitutive efflux; OprD downregulation; intrinsic AmpC β-lactamase; low outer membrane permeability	Major burn and chronic wound pathogen; extremely treatment-resistant; high mortality when systemic

Note. MRSA = methicillin-resistant *S. aureus*; PVL = Panton-Valentine leukocidin; ESBL = extended-spectrum β-lactamase; SSTIs = skin and soft tissue infections; HAIs = healthcare-associated infections; TSST-1 = toxic shock syndrome toxin-1.

inhibitory threshold. The development of topical delivery systems capable of generating and sustaining intracellular norfloxacin concentrations sufficient to transiently saturate NorA efflux capacity represents a central mechanistic objective of

the NFX-NLC gel. *Pseudomonas aeruginosa* is the second most frequently isolated pathogen from chronic wound infections and the dominant organism in burn wound infections [10].

Its extraordinary intrinsic multidrug resistance arises from the synergistic action of restricted outer membrane permeability, a limited repertoire of general diffusion porins substantially reduces passive antibiotic influx, and constitutive MexAB-OprM efflux pump expression, which actively extrudes fluoroquinolones (as well as β-lactams, tetracyclines, and chloramphenicol) across both inner and outer membranes before they accumulate to inhibitory intracellular concentrations.

Biofilm formation by *P. aeruginosa*, characterised macroscopically by greenish wound discolouration and a characteristic grape-like malodour (from 2-aminoacetophenone), establishes a treatment-resistant state of particular clinical intractability.

Achieving intracellular norfloxacin concentrations sufficient for bactericidal topoisomerase II inhibition in *P. aeruginosa* requires extracellular concentrations substantially above the planktonic MIC, a pharmacokinetic demand that the sustained high-concentration NLC-mediated release profile is specifically designed to address.

Escherichia coli is an increasingly significant wound pathogen, particularly in wounds associated with faecal flora contamination, perineal wounds, parastomal infections, abdominal surgical dehiscence, and in diabetic foot ulcers and pressure injuries in incontinent patients. Pathogenic *E. coli* express type 1 fimbriae mediating adhesion to wound fibronectin, α-haemolysin, and iron-acquisition systems (aerobactin, enterobactin). The global dissemination of extended-spectrum β-lactamase (ESBL)-producing *E. coli*, particularly CTX-M-15 associated with the pandemic O25b-ST131 clonal lineage, has substantially complicated wound infection management, eliminating most orally bioavailable β-lactam options. Norfloxacin retains activity against the majority of non-ESBL *E. coli* wound isolates at MICs of 0.06–0.25 µg/mL, making it pharmacologically rational for topical delivery when administered at adequate local concentrations [14, 16].

2.2.3 Antimicrobial Resistance and Its Consequences for Wound Management

The epidemiological trajectory of antimicrobial resistance in wound pathogens over the past two decades has been characterised by the progressive accumulation of resistance determinants within individual isolates, producing multidrug-resistant (MDR), extensively drug-resistant (XDR), and pandrug-resistant (PDR) phenotypes, and the horizontal dissemination of resistance genes across species through plasmids, transposons, and integrons. The WHO designation of MRSA and carbapenem-resistant *P. aeruginosa* as critical-priority pathogens for new antimicrobial agent development reflects the severity of the therapeutic crisis these organisms represent. In the wound infection context, MDR pathogens narrow the spectrum of effective systemic antimicrobials while simultaneously rendering conventional topical formulations, which fail to achieve sustained above-MIC drug concentrations, therapeutically futile. Advanced formulation strategies that restore therapeutic efficacy against MDR wound pathogens using established antibiotics, by overcoming formulation-level barriers, represent the highest-priority research direction directly addressed by the present study.

2.3 Current Therapeutic Approaches for Wound Infections and their Limitations

2.3.1 Systemic Antibiotic Therapy

The pharmacokinetic basis for the limited clinical efficacy of systemic antibiotic therapy in wound infections is well established. Antibiotic penetration into wound tissue is governed by plasma protein binding, tissue perfusion, the physicochemical properties of the antibiotic, and the anatomical characteristics of the wound microenvironment [7]. In the diabetic foot ulcer, the most therapeutically challenging wound infection context, peripheral arterial disease may reduce tissue perfusion

to 10–20% of normal values, creating a pharmacokinetic dead zone in which systemically administered antibiotics fail to achieve effective wound-bed concentrations despite therapeutic plasma levels. Microdialysis studies in diabetic patients have demonstrated that tissue concentrations of systemically administered fluoroquinolones in the foot fall below MIC values for target organisms despite nominally therapeutic plasma concentrations.

Systemic fluoroquinolone administration subjects the drug to hepatic first-pass metabolism and exposes all body tissues to drug concentrations, generating class-specific adverse effects including gastrointestinal intolerance, central nervous system toxicity (headache, dizziness, seizure risk in predisposed patients), QT interval prolongation, tendinopathy and tendon rupture (particularly Achilles tendon rupture in elderly patients receiving concurrent corticosteroids), phototoxicity, and hypersensitivity reactions. These adverse effects carry disproportionate impact in the elderly, immunocompromised patients who constitute the majority of the chronic wound population. Systemic antibiotic prescribing additionally exposes the entire body microbiome to selection pressure, accelerating resistance emergence at anatomical sites remote from the wound, a concern with substantial public health implications in the contemporary antimicrobial stewardship context.

2.3.2 Conventional Topical Formulations

Topical antibiotic creams and ointments provide the theoretical advantage of direct wound-site delivery without systemic distribution. However, they suffer from profound physicochemical and pharmacokinetic limitations that constrain clinical utility. Wound exudate continuously flowing across the wound surface displaces non-adhesive ointment vehicles, reducing drug-wound contact time to minutes rather than the hours required for sustained antibacterial coverage. Cream bases (oil-in-water emulsions) spread easily but exhibit even lower wound retention than ointments. Both formulation types lack controlled sustained release mechanisms: drug concentrations decline exponentially after initial application as the concentration gradient dissipates, generating only a brief burst of drug delivery followed

by rapid decay to subtherapeutic levels. For norfloxacin specifically, dissolution from crystalline particles in conventional gel bases is further limited by the low aqueous solubility of the drug at wound-bed pH 7.0, creating a concentration ceiling on dissolved drug available for diffusion that is pharmacokinetically insufficient to sustain inhibitory concentrations against MRSA or *P. aeruginosa*.

2.3.3 Advanced Wound Delivery Systems and their Remaining Limitations

The recognised limitations of conventional formulations have driven intense research into advanced drug delivery platforms for wound infection management [12, 30]. Liposomal formulations, vesicular systems comprising phospholipid bilayers encapsulating an aqueous core, offer enhanced biocompatibility and initial improvement in skin retention but suffer from poor physical stability (drug leakage at 37°C and particle aggregation over shelf-life), limited drug loading for hydrophilic BCS Class IV molecules typically below 5% w/w, and high manufacturing costs that constrain clinical translation. Niosomal systems (non-ionic surfactant vesicles) offer improved chemical stability relative to phospholipid liposomes but share similar loading and penetration limitations [12].

Chitosan-based nanofiber dressings produced by electrospinning provide a high surface area-to-volume ratio enabling rapid initial drug release, but this same property generates unacceptable burst release exhausting the drug reservoir within 1–2 hours, failing to provide the sustained coverage required for biofilm suppression. Chitosan-grafted norfloxacin constructs, where the drug is covalently conjugated to the chitosan backbone, sacrifice the concentration-dependent bactericidal kinetics of free norfloxacin. Solid lipid nanoparticles (SLNs) represent the closest conceptual approach to NLC technology but are limited by polymorphic crystallisation of the solid lipid matrix during storage, progressively reducing drug accommodation volume and generating uncontrolled drug expulsion, a critical limitation that NLC architecture is specifically engineered to overcome. Collectively, no existing system simultaneously satisfies all criteria of the ideal topical antimicrobial

formulation: solubilised drug delivery at wound-bed pH, sustained 12–24 hour above-MIC release, wound bioadhesion, adequate stratum corneum penetration, biocompatibility with wound healing processes, and physicochemical stability under tropical storage conditions.

2.4 Norfloxacin: Pharmacology Physicochemical Properties and Wound Healing Relevance

2.4.1 Introduction to Fluoroquinolone Antibiotics

Fluoroquinolones are synthetic broad-spectrum antibacterial agents derived from nalidixic acid through iterative structural optimisation commencing in the 1960s [14, 15]. The introduction of a fluorine substituent at position 6 of the quinolone core, defining the fluoroquinolone class, substantially enhanced antibacterial potency and broadened the spectrum to encompass both gram-negative and gram-positive organisms. Norfloxacin, the first clinically approved fluoroquinolone (United States FDA approval, 1986), retains foundational antibacterial properties against cutaneous and wound-associated bacteria, and its well-characterised pharmacological and safety profile accumulated over four decades of clinical use provides a robust framework for evaluating the formulation-specific performance improvements afforded by NLC encapsulation [14, 16].

2.4.2 Physicochemical Properties and BCS Classification

The Biopharmaceutics Classification System (BCS), developed by Amidon and colleagues, classifies drug substances according to aqueous solubility and membrane permeability [17]. BCS Class IV drugs, characterised by simultaneously low solubility and low permeability, present the most challenging biopharmaceutical

profile, requiring simultaneous enhancement of both parameters for effective delivery. Norfloxacin's BCS Class IV classification represents a fundamental constraint on conventional topical formulations that the NLC approach addresses at the molecular level: lipid nanoencapsulation maintains norfloxacin in an amorphous state, abolishing the crystalline solubility barrier, while the lipophilic NLC surface and follicular penetration route enhance stratum corneum permeation [11, 21, 22].

TABLE 2.3: Physicochemical Properties of Norfloxacin Relevant to Topical NLC Delivery [32, 33].

Physicochemical Property	**Value / Description**	**BCS Relevance**	**Implication for Topical NLC Delivery**
Molecular Formula / MW	CHFNO / 319.33 g/mol	Below 500 Da Lipinski limit	Favourable MW for membrane permeation; however, other parameters limit passive flux
BCS Classification	Class IV , low solubility / low permeability	Dual formulation challenge	Requires simultaneous solubility and permeability enhancement; primary rationale for NLC
Aqueous Solubility	∼0.32-0.39 mg/mL (minimum near isoelectric point pH (7.4-7.5)	Critical BCS solubility parameter	Minimum availability at wound-bed pH; NLC amorphous dispersion circumvents this barrier
pKa (Piperazinyl N)	6.35	Governs cationic species at skin pH	At pH 5.5, predominantly cationic (∼88%); increased solubility and flux at skin surface pH

Table 2.3 continued from previous page

Physicochemical Property	**Value / Description**	**BCS Relevance**	**Implication for Topical NLC Delivery**
pK_{a2} (Carboxylic acid)	8.80	Amphoteric character	Zwitterionic form at pH 7.0–8.5 with minimum solubility and permeability
LogP (octanol/water)	1.03 (zwitterionic form)	BCS permeability determinant	Pronounced hydrophilicity; unfavourable for passive transcellular stratum corneum permeation
Melting Point	227–228°C (crystalline)	Reflects crystal lattice energy	High melting point indicates strong crystal lattice; NLC eliminates this energy barrier by amorphisation
Membrane Permeability (Papp)	$<2 \times 10$ cm/s (Caco-2)	BCS Class IV permeability criterion	Low passive permeability; NLC lipid-SC interaction enhances transcutaneous drug flux
λmax (UV)	273 nm	Analytical parameter	Basis for spectrophotometric quantification in release and permeation studies

Note. BCS = Biopharmaceutics Classification System; SC = stratum corneum; NLC = nanostructured lipid carrier; Papp = apparent permeability coefficient.

The amphoteric character of Norfloxacin, arising from the piperazinyl nitrogen (pKa = 6.35) and the carboxylic acid (pK_{a2} = 8.80), generates a pH-dependent solubility profile with critical implications for topical wound delivery [18]. At skin surface pH 4.5–5.5, the protonated cationic species exhibits enhanced solubility (up to 6–8 mg/mL at pH 4.0) but limited membrane permeability. At wound-bed pH 7.0–8.5, norfloxacin approaches its isoelectric point with minimum solubility (∼0.32-0.39 mg/mL), creating the paradox of minimum drug availability at the site of maximum therapeutic need. NLC encapsulation circumvents this by maintaining norfloxacin in a lipid-dissolved, pH-independent amorphous state [21, 25]. The topological polar surface area (TPSA) of approximately 72.9 $Å^2$ approaches the 75–80 $Å^2$ threshold above which transcellular passive permeation is substantially impaired, reinforcing the need for a carrier-mediated delivery strategy.

Norfloxacin exerts bactericidal activity through dual inhibition of two essential bacterial type II topoisomerases [14, 15]. DNA gyrase ($GyrA_2/GyrB_2$ heterotetramer) catalyses the introduction of negative supercoils into the bacterial chromosome, relieving torsional stress ahead of the replication fork and transcription machinery; norfloxacin intercalates between cleaved DNA base pairs and contacts residues in the quinolone resistance-determining region (QRDR) of GyrA, particularly Ser83 and Asp87 in *E. coli*, stabilising the enzyme-DNA cleavage complex and preventing strand relegation [14, 16].

Topoisomerase IV ($ParC_2/ParE_2$ heterotetramer) decatenates replicated chromosomes during cell division; fluoroquinolone stabilisation of the topoisomerase IV-DNA cleavage complex prevents chromosome segregation. These stabilised cleavage complexes generate protein-linked double-strand breaks at above-MIC concentrations when the replication fork encounters the stalled enzyme-DNA adduct, triggering SOS response activation that exceeds cellular repair capacity and leads to chromosomal fragmentation and cell death [15]. The concentration-dependent bactericidal kinetics of Norfloxacin, achieving maximum kill rates of ≥ 3 log reduction within 4-6 hours at 4–10× MIC, provides the pharmacodynamic rationale for the sustained high-concentration wound-site drug delivery targeted by the NLC formulation.

2.4.3 Role of Norfloxacin in Wound Healing

Bacterial burden within the wound, particularly from *S. aureus* and *P. aeruginosa*, perpetuates a destructive pro-inflammatory state characterised by elevated TNF-α, IL-1β, and IL-6, which sustains M1 macrophage dominance and impairs the transition to the M2 wound-healing phenotype required for tissue repair [34, 35]. In infected wounds, *P. aeruginosa* promotes excessive M1 macrophage activation with a relatively inadequate M2 phenotype induction, locking the wound in a state of persistent inflammation that arrests the proliferative phase of healing [36]. By eradicating these pathogens, norfloxacin removes the primary bacterial stimulus driving this dysregulated inflammatory cascade, thereby permitting macrophage reprogramming toward the M2 wound-healing phenotype and resolution of chronic wound inflammation.

Critically, *P. aeruginosa* secretes the zinc metalloprotease LasB (pseudolysin), which directly inhibits fibroblast and keratinocyte migration and survival, degrades collagen, impedes neovascularization, and sustains elevated IL-6, collectively arresting the proliferative phase of wound healing [37].

Elastase-producing *P. aeruginosa* isolates have further been shown to degrade plasma proteins, antiproteinases, proteoglycans, and fibroblast-derived ECM components *in vitro*, thus mimicking the proteolytic activity observed in chronic ulcer fluid in vivo [38].

Concurrently, *S. aureus* exploits ECM proteins including fibronectin, laminin, and collagen as adhesion substrates, [39] and its proteases disrupt these structural components, destabilising the scaffold essential for keratinocyte and fibroblast attachment and migration [40].

The suppression of these bacterial protease-driven ECM degradation mechanisms through norfloxacin-mediated pathogen eradication restores the MMP/TIMP balance and preserves the structural integrity of the wound ECM, creating a permissive environment for re-epithelialisation and dermal regeneration [41].

These indirect mechanisms, acting through bacterial burden clearance rather than direct pharmacological modulation of host cell signaling, provide additional therapeutic rationale for the selection of norfloxacin in topical wound infection management beyond its primary bactericidal function.

2.4.4 Previous Norfloxacin Delivery Systems and their Limitations

The pharmaceutical literature reports a diverse range of nanocarrier approaches investigated for enhancing norfloxacin delivery, each with characteristic advantages and well-defined limitations.

Liposomes demonstrated improvements in skin retention relative to free drug but suffered from poor physical stability, drug leakage at physiological temperatures, and drug loading below 5% w/w for the hydrophilic zwitterionic form of norfloxacin.

Niosomes offered improved chemical stability but shared similar loading and penetration limitations.

Polymeric nanoparticles (PLGA, chitosan, albumin) and lipid-polymer hybrids improved encapsulation efficiency and release kinetics but have not been comprehensively characterised in the wound exudate environment.

Chitosan-based nanofiber dressings uniformly exhibited critical burst release exhausting the drug reservoir within 1–2 hours. SLNs represent the closest conceptual approach to the present NLC system but are critically limited by lipid polymorphism and drug expulsion during storage [24, 25].

None of the previously investigated systems has simultaneously provided amorphous drug solubilisation, wound bioadhesion, sustained above-MIC drug release, and demonstrated antibacterial efficacy against both MRSA and *P. aeruginosa*, the combination of attributes targeted by the present NFX-NLC Carbopol gel.

2.5 Nanostructured Lipid Carriers: An Evolved Lipid-Based Drug Delivery System

2.5.1 Introduction Classification of Nanocarriers and NLC Historical Evolution

Nanotechnology, the science of structures and materials at the 1–1,000 nm scale, has emerged as a transformative platform for pharmaceutical drug delivery, enabling the engineering of carrier systems with precisely controlled nanoscale dimensions, surface chemistry, and release kinetics [21, 22]. At the nanoscale, the high surface area-to-volume ratio facilitates rapid drug dissolution through amorphous drug dispersion eliminates crystalline lattice energy barriers, enhancing apparent solubility, while size-dependent biological interactions can be exploited to overcome fundamental barriers to drug absorption and therapeutic efficacy [42, 43]. Table 2.4 provides a comparative classification of the principal nanocarrier systems employed in topical drug delivery, highlighting the specific advantages that distinguish NLCs for the present application. Nanostructured lipid carriers were conceptually developed by Müller, Radtke, and Wissing in the late 1990s as a second-generation solid lipid nanoparticle platform that retains the advantages of SLNs, biocompatibility, scalability, physical stability superior to liquid nanoemulsions, and stratum corneum permeation enhancement, while fundamentally overcoming their drug loading and polymorphic instability limitations [23]. SLNs, composed entirely of physiologically compatible lipids solid at body temperature (glycerides such as Compritol® 888 ATO, Precirol® ATO 5, cetyl palmitate), suffer from well-characterised limitations: drug loading is severely constrained because drug molecules can only be accommodated in crystal imperfections and grain boundaries (typically 5–10% w/w); lipid crystal polymorphism, the thermodynamically driven conversion from metastable α and β polymorphs to the stable β polymorph, progressively reduces drug accommodation space, causing drug expulsion during storage; and the resulting burst release substantially reduces suitability for sustained drug delivery applications [24, 25].

TABLE 2.4: Classification and Comparative Properties of Principal Nanocarrier Systems for Topical Drug Delivery

Nanocarrier Type	**Matrix Composition**	**Size (nm)**	**Drug Loading**	**Release Profile**	**Key Advantage**	**Main Limitation**
Liposomes	Phospholipid bilayers	100–400	Low–moderate	Burst; pH-sensitive	Biocompatible; cell membrane-mimetic	Poor stability; drug leakage at 37°C
Niosomes	Non-ionic surfactant vesicles	100–500	Low–moderate	Sustained	Improved chemical stability vs liposomes	Limited loading for hydrophilic drugs
Polymeric NPs	PLGA, chitosan, PLA	100–400	Moderate	Sustained; pH-responsive	Versatile surface functionalisation	Organic solvents in preparation; higher cost
Dendrimers	Branched polymers	<10	Low (surface only)	Fast	Precise size; multivalent surface	Cytotoxicity; complex synthesis
SLNs	Solid lipid only	50–400	Moderate	Controlled; burst risk	Biocompatible; scalable	Polymorphic transitions; drug expulsion on storage
NLCs	Solid + liquid lipids	100–400	High	Sustained; biphasic	Amorphous drug dispersion; high loading; stable	Preparation optimisation required

Note. SLNs = solid lipid nanoparticles; NLCs = nanostructured lipid carriers; PLGA = poly(lactic-co-glycolic acid); PLA = polylactic acid.

NLC technology overcomes each of these limitations by incorporating structurally incompatible liquid lipids that prevent complete crystallisation of the matrix.

2.5.2 Structural Characteristics: The Imperfect Lipid Matrix Concept

The structural basis of NLC superiority over SLNs lies in the deliberate creation of an imperfect lipid matrix.

TABLE 2.5: Classification of NLC Structural Types with Drug Loading Mechanisms and Applications

NLC Type	**Structural Description**	**Lipid Matrix Organization**	**Drug Loading Capacity**	**Preferred Application**
Imperfect Type	Solid lipid predominates with small amounts of liquid lipid creating crystalline defects	Partially crystalline with amorphous domains; liquid lipid creates nanospaces in the crystal lattice	Moderate to high; substantially enhanced over SLN baseline	Lipophilic drugs requiring enhanced skin retention
Multiple Type	Higher liquid lipid content generating oil nanodroplets within the solid lipid matrix	Solid lipid shell encapsulating liquid oil core; nanoemulsion-within-nanoparticle architecture	High; drug partitions preferentially into oil nanodroplets	Highly lipophilic drugs; prolonged extended release

Table 2.5 continued from previous page

NLC Type	Structural Description	Lipid Matrix Organization	Drug Loading Capacity	Preferred Application
Amorphous Type	Fully amorphous solid matrix produced by lipid blends that resist crystallisation on cooling	Completely amorphous; no crystalline domains; maximum drug accommodation space; prevents drug expulsion	Highest; amorphous solubility exceeds crystalline solubility by 1.1–1.7-fold	BCS Class II/IV drugs requiring amorphous solubility enhancement; present study

Note. The present study employs an amorphous/imperfect hybrid NLC matrix using Precirol ® ATO 5 (solid lipid) and Labrafac ® WL 1349 (liquid lipid) at optimised solid-to-liquid ratios.

In a conventional SLN composed of structurally similar solid lipids (e.g., tristearin and tripalmitin), the lipid molecules pack efficiently into a well-ordered crystalline lattice with minimal free volume, excluding drug molecules from the interior. In an NLC, the introduction of a structurally disparate liquid lipid, typically a medium-chain triglyceride, an unsaturated fatty acid, or a mixed glyceride with branched or short-chain fatty acid residues such as oleic acid or caprylic/capric acid, generates spatial incompatibilities with the regular solid lipid crystal lattice. These structural incompatibilities prevent complete crystallisation, creating domains of amorphous or nanocrystalline lipid in which drug molecules are accommodated within the spaces between disordered lipid chains. The greater the structural dissimilarity between solid and liquid lipid components, the more profoundly is crystallinity disrupted and the greater the drug loading capacity and physical stability achievable.

2.5.3 Composition of the Proposed NFX-NLC Formulation

Precirol® ATO 5 (glyceryl palmitostearate) is selected as the solid lipid component on the basis of its established use in numerous published NLC formulations for topical drug delivery, its relatively low melting point (50–60°C) enabling NLC preparation at temperatures compatible with norfloxacin thermal stability, its superior norfloxacin lipid solubility compared with long-chain saturated glycerides, and its regulatory acceptability as a GRAS-designated pharmaceutical excipient [25, 44]. Labrafac® WL 1349 (caprylic/capric triglycerides) is selected as the liquid lipid on the basis of its structural incompatibility with Precirol ATO 5, which generates the imperfect matrix required for enhanced drug loading, its widely reported use in Precirol-based NLC formulations, and its demonstrated ability to solubilise norfloxacin in the liquid lipid phase. Transcutol® P (diethylene glycol monoethyl ether) serves the dual function of drug solubiliser , substantially increasing norfloxacin's apparent solubility in the lipid phase and improving encapsulation efficiency , and permeation enhancer that modifies stratum corneum hydration and lipid organisation to facilitate transcutaneous drug transport [11, 45].

2.5.4 Mechanisms of Drug Release from NLCs

Drug release from NLC formulations proceeds through multiple simultaneous mechanisms whose relative contributions depend upon lipid matrix composition, degree of crystallinity, and the environmental conditions at the site of application [28, 46]. Diffusion-controlled release, described by Fickian diffusion theory, occurs as drug molecules dissolved in the NLC lipid matrix diffuse down their concentration gradient through the lipid core to the lipid-water interface, where they partition into the aqueous phase and become available for biological activity. Surface desorption contributes an initial rapid release component from weakly adsorbed drug at the NLC surface, a burst phase that may be beneficial for initiating rapid antibacterial activity.

Table 2.6: Composition of the NFX-NLC Formulation: Excipient Roles and Selection Justification

Component	**Chemical Identity**	**Functional Role**	**Concentration Range**	**Key Property**	**Regulatory Status**
Precirol® ATO 5	Glyceryl palmitostearate (C16/C18 mixed glycerides)	Solid lipid matrix former	3–8% w/w	Melting point 50–60°C; excellent norfloxacin lipid solubility	GRAS; pharmacopoeial excipient
Labrafac® WL 1349	Medium-chain triglycerides (C8/C10 caprylic/capric esters)	Liquid lipid; crystallinity disruptor	1–3% w/w	Structural incompatibility with Precirol generates imperfect matrix	GRAS; widely used in topical formulations
Transcutol® P	Diethylene glycol monoethyl ether (DGME)	Co-surfactant; drug solubiliser; permeation enhancer	2–5% w/w	Enhances norfloxacin lipid-phase solubility; promotes SC hydration and partitioning	Pharmacopoeial; GRAS-designated
Tween® 80	Polysorbate 80 (polyoxyethylene sorbitan monooleate)	Primary surfactant; emulsifier; particle stabiliser	1.5–3% w/w	HLB 15; excellent O/W emulsification; prevents nanoparticle aggregation	GRAS; pharmacopoeial

Table 2.6 continued from previous page

Component	Chemical Identity	Functional Role	Concentration Range	Key Property	Regulatory Status
Poloxamer 188	Polyoxyethylene-polyoxypropylene block copolymer	Co-surfactant; steric stabiliser	0.5–1.5% w/w	PEO chains provide steric stabilisation; prevents Ostwald ripening	GRAS; widely used stabiliser
Carbopol® 940	Crosslinked polyacrylic acid (Carbomer 940)	Gel former; bioadhesive agent	0.3–0.9% w/w	Pseudoplastic rheology; wound bioadhesion; transparent gel; pH-sensitive gelation	FDA GRAS; pharmacopoeial

Note. GRAS = generally recognised as safe; HLB = hydrophile-lipophile balance; SC = stratum corneum.

Matrix erosion by tissue lipases at the wound surface provides a third mechanism of therapeutic relevance, progressively exposing encapsulated drug in a degradation-rate-dependent manner.

The Korsmeyer-Peppas power law relates cumulative drug release to a release exponent n: $n \leq 0.43$ indicates Fickian diffusion; $0.43 < n < 0.85$ indicates anomalous (non-Fickian) transport combining diffusion with matrix relaxation or erosion; $n \geq 0.85$ indicates Case II erosion-controlled transport [28]. NLC formulations incorporating lipophilic or poorly water-soluble drugs typically exhibit anomalous transport ($n = 0.5$–0.7), consistent with the dual-barrier mechanism of lipid core diffusion followed by Carbopol gel network retardation.

2.5.5 Skin Permeation Enhancement by NLCs

The molecular mechanisms by which NLCs enhance transcutaneous drug permeation are multifactorial. At the stratum corneum-formulation interface, NLC lipid components interact with the lamellar lipid bilayers of the stratum corneum through lipid exchange and partial miscibility, introducing the liquid lipid component (medium-chain triglycerides) into the highly ordered ceramide-rich lamellae. This lipid intercalation perturbs the crystalline lipid phase organisation, increasing bilayer fluidity and transiently reducing the diffusional resistance of the stratum corneum to drug permeation, an effect that is reversible and dose-dependent, providing enhancement without permanent barrier disruption [11]. Application of lipid nanoparticle formulations additionally creates an occlusive film that reduces transepidermal water loss, increasing stratum corneum hydration and expanding the aqueous pore pathways that represent the principal transcutaneous route for polar drugs. Hair follicles provide a third and distinct permeation pathway: NLC particles in the 100–400 nm size range preferentially accumulate in hair follicle ostia by a physical funnel effect driven by the cyclical hair movement cycle, delivering drug to the dermal compartment at 1–2 mm depth and bypassing the interfollicular stratum corneum entirely [11, 45]. The combination of these three mechanisms, lipid exchange, occlusive hydration, and follicular shunt penetration,

collectively generates the enhanced flux demonstrated for NLC formulations in *ex vivo* Franz diffusion cell studies.

2.5.6 Carbopol 940 as the Gel Matrix for NLC Integration

The incorporation of norfloxacin-loaded NLCs into a semisolid Carbopol 940 gel matrix addresses the fundamental limitation of liquid NLC dispersions for topical wound application: inadequate wound residence time [26, 27]. Carbopol 940, a high-molecular-weight crosslinked polyacrylic acid homopolymer (MW ∼4,000 kDa; crosslinked with allyl sucrose at ∼1–2% w/w), forms clear, highly viscous gels at concentrations of 0.1–2.0% w/w upon neutralisation with triethanolamine (pKa ∼4.5-5), converting -COOH to -COO groups whose electrostatic repulsion extends polymer chains and dramatically increases network mesh density and hydrodynamic volume [26].

Carbopol 940 gels exhibit pseudoplastic (shear-thinning) behaviour with thixotropic recovery, the rheological profile ideally suited for topical wound application. Under low-shear conditions, high viscosity prevents gravitational displacement from wound surfaces; application shear reduces viscosity for uniform distribution with minimal discomfort; and rapid viscosity recovery after shear cessation restores wound retention. Bioadhesion, arising from hydrogen bonds and van der Waals forces between polyanionic carboxylate groups and wound-surface glycoproteins, provides the sustained formulation-wound contact essential for drug delivery in the dynamic wound environment, an adhesive performance reported to exceed that of HPMC, HEC, and carbomer 934P at equivalent concentrations [**?**]. Incorporation of the NLC dispersion into the Carbopol gel matrix additionally prevents nanoparticle aggregation and sedimentation, ensuring uniform dose distribution throughout the product shelf-life. The dual NLC-gel release system generates a biphasic drug release profile: initial burst from NLC surface drug providing rapid antibacterial activity, followed by sustained release from the lipid core retarded further by the Carbopol gel network, maintaining above-MIC concentrations over clinically relevant periods [28, 46].

2.6 Previous NLC-Based Topical Gels for Anti-Infective and Wound Healing Applications

The application of NLC gel systems to topical anti-infective and wound healing drug delivery has been explored across several drug classes, collectively establishing the platform feasibility and clinical potential of the Carbopol 940-NLC gel approach [21, 47]. Table 2.7 summarizes the most directly relevant published formulation studies, providing a structured comparison of NLC composition, gel base, key outcomes, and the specific limitations or gaps that distinguish each study from the present investigation.

Among the most directly relevant published studies is the work of Zafar and colleagues, who developed and characterised erythromycin-loaded NLC gel formulations using Precirol ATO 5 as solid lipid, oleic acid as liquid lipid, and Carbopol 940 as the gel former , the same principal excipient combination adopted in the present study , demonstrating significantly enhanced skin retention, drug release kinetics, and zone of inhibition against *S. aureus* relative to plain erythromycin gel [47]. This study provides direct experimental precedent for the antibacterial performance enhancement achievable through the Carbopol 940-NLC platform. Joshi and Patravale's gatifloxacin nano lipid carrier system for ophthalmic delivery [48] is mechanistically relevant as a precedent for fluoroquinolone-specific NLC encapsulation advantages , enhanced fluoroquinolone solubilisation in the lipid matrix, sustained release, and superior antibacterial efficacy , directly applicable to norfloxacin as a structurally related first-generation fluoroquinolone. Lohan and Bhatia's amphotericin B NLC gel [19], employing the identical Precirol ATO 5/Labrafac WL 1349 excipient combination as the present study, demonstrated a 3.2-fold enhancement in skin permeation relative to plain drug gel, providing the closest compositional precedent in the published literature. The absent category in the published NLC gel literature is norfloxacin itself, specifically, a norfloxacin NLC gel evaluated against all four principal wound pathogens at multiple dose levels, *ex vivo* skin permeation at both physiologically relevant pH conditions, and ICH-compliant stability under accelerated tropical conditions.

TABLE 2.7: Representative Published NLC-Based Topical Gel Formulations for Anti-Infective and Wound Healing Applications

Reference Drug	NLC Composition	Gel Base	Key Outcome	Limitation / Gap Relative to Present Study
Zafar et al. (2022) [47]	Erythromycin Stearic acid (solid lipid), Oleic acid (liquid lipid), Pluronic F127 (surfactant)	Carbopol 940 + Chitosan blend (pH-sensitive in situ gel)	Particle size 169.6 ± 4.8 nm; EE 81.7 ± 1.4%; 1.51-fold enhanced permeation flux vs plain drug gel; sustained release >24 h; superior ZOI against *S. aureus* and *E. coli*	Ophthalmic (bacterial conjunctivitis) application, not topical wound delivery; no evaluation against MRSA or *P. aeruginosa*; no *ex vivo* skin permeation at wound-bed pH 7.4; no ICH Q1A(R2) Zone IVb accelerated stability data

Table 2.7 continued from previous page

Reference	Drug	NLC Composition	Gel Base	Key Outcome	Limitation / Gap Relative to Present Study
Mahdi et al. (2021) [49]	Butenafine HCl	Compritol 888 ATO (solid lipid), Labrasol (liquid lipid), Tween 80 (surfactant); Box Behnken design optimisation	Carbopol 934 (1% w/v)	Particle size 111 nm; EE 86.35%; prolonged drug release 65.09% ± 4.37%; drug permeation 641.37 ± 46.59 μ g (3.2-fold vs conventional gel); negligible irritation score (0.17); superior antifungal ZOI at both 12 h and 24 h	Antifungal application only; no antibacterial wound pathogen evaluation; no MRSA or *P. aeruginosa* data; no dual-pH (5.5 / 7.4) *ex vivo* skin permeation; no wound bioadhesion characterisation; Carbopol 934 base, not Carbopol 940

Table 2.7 continued from previous page

Reference Drug	NLC Composition	Gel Base	Key Outcome	Limitation / Gap Relative to Present Study
Shettigar et al. (2021) [50]	Clarithromycin Precirol ATO 5 (solid lipid), Capryol 90 (liquid lipid), Tween 80 (surfactant)	Carbopol 934P (0.5% w/v)	Particle size 164.8 nm; ZP - 39.2 mV; EE 88.16%; improved sustained-release kinetics (diffusion-controlled); *ex vivo* permeation 89.5% vs marketed gel 65%; enhanced anti-acne efficacy	Limited to Cutibacterium acnes (acne vulgaris); no evaluation against MDR wound pathogens (MRSA, *P. aeruginosa*); no ZOI interpretation against CLSI M100 susceptibility breakpoints; no ICH Q1A(R2) stability under tropical conditions (40 °C/75% RH); no dual-pH permeation

Table 2.7 continued from previous page

Reference	Drug	NLC Composition	Gel Base	Key Outcome	Limitation / Gap Relative to Present Study
Joshi et al. (2023) [51]	Gatifloxacin (4th-generation fluoroquinolone)	Compritol 888 ATO and Precirol ATO 5 (solid lipids), Tween 80, Poloxamer 407 (surfactants); hot homogenisation + probe sonication	HPMC-based in situ ophthalmic gel	Particle size <200 nm; enhanced corneal drug levels and transcorneal permeation vs commercial GTX eye drops; superior ZOI against *S. aureus* and *P. aeruginosa*; improved precorneal retention; sustained ocular release	Ophthalmic delivery, not topical cutaneous wound application; no *ex vivo* skin permeation through stratum corneum at any pH; 4th-generation fluoroquinolone with distinct resistance profile from 1st-generation norfloxacin; no MRSA susceptibility profiling; no ICH wound-relevant stability

Table 2.7 continued from previous page

Reference	Drug	NLC Composition	Gel Base	Key Outcome	Limitation / Gap Relative to Present Study
Lohan & Bhatia (2025) [52]	Amphotericin B (BCS Class IV)	Beeswax (solid lipid), liquid lipid phase; microwave-assisted synthesis; Tween 80	Carbopol 934 (bioadhesive gel)	Particle size 180 nm; PDI 0.32; ZP-28.8 mV; significantly enhanced *ex vivo* skin permeation vs plain drug gel; controlled biphasic release; skin biocompatibility confirmed by histopathology; improved drug stability	Antiparasitic/antifungal application (cutaneous leishmaniasis); not antibacterial; no evaluation against MRSA or *P. aeruginosa*; no dual-pH *ex vivo* permeation; Carbopol 934 (not 940); distinct NLC excipient system from present study; no ICH Zone IVb stability

Table 2.7 continued from previous page

Reference	Drug	NLC Composition	Gel Base	Key Outcome	Limitation / Gap Relative to Present Study
Present Study	Norfloxacin (BCS Class IV)	Precirol ATO 5 (solid lipid), Labrafac WL 1349 (liquid lipid), Tween 80, Poloxamer 188 (surfactants), Transcutol P (co-surfactant / permeation enhancer)	Carbopol 940 (0.3%, 0.6%, 0.9% w/w); three gel strengths evaluated	Broad-spectrum topical wound antibacterial activity against *S. aureus* ATCC 6538, MRSA ATCC 43300, *E. coli* ATCC 25922, and *P. aeruginosa* ATCC 27853 by agar well diffusion at 2.5, 5, and 10 mg dose levels; ZOI interpreted against published norfloxacin susceptibility thresholds (susceptible $\geq$ 17 mm, intermediate 13 -16 mm, resistant $\leq$ 12 mm); dual-pH *ex vivo* permeation (pH 5.5 and 7.4) via Franz static diffusion cells; ICH Q1A(R2)-compliant accelerated stability at 40 °C/75% RH (Zone IVb)	First study integrating NFX-NLC into Carbopol 940 gel; first to simultaneously demonstrate susceptible-range ZOI against MRSA and *P. aeruginosa* from a norfloxacin NLC topical formulation; first dual-pH *ex vivo* skin permeation and quantified enhancement ratio (ER) for norfloxacin NLC gel; first ICH Zone IVb stability dataset for this formulation class

Note. ZOI = zone of inhibition; CLSI = Clinical and Laboratory Standards Institute; API = active pharmaceutical ingredient; MRSA = methicillin-resistant *S. aureus*; MDR = multidrug-resistant.

No published study has simultaneously demonstrated susceptible-range antibacterial activity against MRSA and *P. aeruginosa* from a norfloxacin topical formulation, the most clinically important and therapeutically recalcitrant organisms in the chronic wound infection landscape. The present study directly and comprehensively addresses each of these gaps.

2.7 Literature Gap and Rationale of the Present Study

2.7.1 Summary of Identified Literature Gaps

A systematic review of the published literature on norfloxacin topical delivery, NLC-based anti-infective formulations, and Carbopol gel systems for wound management identifies six specific, well-defined gaps that collectively provide the scientific justification for the present study.

First, no published study has developed, characterised, or evaluated a norfloxacin-loaded NLC incorporated into a Carbopol 940 gel matrix for topical wound healing applications [21, 47]. Norfloxacin has been investigated in SLN, polymeric nanoparticle, liposomal, and chitosan-based nanofiber systems, but the NLC-Carbopol 940 gel combination, which uniquely offers amorphous drug dispersion (overcoming the BCS Class IV crystalline solubility barrier), lipid-mediated stratum corneum permeation enhancement (overcoming the low-permeability barrier), bioadhesive wound retention, and sustained controlled release , has not been reported in the published pharmaceutical literature.

Second, existing norfloxacin delivery systems have not been systematically evaluated against all four principal wound pathogens, *S. aureus* (ATCC 6538), MRSA

(ATCC 43300), *E. coli* (ATCC 25922), and *P. aeruginosa* (ATCC 27853), at multiple dose levels with rigorous ZOI-based susceptibility profiling. Dave et al. [53] developed norfloxacin-loaded lipid-polymer hybrid nanoparticles for topical burn wound therapy and confirmed retained antimicrobial efficacy against *S. aureus* and *P. aeruginosa*. Mohammed et al. [54] formulated positively charged norfloxacin-loaded lipid-polymer hybrid nanoparticles in gel form and demonstrated enhanced antibacterial activity against *S. aureus*, and *P. aeruginosa*.

El-Saghier et al. [55] screened norfloxacin and its analogues using the agar cup diffusion method against *S. aureus* (ATCC 6538), *E. coli* (ATCC 25923), *K. pneumoniae* (ATCC 10031), and *P. aeruginosa* (ATCC 27853), reporting norfloxacin MIC values of 7.83 µM against *S. aureus* and 1.96 µM against MRSA; however, these work did not involve a drug delivery system or topical gel formulation.

No study to date has integrated NFX-NLC into a Carbopol gel system and simultaneously assessed susceptibility across all four wound pathogens including MRSA at multiple dose levels, representing the primary novelty of the present work.

Third, comprehensive *ex vivo* skin permeation data at both pH 5.5 and pH 7.4 receptor conditions are absent for any norfloxacin NLC gel formulation [56, 57]. This dual-pH permeation evaluation is pharmacokinetically critical: the cationic norfloxacin species predominant at pH 5.5 (piperazinyl protonation, pKa = 6.35) exhibits substantially higher aqueous solubility than the minimum-solubility zwitterion at pH 7.4, generating a larger concentration gradient and consequently superior transcutaneous flux at the primary topical application condition. No published study has quantified this pH-dependent permeation advantage for norfloxacin NLC formulations or established its pharmacokinetic significance for wound-site drug delivery.

Fourth, stability data under ICH Q1A(R2) accelerated storage conditions (40°C/75% RH, Pakistan's Zone IVb climate) are absent for norfloxacin NLC gel formulations [58]. Without such data, no regulatory submission for clinical use in tropical climates is feasible, and the long-term physical and chemical integrity of NLC formulations under relevant storage conditions cannot be established.

Fifth, no comparative evaluation has established the pharmacokinetic value-added contribution of NLC encapsulation versus plain norfloxacin Carbopol gel in the wound healing context, leaving clinicians and formulators without evidence-based guidance for selecting between NLC and conventional gel options. The enhancement ratio (ER = Jss,NLC-gel / Jss,plain-gel) at clinically relevant pH conditions is a particularly important metric for which published data are unavailable.

Sixth, the characterisation of norfloxacin-loaded NLC gels by DSC, XRD, and FTIR in combination, the methodological triad required to confirm amorphous drug dispersion, assess lipid crystallinity reduction, and establish drug-excipient chemical compatibility , has not been reported for this drug-excipient system, leaving the physicochemical basis for any NLC-mediated performance advantage unestablished.

2.7.2 Rationale and Justification for the Present Formulation Strategy

The scientific rationale for the present study rests upon the convergence of three independently compelling lines of evidence. First, the unambiguous clinical significance of wound infections caused by the four target organisms, *S. aureus* (ATCC 6538), MRSA (ATCC 43300), *E. coli* (ATCC 25922), and *P. aeruginosa* (ATCC 27853) , and the demonstrably inadequate performance of all currently available topical antimicrobial formulations in managing these infections with the sustained, penetrating drug delivery that resistant organisms require. Second, the well-established pharmacological basis for norfloxacin's broad-spectrum bactericidal activity against precisely these wound pathogens, combined with its BCS Class IV physicochemical characteristics that conventional topical formulations are structurally incapable of overcoming. Third, the mechanistic, *in vitro*, and *ex vivo* evidence base demonstrating that NLC-mediated encapsulation consistently enhances apparent solubility, stratum corneum permeation, and sustained controlled release of poorly soluble drugs , a body of evidence directly applicable to the present formulation strategy [19, 21, 22, 47].

NLCs are justified over alternative nanocarrier platforms on the basis of their unique combination of attributes: high drug loading for BCS Class IV molecules through amorphous lipid matrix drug dispersion; physical and chemical stability over storage periods and temperature conditions relevant to clinical use in tropical Pakistan; intrinsic biocompatibility of physiological glyceride lipid components with the wound healing environment; lipid composition-mediated stratum corneum permeation enhancement; and scalable manufacture using hot homogenisation followed by ultrasonication. All NLC components, Precirol ATO 5, Labrafac WL 1349, Tween 80, Poloxamer 188, Transcutol P, and Carbopol 940 , are GRAS-designated or pharmacopoeially established excipients with extensive pharmaceutical safety profiles, providing a regulatory-compliant excipient selection that facilitates eventual clinical translation. Carbopol 940 is justified over alternative hydrophilic gelling agents (HPMC, HEC, carbomer 934P) on the basis of its superior bioadhesive properties, pseudoplastic rheological profile, optical transparency enabling wound inspection through the applied gel, and demonstrated biocompatibility with wound healing processes [27, 36, 59].

The proposed NFX-NLC Carbopol 940 gel exploits the complementary and synergistic advantages of lipid nanoencapsulation and bioadhesive gel-based topical delivery. The NLC component provides norfloxacin solubilisation through amorphous dispersion, sustained release through matrix diffusion, and stratum corneum permeation enhancement through lipid exchange and follicular penetration. The Carbopol 940 gel matrix provides wound bioadhesion extending contact time, physical NLC stabilisation preventing aggregation, an additional release-retarding diffusion barrier, pseudoplastic application characteristics, and patient acceptability. Together, these components are designed to deliver norfloxacin at sustained concentrations exceeding the MIC of all four target organisms at the wound site over clinically relevant periods, an outcome that is demonstrably unachievable with conventional norfloxacin gel formulations and that constitutes the novel, clinically significant contribution of the present thesis to the topical anti-infective formulation literature.

Chapter 3

Materials and Methods

3.1 Materials

Norfloxacin (purity $\geq$ 98%) was acquired from OBS Pakistan (Pvt), Ltd. The solid lipid Precirol® ATO 5 (glyceryl palmitostearate) and liquid lipid Labrafac® WL 1349 (medium-chain triglycerides) were generously supplied by Gattefosse (France).

The co-surfactant and permeation enhancer used was Transcutol® P (diethylene glycol monoethyl ether) which was purchased from Gattefossé.

The nonionic surfactants used were Tween 80 (polysorbate 80) and Poloxamer 188, which were bought from Merck (Germany). The gelling agent used was Carbopol 940 (crosslinked polyacrylic acid polymer) which was purchased from Lubrizol (USA).

Triethanolamine and NaOH (sodium hydroxide) were purchased from Merck (Germany) as pH adjustors. Solvents used were acetic acid, absolute ethanol and distilled water.

All additional chemicals and reagents were of analytical grade and utilized without further purification.

3.2 Preparation of Norfloxacin-Loaded Nanostructured Lipid Carriers

The Norfloxacin loaded NLCs were formulated by the hot homogenization and ultrasonication technique which is a well-established procedure for preparing nanoscale lipid dispersions with narrow size distribution and high EE [60]. The solid and liquid lipids (Precirol® ATO 5, glyceryl palmitostearate and Labrafac® WL 1349, medium-chain triglycerides, respectively) were precisely weighed in determined proportions and then melted in a water bath over 75–80°C (about 10°C above the melting point of the solid lipid). Next, norfloxacin was dissolved in the molten lipid phase by continuous magnetic stirring with a speed of 500 rpm until it was transparent and homogeneous. Then the lipid melt was added to Transcutol® P (diethylene glycol monoethyl ether) to improve the drug solubilization and better the interfacial properties of the lipid matrix [61]. Meanwhile, the aqueous phase was also prepared by dissolving the nonionic surfactants, Tween 80 and Poloxamer 188, in distilled water and heated to 75 to 80°C to prevent solidification of the mixture due to the premature solidification of the nonionic surfactant. In order to create a coarse oil-in-water emulsion, the hot aqueous surfactant solution was subsequently introduced dropwise to the molten lipid phase under high-shear homogenization using a high-speed homogenizer (IKA T25 digital Ultra-Turrax, Germany) at 10,000–15,000 rpm for two to three minutes. The resulting coarse emulsion was immediately subjected to ultrasonication (QSonica Q700, USA) at 70% amplitude with 10-second on/off cycles for 5–15 minutes to reduce the droplet size to the nanometer range and ensure uniform dispersion [62]. The hot nanoemulsion was then rapidly cooled by immersion in an ice bath under continuous magnetic stirring at 500 rpm for 30 minutes to promote recrystallization of the lipid phase and formation of solidified nanostructured lipid carriers. The obtained NLC dispersion was stored in airtight amber glass vials at 25°C until further characterization. Blank NLCs were prepared without incorporation of drug using the same process [63]. A total of thirteen NLC formulations (F1–F13) were prepared by systematically varying the independent formulation parameters,

including total lipid concentration (3–7% w/w), solid-to-liquid lipid ratio (50:50 to 90:10), surfactant concentration (0.5–2.5% w/v), Transcutol P content (10–30% v/v), homogenization speed (8,000–20,000 rpm), and processing time (5–15 min). The detailed composition of all formulations is presented in Table 3.1.

TABLE 3.1: Composition of Norfloxacin NLC Formulations (F1–F13)

Form.	**Lipid (% w/w)**	**Precirol: Labrafac (Solid: Liquid)**	**Surfactant (% w/v)**	**Transcutol P (% v/v)**	**Homog. Speed (rpm)**	**Time (min)**
F1	5	70:30	1.5	30	12,000	10
F2	3	70:30	1.5	30	12,000	10
F3	7	70:30	1.5	30	12,000	10
F4	5	50:50	1.5	30	12,000	10
F5	5	90:10	1.5	30	12,000	10
F6	5	70:30	0.5	30	12,000	10
F7	5	70:30	2.5	30	12,000	10
F8	5	70:30	1.5	10	12,000	10
F9	5	70:30	1.5	20	12,000	10
F10	5	70:30	1.5	30	8,000	10
F11	5	70:30	1.5	30	20,000	10
F12	5	70:30	1.5	30	12,000	5
F13	5	70:30	1.5	30	12,000	15

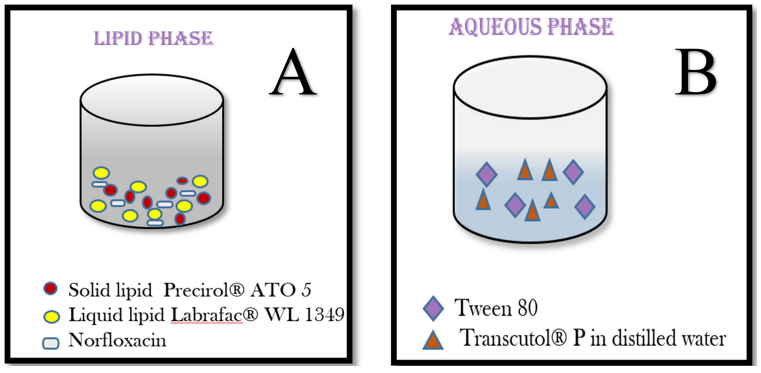

FIGURE 3.1: Preparation of Lipid Phase (A) and Aqueous Phase (B)

3.3 Characterization of Norfloxacin-Loaded NLCs

3.3.1 Particle Size, Polydispersity Index, and Zeta Potential

Dynamic light scattering (DLS) was executed using a Zetasizer Nano ZS (Malvern Instruments, UK) to determine the mean particle size, polydispersity index (PDI) and zeta potential of the prepared NLC formulations. Samples were diluted with filtered distilled water (1:100 v/v) as necessary to prevent multiple scattering and allowed to equilibrate at 25°C for 2 minutes before measuring. The results of particle size and PDI gave an idea of the size of the nanoparticles and the homogeneity of the size distribution, while the results of zeta potential on the surface charge and the stability of the nanoparticles as a colloidal system. All measurements were performed in triplicate (n = 3), and results were expressed as mean ± standard deviation (SD) [64].

3.3.2 Encapsulation Efficiency

The encapsulation efficiency of norfloxacin in NLCs was determined using an ultracentrifugation method. A known volume of NLC dispersion (1 mL) was placed in ultracentrifuge tubes and centrifuged at 15,000 rpm for 30 minutes at 4°C (Beckman Coulter Optima XPN-100, USA) to separate the drug-loaded nanoparticles from the unentrapped free drug. The supernatant containing the free drug was carefully collected and filtered through a 0.45 μm membrane filter (Millipore, USA). The concentration of free norfloxacin in the supernatant was determined spectrophotometrically at λmax = 273 nm using a UV-Vis spectrophotometer (Shimadzu UV-1800, Japan) against a blank NLC supernatant as reference [65].

The %EE was calculated using the following equation 3.1:

$$\%EE = \frac{\text{Total drug added} - \text{Free drug in supernatant}}{\text{Total drug added}} \times 100 \qquad (3.1)$$

All measurements were performed in triplicate (n = 3), and results were expressed as mean ± standard deviation (SD) [66].

3.3.3 Scanning Electron Microscopy

The surface morphology and shape of the optimized norfloxacin-loaded NLCs were examined using scanning electron microscopy (SEM, JEOL JSM-6490LA, Japan) [67]. A small drop of NLC dispersion was placed on a carbon-coated copper grid, air-dried at room temperature, and sputter-coated with gold under argon atmosphere using a sputter coater (SC7620, Quorum Technologies, UK) to render the samples conductive. The samples were then imaged at an accelerating voltage of 15 kV at various magnifications (1,000× to 100,000×). The micrographs were analyzed for particle shape, surface characteristics, and the existence or absence of crystalline drug deposits.

3.3.4 Differential Scanning Calorimetry

DSC analysis was performed using a differential scanning calorimeter (DSC 8500, PerkinElmer, USA) to investigate the crystalline behavior of lipids and possible drug-excipient interactions. Samples of pure norfloxacin, pure Precirol ATO 5, blank NLCs (without drug), and optimized norfloxacin-loaded NLCs were accurately weighed (5–10 mg) and sealed in aluminum pans. The analysis was conducted under nitrogen purge (20 mL/min) at a heating rate of 10°C/min over a temperature range of 25–300°C. An empty sealed aluminum pan served as reference. Thermograms were obtained and analyzed for variation in the melting endotherm, peak temperature and enthalpy values with the help of Pyris Software (PerkinElmer). The changes in the melting endotherms suggested the incorporation of drugs in the lipid matrix and possible solid-state modifications [68].

3.3.5 Fourier Transform Infrared Spectroscopy

FTIR spectroscopy was used to evaluate potential chemical interactions between norfloxacin and excipients in the optimized formulation. Pure norfloxacin, individual excipients, blank NLCs, and drug-loaded NLCs were analyzed directly without prior sample preparation. Each sample was placed onto the diamond attenuated total reflectance (ATR) crystal of the FTIR spectrophotometer (Bruker Tensor II, Germany) and firmly pressed to ensure optimal contact. Spectra were recorded in ATR mode over the wavenumber range of 4000–400 cm^{-1} at a resolution of 4 cm^{-1} with 32 scans per sample. The characteristic absorption peaks of norfloxacin were analyzed for any shifts, broadening, disappearance, or appearance of new peaks indicative of chemical interactions between the drug and the lipid matrix [20].

3.3.6 X-Ray Diffraction

X-ray diffraction analysis was performed using an X-ray diffractometer (Bruker D8 Advance, Germany) with Cu Kα radiation ($\lambda = 1.54$ Å) at 40 kV and 30 mA to assess the crystalline or amorphous nature of pure norfloxacin, pure Precirol ATO 5, blank NLCs, and optimized drug-loaded NLCs. Samples were scanned throughout a 2θ range of 10–80° at a scanning speed of 2°/min at room temperature in a flat sample holder with a uniform surface. The diffractograms were compared to identify alterations in characteristic diffraction peaks, peak intensities, or peak broadening that may indicate a transition from crystalline to amorphous state following drug incorporation into the lipid matrix [69, 70].

3.3.7 *In Vitro* Drug Release and Release Kinetics

The *in vitro* release profile of norfloxacin from the NLC formulations was determined using the dialysis bag diffusion method. A known volume of NLC dispersion (2 mL, equivalent to 6 mg norfloxacin) was placed inside a pre-soaked dialysis membrane (MWCO 12–14 kDa, Sigma-Aldrich, USA) and sealed securely. The dialysis

bag was immersed in 100 mL of phosphate buffer (pH 7.4) and acetate buffer (pH 5.5) maintained at 37 ± 0.5°C with constant magnetic stirring at 100 rpm. After a set period of time (0.5, 1, 2, 4, 6, 8, 12, 16, 20, and 24 h), 2 mL aliquots were removed from the receptor medium and replaced with fresh pre-equilibrated receptor medium to preserve the sink conditions.

Norfloxacin in withdrawn samples was measured spectrophotometrically at the wavelength of maximum absorbance value (λmax) of 273 nm [47].

The drug release kinetics were studied by fitting the release data to four mathematical models namely zero order, first order, Higuchi model and Korsmeyer–Peppas model.

The model which showed the highest correlation coefficient (R^2) was determined as the best fit model and the release mechanism was interpreted based on the diffusion exponent (n) obtained from the Korsmeyer–Peppas model, where $n \leq 0.45$ specified Fickian diffusion, $0.45 < n < 1.0$ indicated anomalous (non-Fickian) transport, and $n = 1.0$ indicated Case II (relaxation-controlled) transport [71].

3.4 Preparation of Norfloxacin-Loaded NLC Gel

The optimized norfloxacin-loaded NLC dispersion was incorporated into Carbopol 940 hydrogel to produce a semi-solid topical formulation with enhanced bioadhesive properties and prolonged skin contact time. Three gel formulations were prepared using varying concentrations of Carbopol 940 (0.3%, 0.6%, and 0.9% w/w) to determine the optimal polymer concentration for desired rheological properties and wound compatibility.

Briefly, accurately weighed Carbopol 940 was dispersed slowly in distilled water at room temperature under continuous magnetic stirring at 100 rpm for 3 hours to ensure complete hydration and polymer swelling.

The hydrated dispersion was then left overnight at 4°C to remove entrapped air bubbles and achieve complete polymer network formation.

A dispersion of the prepared NLC was then added dropwise to the prepared hydrated Carbopol dispersion under magnetic stirring at 100 rpm for 30 minutes to ensure the homogeneity of the dispersion.

Then the mixture was neutralized to pH 5.5–6.0 by dropwise addition of triethanolamine (0.5 mL) under gentle stirring to induce gelation and provide the final gel consistency.

Appropriate amounts of 0.1 M NaOH or 0.1 M acetic acid were added to adjust the pH to the wound compatible range (5.5–6.5). The gels were then prepared and allowed to equilibrate for 30 minutes at 2–8°C to ensure that the gels were uniform and stable.

The optimized NLC gel with 0.3% of Carbopol 940 was chosen for further characterization due to optimum viscosity and spreadability. A plain norfloxacin gel (without NLC encapsulation) was prepared by dispersing the same amount of free norfloxacin in Carbopol 940 gel using the same method. All the gel formulation were kept in sealed containers at room temperature for characterization [72].

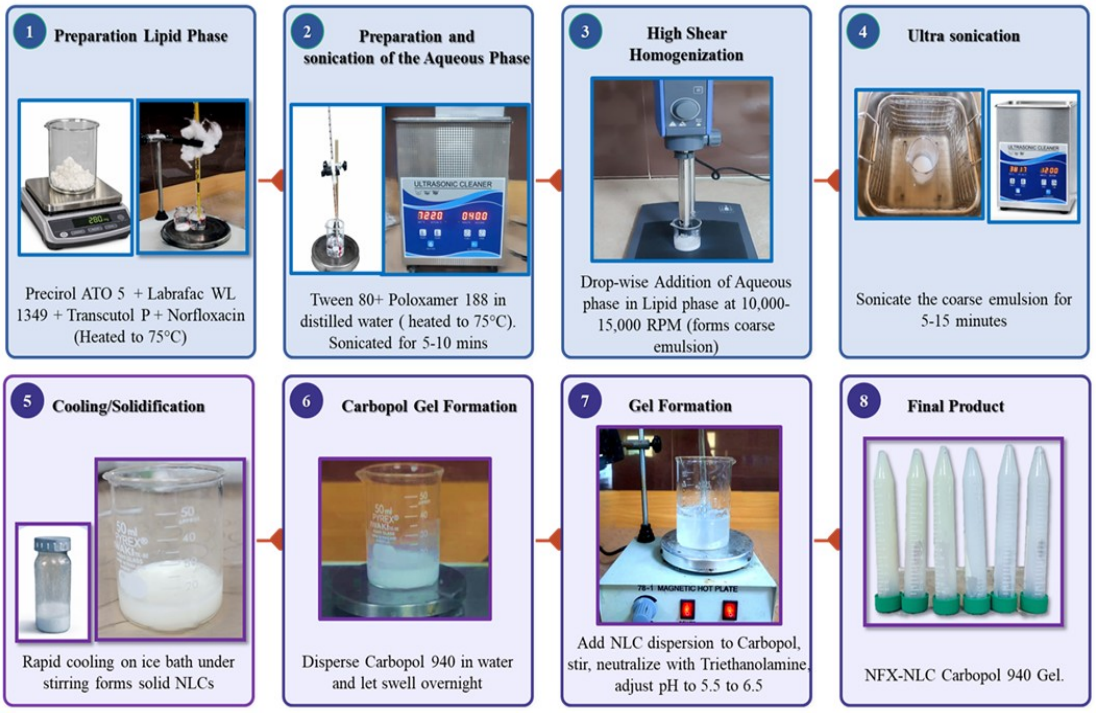

FIGURE 3.2: Schematic diagram of the preparation of NFX loaded NLC based Carbopol Gel

3.5 Characterization of Norfloxacin-Loaded NLC Gel

3.5.1 Physical Appearance pH Viscosity and Spreadability

The physical appearance of the prepared gel formulations was visually evaluated against white and black background for consistency, texture, homogeneity and color uniformity. A small quantity of gel was rubbed between the thumb and forefinger to assess smoothness and also see if there was any grittiness and/or particulate matter present [73].

Gel formulations pH was determined by dispersing 250 mg of gel in 50 mL distilled water and the pH value was measured at room temperature using calibrated digital pH meter (Mettler Toledo FE20, Switzerland). Measurements were taken in triplicate and expressed as Mean ± SD [50]. The viscosity was measured at different speeds of rotation (0.5 to 100 rpm) using a Brookfield DV-II Pro viscometer (Brookfield Engineering, USA) fitted with spindle S64 at 25°C to determine the shear-thinning (pseudoplastic) behavior. The viscosity data was fitted to the power law model ($\tau = K\gamma^n$) and flow index (n) values were calculated. All measurements were done three times (n = 3) [74].

Spreadability was measured by horizontal glass plate method. Then about 1 g of gel was poured on a glass plate (diameter: 2 cm) marked, and the other glass plate weighing 50 g was carefully laid on the glass plate and kept for 5 minutes. Changes in diameter were measured due to spreading and spreadability (g·cm/s) was calculated according to the following formula:

$$\text{Spreadability} = \frac{M \times L}{T} \tag{3.2}$$

where M is the weight applied (50g), L is the spread diameter (cm) and T is the time required for separation [75].

Extrudability was measured by exerting equal pressure on collapsible tubes containing gel and determining the pressure required to extrude 1g of gel (g/cm^2). All measurements were carried out in triplicate (n = 3), and the data are presented as the mean ± standard deviation (SD) [49].

3.5.2 Drug Content Uniformity

The amount of drug in the gel formulations was determined by dissolving accurately weighed gel (100mg) in 100mL phosphate buffer pH 7.4, which was continuously stirred for 4 hours to extract the drug completely. After filtering the mixture through a 0.45 μm membrane filter, the norfloxacin concentration was determined using spectrophotometry at λmax=273 nm. The drug content was determined using the theoretical drug loading %. The measurements were performed in triplicate (n = 3) and reported as mean ± SD [76, 77].

3.5.3 *Ex Vivo* Skin Permeation Study

The *ex vivo* skin permeation potential of the optimized norfloxacin-loaded NLC gel was evaluated using Franz diffusion cells (PermeGear, USA) with excised ear skin of rabbits. The study was conducted in accordance with the institutional ethical standards. Ear lobes skin was removed from sacrificed New Zealand White rabbits (2.5kg to 3.5kg), carefully cleaned to eliminate hairs, and placed in phosphate-buffered saline (PBS) solution (pH 7.4) for 1 hour before use. The samples of skin were kept frozen at -20°C and thawed to room temperature prior to mounting [78, 79].

The skin samples were carefully placed between the donor and receiver compartments of the Franz diffusion cell with the stratum corneum towards the donor chamber (effective diffusion area = 1.77 cm^2). The two-receptor media used were PBS pH 5.5 (acidic wound surface environment) and PBS pH 7.4 (physiological environment). The receptor compartment was filled with 20 mL of the respective PBS medium and the temperature was kept at 37 ± 0.5°C and stirring at 600 rpm

to ensure sink conditions throughout the experiment. An optimized NLC gel (F1) was prepared and an accurately weighed amount (1 g, corresponding to 3 mg of norfloxacin) was evenly spread over the surface of stratum corneum in the donor compartment, along with a plain gel (free norfloxacin without NLC encapsulation).

Aliquots of 1ml were taken from the receptor compartment after 0.5, 1, 2, 4, 6, 8, 12, 16, 20 and 24 hours and replaced with fresh PBS of the same pH. The contents of norfloxacin in the withdrawn samples was estimated spectrophotometrically at the λmax equal to 273 nm.

The skin permeation profile was obtained by plotting the cumulative amount of medication permeated per unit area (μg/cm^2) against time. The steady-state flux (Jss) was computed using the linear section of the cumulative permeation curve that represents steady state:

$$J_{\text{ss}} = \frac{\Delta Q}{A\,\Delta t} \tag{3.3}$$

where A is the effective diffusion area (cm^2), Δt is the time interval during the steady-state linear region (h), and ΔQ is the total amount of medication penetrated during steady state (μg).

The permeability coefficient (Kp) was calculated as:

$$K_p = \frac{J_{\text{ss}}}{C_d} \tag{3.4}$$

Where Cd is the initial drug concentration in the donor compartment (μg/mL).

The enhancement ratio (ER) was calculated to evaluate the permeation enhancement conferred by NLC encapsulation:

$$ER = \frac{J_{\text{ss}}(\text{NLC gel})}{J_{\text{ss}}(\text{Plain gel})} \tag{3.5}$$

All skin permeation experiments were conducted in triplicate (n = 3). Data are expressed as mean ± SD. Statistical comparison between formulations was performed using unpaired two-tailed Student's t-test, with $p < 0.05$ considered statistically significant [52, 80].

3.5.4 Skin Irritation Test

The Draize skin irritation test was used to assess the dermal biocompatibility of the optimized norfloxacin NLC Carbopol 940 gel in nine healthy adult New Zealand White rabbits (Oryctolagus cuniculus), in compliance with OECD (Organization for Economic Co-operation and Development) Test Guideline 404 for acute dermal irritation/corrosion [81]. The Research Ethics Committee, Faculty of Pharmacy, Capital University of Science and Technology, Islamabad, accepted the study protocol (Approval Ref: REC/FOP/CUST/2025/08). All animals were acclimatized under standard laboratory conditions (22 ± 2°C, 55 ± 5% RH, 12 h light/dark cycle) with unrestricted access to standard food and water.

Three groups (n=3 per group) were formed randomly. Test group consisted of optimized norfloxacin NLC Carbopol 940 gel. The positive control was SLS solution (0.8% w/v) and the negative control was the site that was not treated (baseline skin response).

To prevent any microscopic damage to the skin, rabbits had the dorsal side of their skin shaved using an electric clipper a day before the application of the formulation. An area of approximately 6 cm^2 on the skin was marked. An exact weight (0.1 g) of the test material was applied to the designated area using a sterile polypropylene spatula and was secured with an occlusive patch to ensure sustained contact with skin. Clinical observations for erythema and edema were conducted at 24, 48, and 72 hours after application. Measurements were based upon the Draize scoring system (0 = None; 1 = Mild; 2 = Moderate; 3 = Severe) [82]. At 72 hours the Primary Irritation Index (PII) was calculated. Based on OECD classification: PII < 0.5 = non-irritant; PII 0.5–2.0 = slightly irritant; PII > 2.0 = moderately to severely irritant [83].

3.5.5 Stability Studies

The optimized NLC gel formulation was subjected to the physical and chemical stability testing under three storage conditions (refrigerated (4 ± 2°C), ambient (25 ± 2°C / 60 ± 5% RH) and accelerated (40 ± 2°C / 75 ± 5% RH)) as per the ICH Q1A(R2) guidelines. Amber glass vials were used to store samples for 3 months with aluminum foil to prevent air leakage.

Samples were taken at fixed time intervals (0, 1, 2 and 3 months) and analyzed for particle size, polydispersity index, zeta potential, pH, viscosity, drug content and physical appearance. One way ANOVA and Tukey's post-hoc test were utilized for statistical analysis. Any changes were deemed statistically significant when the value was < 0.05 [51].

3.6 Antimicrobial Assay

The antibacterial efficacy of the optimized norfloxacin-loaded NLC gel was evaluated against four clinically relevant wound pathogens: *Staphylococcus aureus* (ATCC 6538), methicillin-resistant *Staphylococcus aureus* (MRSA, ATCC 43300), *Escherichia coli* (ATCC 25922), and *Pseudomonas aeruginosa* (ATCC 27853) using the agar well diffusion method [84].

The overnight culture was adjusted to 0.5 McFarland ($\sim 1.5 \times 10^8$ CFU/mL) and uniformly swabbed onto Mueller-Hinton agar (MHA) plates with sterile cotton swabs. Test formulations were punched into the agar and 50 μL of these placed in the well (6 mm) at three concentrations of the drug (10, 5 and 2.5 mg norfloxacin/well). The optimized norfloxacin loaded NLC gel (NFX-NLC gel), plain norfloxacin gel (positive control), blank NLC gel (negative control), blank Carbopol gel (negative control) and DMSO (solvent control) were tested. The plates were then incubated at 37°C for 24 hours and the zones of inhibition (ZOI) were measured with a digital caliper. Each experiment was conducted three times and the results were reported as mean ± SD.

Antibacterial activity was assessed by the agar well diffusion method, a well-validated technique for evaluating the antimicrobial potential of pharmaceutical formulations including topical drug delivery systems [85]. Zones of inhibition were interpreted using the norfloxacin susceptibility thresholds consistently applied across the contemporary norfloxacin antibacterial literature: susceptible $\geq$ 17 mm, intermediate 13–16 mm, and resistant $\leq$ 12 mm, corresponding to MIC breakpoints of $\leq$ 16 μg/mL (susceptible) and $\geq$ 32 μg/mL (resistant). These thresholds continue to serve as the primary reference standard for norfloxacin susceptibility interpretation in published investigations of norfloxacin formulations and analogues, including recent studies employing the agar cup diffusion method against *S. aureus*, MRSA, and Gram-negative wound pathogens. Since the present study employs norfloxacin topically for wound infection management — an indication for which no independently established topical breakpoints exist — application of these widely adopted ZOI thresholds is both scientifically justified and consistent with current practice in the norfloxacin antibacterial literature [86, 87].

3.7 Statistical Analysis

All data are given as mean $\pm$ standard deviation (SD) or standard error of the mean (SEM) as appropriate. GraphPad Prism software version 9.0 (GraphPad Software, USA) was used for statistical analysis. Multiple group comparisons were made using one-way analysis of variance (ANOVA) with Tukey's post-hoc test. Unpaired two-tailed Student's t-test was used for two-group comparisons. A two-way ANOVA with Sidak's multiple comparison test was performed for permeation data with two independent variables (pH and time) to find significant differences between pH conditions throughout the time course. The p value of < 0.05 was set as the significance criterion. All experiments were repeated three times (unless otherwise stated).

Chapter 4

Results and Discussion

4.1 Encapsulation Efficiency

Norfloxacin NLCs were systematically evaluated in terms of encapsulation efficiency (% EE) in all the 13 developed batches. EE values were statistically significantly different between the formulations (one-way ANOVA, Tukey's post hoc analysis, $p<0.05$) and showed a wide range from 61.20±0.48% (F10) to 94.95±0.13% (F1) as presented in Table 4.1. The F1 formulation showed consistently good encapsulation efficiency (94.95 ± 0.13%), which demonstrates the ability of this optimized NLC design to provide high drug loading efficiency.

The systematic change in %EE over the thirteen formulations gives clues to the mechanism of the factors that affect the drug loading capacity. F3 (77.30 ± 0.40%) and F12 (74.38 ± 0.37%) demonstrated comparatively higher EE values among the remaining formulations except F1, while F6 (71.97 ± 0.99%) and F11 (71.82 ± 0.82%) exhibited moderate entrapment. F10 recorded the lowest encapsulation efficiency overall (61.20 ± 0.48%), followed closely by F9 (64.00 ± 0.76%) and F5 (64.69 ± 0.50%). These differences may be systematically explained by the differences in the architecture of the lipid matrix. Formulations containing less than optimum solid lipid concentrations, an imbalanced solid:liquid lipid ratio or insufficient surfactant content demonstrate a reduced drug entrapment ability,

which is in line with the previously described drug loading mechanics in NLCs [88, 89].

These observations can be explained by the "imperfect crystal" model. In this model, by adding liquid lipid (Labrafac WL1349) to the solid lipid (Precirol ATO5), the crystal lattice is disrupted and numerous imperfections and cavities are created into which the drug molecules can move, i.e. drug accommodation sites [90]. The ratio of Precirol:Labrafac in F1 is 70:30, which is an optimum ratio that allows the maximum amount of space for the drug to be accommodated, while at the same time keeping the integrity of the nanoparticles. However, formulations with a high solid lipid content, as in the case of the dominant Precirol ATO5 in F10, create a very ordered crystalline matrix, in which lattice imperfections are very limited and drug accommodation is consequently reduced and EE is reduced [91]. Likewise, formulations containing formulations with imbalanced lipid ratios (F4: 50:50 and F5: 90:10) show suboptimal EE because either too much liquid lipid is used, which negatively affects matrix stability, or too much solid lipid is used with a limited space for accommodating the drug. Surfactant concentration is another important factor and insufficient (F6: 0.5%) and excess (F7: 2.5%) concentrations adversely affect EE by different mechanisms of insufficient emulsification and micellar competition for drug molecules, respectively [92].

TABLE 4.1: Norfloxacin NLC Formulation's Encapsulation Efficiency (EE%) (n = 3) Data displayed as mean ± SD (n = 3).

Formulation	**EE% Mean ± SD**
F1	94.95 ± 0.13
F2	67.95 ± 0.36
F3	77.30 ± 0.40
F4	69.06 ± 0.76
F5	64.69 ± 0.50
F6	71.97 ± 0.99
F7	66.77 ± 0.47
F8	64.85 ± 0.53

Table 4.1 continued from previous page

Formulation	EE% Mean ± SD
F9	64.00 ± 0.76
F10	61.20 ± 0.48
F11	71.82 ± 0.82
F12	74.38 ± 0.37
F13	65.20 ± 0.38

4.2 *In Vitro* Drug Release and Kinetics

The *in vitro* drug release behaviour of the developed norfloxacin NLC formulations (F1-F13) was systematically explored at simulated wound surface (pH 5.5) and physiological (pH 7.4) pH using dialysis bag diffusion technique (MWCO 12-14 kDa). The receptor media were acetate buffer (pH 5.5) and phosphate buffered saline (PBS, pH 7.4) which were kept at 37 ± 0.5°C and stirred continuously at 100 rpm during the 24-hour study period. The cumulative drug release profile at both pH conditions is shown in figure 4.1 and Table 4.2 displays the release kinetic parameters derived from the zero order, first order, Higuchi, and Korsmeyer-Peppas models.

All 13 formulations were found to show sustained controlled release of the drug without reaching a plateau at the pH of 5.5 which corresponds to the mildly acidic microenvironment of healing and infected wound surfaces, reflecting prolonged drug delivery from the lipid matrix architecture [93]. The highest cumulative drug release (90.1 ± 2.50% at 24 h) was observed with formulation F1, statistically superior to all other formulations ($p < 0.05$, one-way ANOVA followed by Tukey's post hoc test).

The increase in the release of norfloxacin from F1 at pH 5.5 is mechanistically consistent with the ionization behaviour of norfloxacin: at pH 5.5, norfloxacin ($pK_{a1} \approx 6.35$) exists primarily as a cationic form, which is more soluble in water

than its zwitterionic form at pH 7.4, causing the concentration gradient (ΔC) to become greater, which in turn increases the diffusion of the drug from the lipid matrix into the receptor medium [94]. Formulation F13 under acidic conditions had the lowest cumulative release at 24 hours (44.80 ± 1.50%). Despite sharing the identical lipid composition and solid-to-liquid ratio as the optimized F1, F13 was subjected to a prolonged processing time of 15 min (versus 10 min for F1).

This extended ultrasonication induced excessive mechanical stress and localized thermal effects, promoting polymorphic transition of the lipid matrix to a more ordered crystalline state and subsequent particle re-aggregation (as reflected by the highest PDI of 0.562 in Table 4.3). The resultant compact crystalline lattice physically entrapped the drug, markedly restricting its diffusion into the receptor medium [95].

All the formulations showed statistically significant and marked decrease in cumulative drug release at pH 7.4 compared to pH 5.5 ($p<0.05$). The cumulative release of F1 at 24 h at pH 7.4 was 27.2 ± 1.5%, which was 62.9 percentage points lower than at pH 5.5. The release reduction was mechanistically attributed to the near-isoelectric state of norfloxacin at physiological pH, characterized by the presence of an electrically neutral zwitterion with minimum aqueous solubility (0.32-0.39 mg/mL), resulting in limited drug concentration gradient to drive the drug diffusion and increased drug retention within the lipid core of Precirol [96].

Among the formulations, F13 showed the least release at pH 7.4 (4 ± 0.3%), while F10 was also severely limited (5.2 ± 0.3%). While F10's restriction was due to insufficient homogenization speed (8,000 rpm) resulting in large particle sizes, F13's hindered release stemmed from over-processing-induced crystallinity and re-aggregation.

In both cases, the inherently limited aqueous solubility of the zwitterionic drug at near-neutral pH further reduced the driving concentration gradient, synergistically restricting diffusion from the crystalline lipid core [97]. The encapsulation efficiency and the composition of the lipid matrix are directly related to the differential release of the formulations at both pH. The formulations with higher EE

(F1) also showed more cumulative release, suggesting that the higher the amount of drug loaded in the lipid matrix, the more the drug can be released via diffusion. On the other hand, formulations with lower EE showed lesser cumulative release which suggested restricted availability of the drug in the formulation matrix.

Four mathematical models (zero-order, first-order, Higuchi and Korsmeyer-Peppas model) were evaluated using release kinetic modelling which revealed that the Korsmeyer-Peppas model was the best fit for all thirteen formulations at both pH with R2 ranging from 0.980 to 0.999.

This model was better than that of zero order (R^2 0.930-0.982), first order (R^2 0.536-0.880) and Higuchi (R^2 0.970-0.996) models, thereby proving that the complex release mechanism from the dual NLC-Carbopol matrix system, could not be suitably explained by simpler kinetic models [98].

Diffusion exponent (n) obtained from Korsmeyer-Peppas model were in the range of 0.570 to 0.741 for all the formulations at both pH levels and is clearly between 0.45 and 1.0, indicating non-Fickian (anomalous) transport. This transport mechanism is a mixture of Fickian diffusion through the NLC lipid matrix and swelling controlled relaxation of the Carbopol 940 polymer network [99]. The n value for formulation F1 at both pH 5.5 (n=0.654) and 7.4 (n=0.615) are in the anomalous transport range, and there is a slightly more polymer relaxation contribution at pH 7.4 compared to pH 5.5.

The significantly lower value of the Korsmeyer-Peppas rate constant (K_{KP}) at pH 7.4 (3.453) compared to pH 5.5 (12.184), further confirms the significantly reduced driving force for the diffusion of the drug at the physiological pH, where norfloxacin acquires a near-isoelectric zwitterionic state, which results in a much lower concentration gradient from the lipid core into the receptor medium. The Higuchi model also fitted well (R^2 = 0.990-0.994 for F1), and it was also found that diffusion through the lipid matrix is a major part of the overall anomalous transport mechanism, which is Fickian. Such kinetic results are typical of NLC-Carbopol gel systems described in the literature, which has a dual matrix structure with a diffusion barrier of NLCs and a polyacrylate gel and is intrinsically not

Fickian, with the release controlled by the resistance of both the lipid core and the hydrogel polymer network.

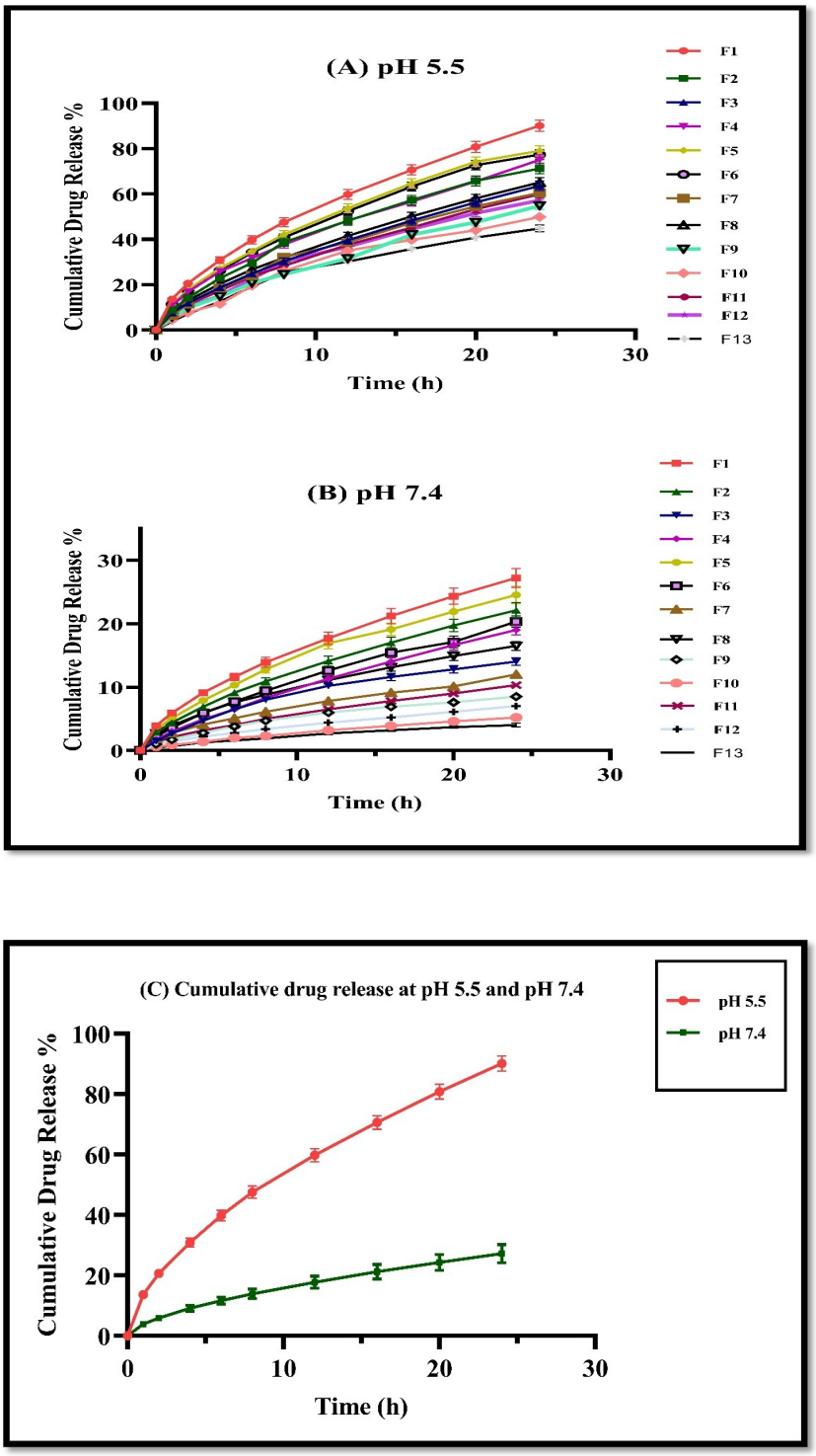

FIGURE 4.1: *In Vitro* drug release profile of Norfloxacin NLC Loaded Gel at (A) pH 5.5, (B) pH 7.4 and (C) Cumulative mean drug release at both pH 5.5 and 7.4. Data are represented as Mean ± SD (n = 3). One-way ANOVA ($p < 0.05$) was used to compare between groups for statistical significant.

TABLE 4.2: The *In Vitro* drug release kinetic parameters of Norfloxacin NLC formulations (F1–F13) at both pH are listed.

Form.	**pH**	**Zero-Order R^2**	K_1	**First-Order R^2**	K_1	**Higuchi R^2**	**K_H**	**K-P R^2**	**K_KP**	**n**
F1	5.5	0.957	4.966	0.536	0.173	0.994	16.473	0.999	12.184	0.654
F1	7.4	0.965	1.469	0.687	0.114	0.990	4.826	0.996	3.453	0.615
F2	5.5	0.958	3.841	0.592	0.159	0.989	12.616	0.991	8.859	0.676
F2	7.4	0.970	1.161	0.737	0.101	0.988	3.807	0.999	2.606	0.636
F3	5.5	0.976	3.272	0.626	0.151	0.983	10.595	0.999	7.132	0.697
F3	7.4	0.936	0.761	0.754	0.080	0.988	2.534	0.991	1.718	0.637
F4	5.5	0.962	4.069	0.558	0.164	0.992	13.335	0.998	9.730	0.661
F4	7.4	0.983	0.925	0.815	0.087	0.970	2.912	0.999	1.592	0.741
F5	5.5	0.955	4.352	0.557	0.167	0.992	14.548	0.996	10.935	0.644
F5	7.4	0.958	1.319	0.707	0.108	0.991	4.349	0.994	3.125	0.611
F6	5.5	0.967	4.361	0.566	0.166	0.990	14.336	0.999	10.237	0.671
F6	7.4	0.976	1.025	0.774	0.094	0.981	3.291	0.997	2.162	0.653
F7	5.5	0.966	3.211	0.626	0.150	0.986	10.285	0.990	6.800	0.704
F7	7.4	0.957	0.658	0.791	0.076	0.992	2.156	0.995	1.590	0.601
F8	5.5	0.970	3.416	0.607	0.154	0.988	11.137	0.999	7.735	0.682
F8	7.4	0.951	0.919	0.728	0.0929	0.996	3.089	0.999	2.417	0.570

Table 4.2 continued from previous page

Form.	pH	Zero-Order R^2	K_0	First-Order R^2	K_1	Higuchi R^2	K_H	K-P R^2	K_KP	n
F9	5.5	0.983	2.747	0.666	0.142	0.975	8.743	0.993	5.605	0.719
F9	7.4	0.972	0.430	0.856	0.053	0.986	1.400	0.999	0.920	0.655
F10	5.5	0.958	2.541	0.687	0.136	0.973	8.111	0.980	4.953	0.735
F10	7.4	0.982	0.258	0.880	0.027	0.977	0.839	0.997	0.527	0.677
F11	5.5	0.977	3.072	0.636	0.148	0.983	9.933	0.999	6.669	0.698
F11	7.4	0.973	0.541	0.824	0.065	0.986	1.747	0.999	1.157	0.653
F12	5.5	0.969	2.994	0.642	0.146	0.981	9.635	0.990	6.419	0.702
F12	7.4	0.972	0.366	0.871	0.046	0.987	1.189	0.998	0.795	0.648
F13	5.5	0.951	2.352	0.672	0.132	0.981	7.559	0.986	4.842	0.713
F13	7.4	0.968	0.202	0.839	0.015	0.983	0.688	0.993	0.480	0.623

K-P = Korsmeyer–Peppas; n = diffusion exponent; $n < 0.45$ = Fickian diffusion; $0.45 < n < 1.0$ = anomalous (non-Fickian) transport; $n = 1.0$ = Case II transport. All formulations exhibit anomalous transport ($n = 3$).

Zero order (0.957-0.965) and first order (0.536-0.687) were also less satisfactory than the Korsmeyer-Peppas model in explaining the drug release of all formulations, which suggested that the drug release from this system was not simply concentration-independent or simple exponential decay [100]. The pH dependent, anomalous transport release profile of the norfloxacin NLC formulations provides an approach that can be clinically rational in treating topical wound infection.

The formulation is designed to deliver the norfloxacin at a faster, more complete rate at pH 5.5 (conditions found in infected and healing wounds), and sustain and prolong the release at pH 7.4 (deeper dermal and physiological tissue conditions). This pH responsive behaviour can allow for greater drug levels to be delivered at the wound surface where there are maximum numbers of bacteria, and to retain and sustain drug levels in the underlying tissues where there is potential for systemic absorption and toxicity. Sustained release profile over 24 hours without reaching a plateau further supports Clinical utility of this formulation which might enable once daily application and increase patient compliance. Drug release behavior under various physiological situations can be described and predicted using the anomalous transport mechanism (diffusion and swelling-controlled release), which will further support formulation development and clinical translation [101].

4.3 Particle Size Polydispersity Index and Zeta Potential

F1's particle size (prepared with 5% w/w total lipid, Precirol ATO5: Labrafac WL1349 ratio of 70:30, 1.5% total surfactant, 30% v/v Transcutol P, homogenization speed of 12,000 rpm, and 10 min processing time) was 102 nm, the PDI was 0.267, and the zeta potential was -37.7 mV, the smallest particle size and the lowest PDI and the highest negative zeta potential when compared with all tested formulations. The influence of total lipid content on particle properties was clearly demonstrated by comparing F2 (3% lipid; 214.1 nm, PDI 0.474, ZP -15.8 mV) and F3 (7% lipid; 216.3 nm, PDI 0.472, ZP -13.6 mV) with F1. Insufficient mass of the

lipid matrix (F2) led to the formation of larger particles with broad particle size distribution and poor surface charge stability at 3% total lipid. Excessive lipid concentration (F3, 7%), on the other hand, encouraged the aggregation of particles and coalescence of lipids during cooling, leading to an increase in particle size and PDI [102]. In contrast, excess lipid concentration (F3, 7%) promoted particle aggregation and lipid coalescence during the cooling phase, increasing both particle size and PDI. This biphasic behaviour is due to the fact that at sufficiently high concentrations of the lipid, the viscosity of the internal phase is sufficiently high such that efficient emulsification during high shear homogenization is not possible [103].

Solid to liquid ratio of the lipids was a key factor for the properties of NLC particles. The particle size of F4 (Precirol: Labrafac = 50:50) was significantly larger (477.1 nm, PDI 0.468, ZP -15.0 mV) because of the high liquid lipid content which decreased the rigidity of the matrix and caused particle aggregation [104]. F5 (Precirol: Labrafac = 90:10) on the other hand, was found to have the highest mean particle size of 485.5 nm, lowest PDI (0.429) and ZP (-12.9 mV), which was obtained due to highly ordered crystalline matrix formed by the highest solid lipid content. The Precirol matrix is a rigid matrix with high crystallinity, which is thermodynamically less favourable for drug accommodation and emulsification and which leads to the development of large particles with the lowest zeta potential of the various lipid ratio variants [22]. The 70:30 ratio Precirol:Labrafac in F1 represents an optimum ratio, and the amount of liquid lipid-derived structural disorder provides imperfections in the lipid crystal lattice leading to increased accommodation space for the drug and subsequently reduced particle size, thus satisfying the well-established "imperfect crystal" NLC model [105].

An obvious influence of the surfactant concentration (Tween 80) on the particle size and the colloidal stability was observed. F6 (0.5% surfactant; PDI 0.344; ZP -15.1 mV) resulted in the largest particle size (492.2 nm) as the surfactant used was not sufficient to completely cover the lipid–water interface, causing incomplete emulsification to be formed and poor steric/electrostatic stabilization of lipid

droplets during the homogenization process. Increasing the surfactant concentration to 2.5% (F7) further reduced the particle size (163.2 nm) through enhanced emulsification compared to F6. However, the excess surfactant molecules formed free micelles in the dispersion, which resulted in a markedly reduced zeta potential (-14.7 mV), indicating compromised electrostatic stabilization. While the PDI of F7 (0.326) was slightly narrower (more uniform) than that of F6 (0.344), both values remained higher than the optimal F1 (0.267), suggesting that either insufficient or excessive surfactant leads to suboptimal size homogeneity. The primary drawback of excess surfactant was therefore the loss of colloidal stability rather than a worsening of size distribution. The concentration of Tween 80 in F1 is 1.5%, which is the optimum concentration for sufficient coverage of the interface but with a minimum of free micellar interference [106, 107].

The physicochemical properties of NLCs significantly changed with the concentration of Transcutol P. Both F8 (10% Transcutol P; P; 300.6 nm, PDI 0.376, ZP -25.8 mV)) and F9 (20% Transcutol P; 305.7 nm, PDI 0.409, ZP -26.2 mV) showed higher particle sizes than F1, indicating that 30% Transcutol P is needed to achieve optimum plasticization of the interface and optimum reduction of the interfacial tension during NLC formation. Transcutol P is used as a co-solvent and penetration enhancer and at adequate concentrations it alters the interfacial properties of the lipid/water interface to improve the formation of nanoparticles with small and homogeneous size distribution [108].

The properties of the particles were significantly affected by the speed of homogenization, which in a certain range was non-linear. The slowest speed (F10, 8,000 rpm; 295.2 nm, PDI 0.476, ZP -25.8 mV) did not generate enough shear energy to break up the lipid droplet fully into the nanometer range, resulting in the highest PDI value of the speed variants. With F11 (20,000 rpm, 213.5 nm, PDI 0.547, ZP -13.8 mV), a higher speed led to lipid overheating and particle coalescence resulting in a high PDI, and a marked deterioration in surface charge.

Likewise, too low a homogenization time (F12, 5 min; 176.1 nm, PDI 0.408, ZP -15.3 mV) led to incomplete emulsification, whereas too high a homogenization

time (F13, 15 min; 167.6 nm, PDI 0.562, ZP -16.0 mV) produced the highest PDI of all due to mechanical over-processing and thermal degradation of the lipids leading to re-aggregation [109].

The zeta potential of F1 (-37.7 mV) exceeded the critical stability value of ±30 mV, which is considered as the universal value for a colloidally stable dispersion with a sufficient electrostatic repulsion between the particles to avoid aggregation and coalescence during storage [110]. In contrast, all other formulations gave the results of zeta potentials in the range of -12.9 mV to -26.2 mV, below this value of stability, indicating a lower value of long-term physical stability. The formulation F1 with the smallest particle size (102 nm), lowest PDI (0.267) indicating narrow and monodisperse size distribution and largest negative zeta potential (-37.7 mV) was identified as the formulation with the most promising physicochemical properties among all the formulations tested [111].

TABLE 4.3: Physicochemical Characterization of Norfloxacin NLC Formulations (F1–F13)

Formulation	**Particle Size (nm)**	**Polydispersity Index (PDI)**	**Zeta Potential (mV)**
F1	102.0	0.267	-37.7
F2	214.1	0.474	-15.8
F3	216.3	0.472	-13.6
F4	477.1	0.468	-15.0
F5	485.5	0.429	-12.9
F6	492.2	0.344	-15.1
F7	163.2	0.326	-14.7
F8	300.6	0.376	-25.8
F9	305.7	0.409	-26.2
F10	295.2	0.476	-25.8
F11	213.5	0.547	-13.8
F12	176.1	0.408	-15.3
F13	167.6	0.562	-16.0

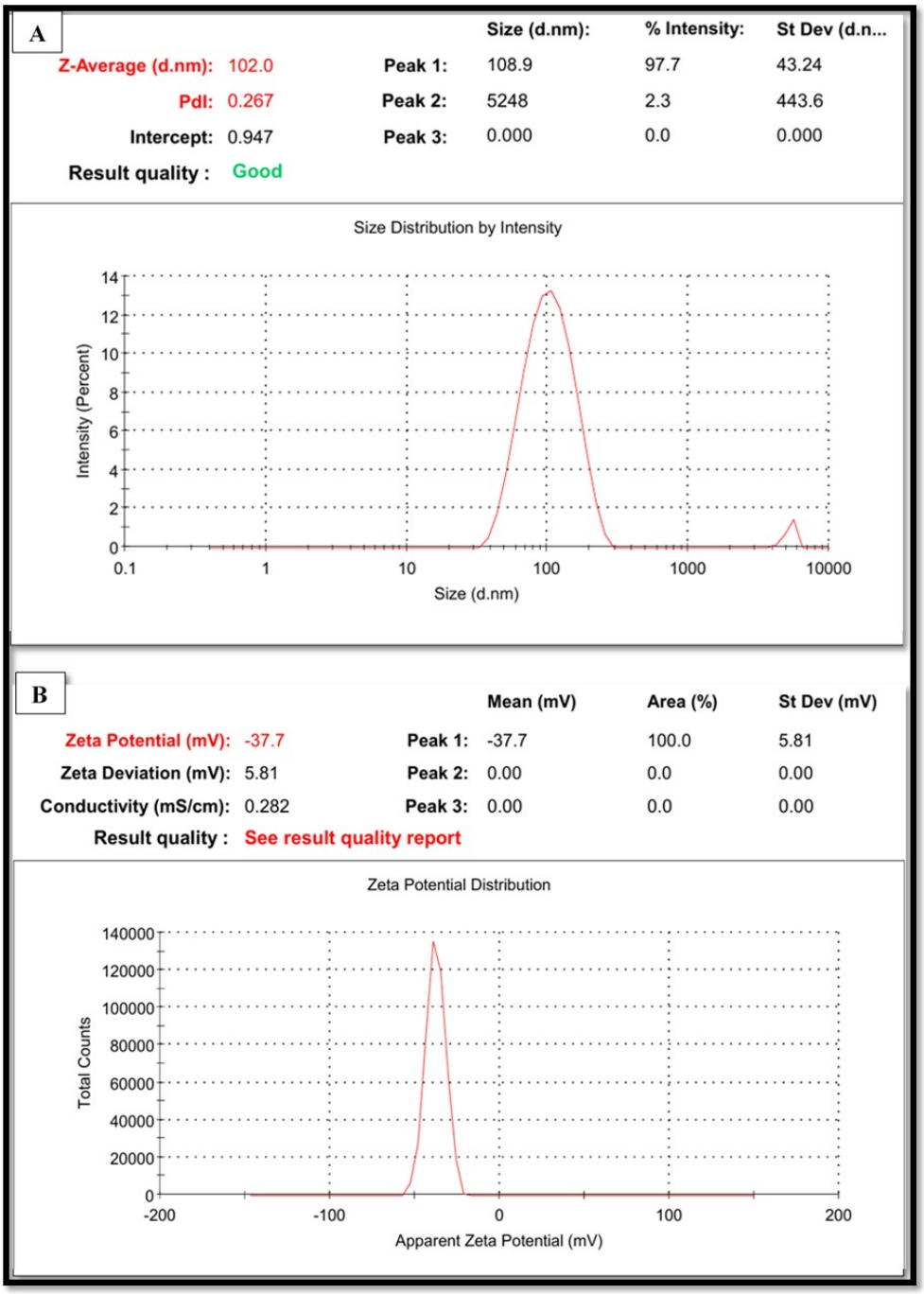

FIGURE 4.2: The particle size distribution and zeta potential of F1 formulation. (A) The particle size histogram displayed monomodal distribution with mean diameter of 102 nm and PDI of 0.267 and the Zeta potential distribution (B) showed excellent colloidal stability with surface charge of -37.7 mV. Data are the average of triplicates (n = 3).

Based on the results of the extensive physiochemical characterization, encapsulation efficiency and *in vitro* drug release, F1 was selected as the optimized formulation for further development. F1 had the smallest particle size (102 nm), the

narrowest polydispersity index (0.267), and the highest zeta potential (-37.7 mV) among all thirteen formulations, which all indicate the best possible combination of critical quality attributes that give the product the most favorable colloidal stability and homogeneous dispersion. F1 had also shown the highest encapsulation efficiency (94.95 ± 0.13%) with an extraordinary ability to load the drug in the lipid matrix [112].

F1's *in vitro* drug release profile was also impressive which revealed highest drug release at pH 5.5 (90.1 ± 2.5% after 24 hours) and sustained release at pH 7.4 (27.2 ± 1.5%) with the anomalous non-Fickian transport kinetics (Korsmeyer – Peppas R2 = 0.999, n = 0.654 at pH 5.5) indicating dual diffusion/swelling controlled release. The pH dependent release behaviour (increased delivery at low pH at the wound surface and sustained release at the physiological pH) offers a pharmacokinetically rational basis for topical management of wound infections. Based on the results obtained for various parameters such as particle characteristics, drug loading capacity and drug release kinetics, it is clear that F1 is the most promising formulation to be incorporated in the gel matrix of Carbopol 940 for further investigation of *ex vivo* permeation, dermal safety, antibacterial activity and stability. Thus, the optimized formulation of F1 was chosen for all the subsequent characterization studies.

4.4 Scanning Electron Microscopy

To evaluate particle shape, surface morphology and the uniformity of the structure which influences the colloidal stability, the drug release behaviour and the functional performance of optimum NLC formulation (F1) was characterized using scanning electron microscopy (SEM). The SEM micrographs (Fig. 4.3) taken at a wide range of magnification (1,000× to 100,000×) showed mostly well-formed, spherical to near-spherical nanoparticles with smooth, dense surfaces and nanoscale dimension which are typical characteristics of good nanostructured lipid carriers. The particles were evenly distributed and had good structural integrity and low

aggregation at lower magnifications (1,000×-7,000×) demonstrating that the formulation process was successful showing no phase separation, coalescence or large crystalline domains. Minor surface irregularities and indentations observed are likely to be due to the inherent imperfections that occur when liquid lipid (Labrafac WL1349) is incorporated into the solid lipid (Precirol ATO5) crystalline lattice, and are a typical morphological feature of the "imperfect crystal" architecture of NLC systems [113, 114]. The images showed that at high magnifications (13,000× – 100,000×) the particle boundaries were well defined with a compact matrix structure lacking any sharp, needle-like or angular crystalline structures. The lack of any crystalline drug deposits on the surface of the nanoparticles suggests that norfloxacin was encapsulated and not deposited into the lipid matrix as free surface-adsorbed crystals or free unentrapped drug particles [115]. This morphological observation has a mechanistically significant impact because the efficiency of drug loading, the release kinetics, and the potential for nanoparticle aggregation via crystal bridging would all be affected if there was surface crystallization [116]. The smooth surface characteristics and spherical shape is especially beneficial for topical use. The smooth surfaces of spherical nanoparticles result in minimum interparticle friction which helps in even dispersion in the Carbopol 940 gel matrix and hence even drug distribution in the applied gel [117]. Moreover, the compact and dense matrix structure ensures physical protection for the encapsulated drug, reducing the risk of premature leakage and degradation during storage and use. The XRD and DSC results independently suggested the amorphous nature of norfloxacin in the lipid matrix and the same result was also confirmed from the micrographs where no crystalline domains were observed. The unique combination of the morphological and solid-state characterization data gives strong support to the dispersion of molecules at the molecular level, which is a key requirement to improve the solubility and dissolution behaviour in BCS Class IV compounds. Some of the micrographs showed occasional clustering of nanoparticles, which was believed to be caused by the dehydration and vacuum-induced artifacts during the preparation of the samples for SEM and not due to inherent formulation instability, as excellent colloidal stability evident by DLS (PDI = 0.267; zeta potential = -37.7 mV) was observed in the dispersed state. It is worth noting that the particle

size distribution obtained from SEM analysis (around 100-120 nm) agrees well with the mean diameter value determined by DLS analysis (102 nm) indicating the reliability of the characterization techniques [118].

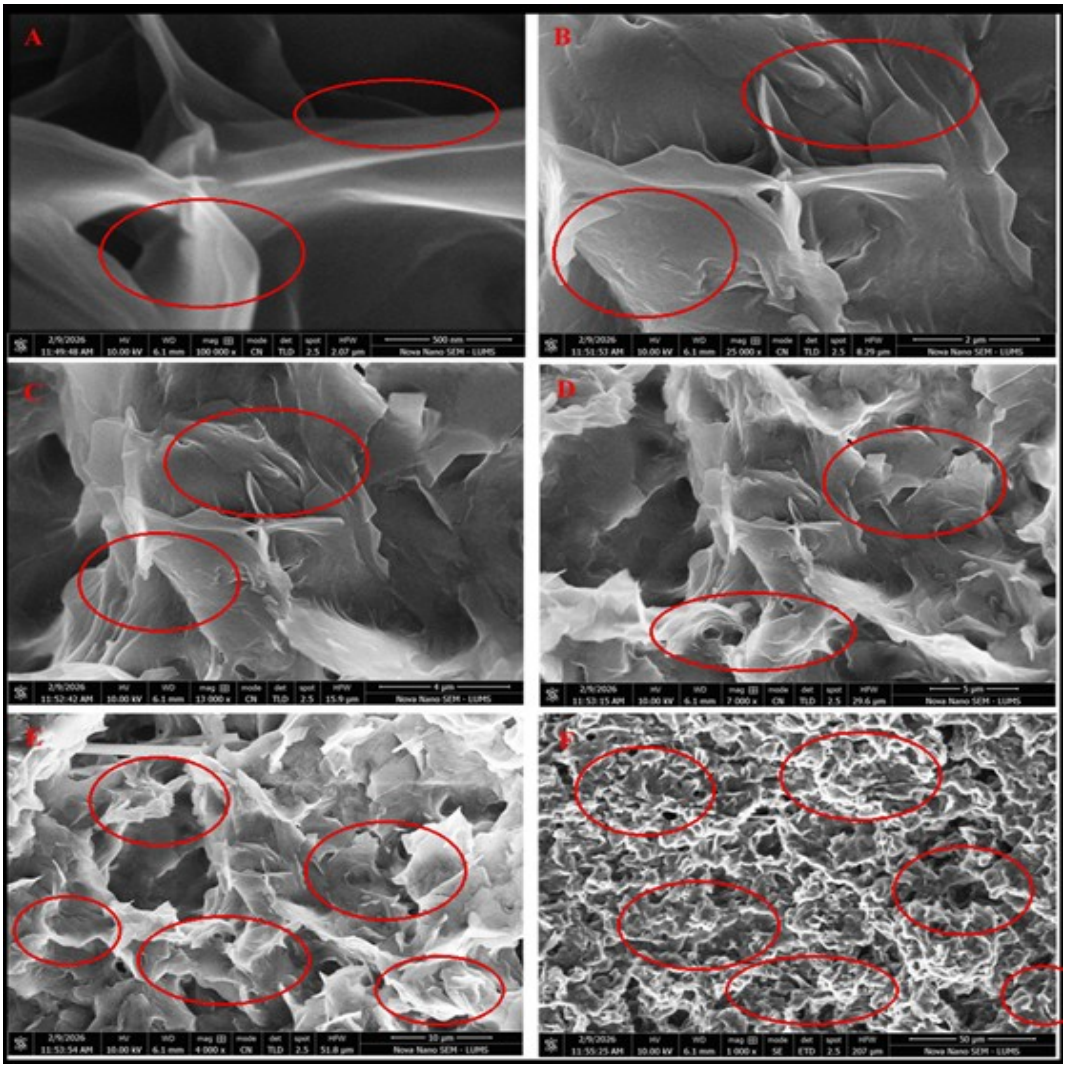

FIGURE 4.3: Representative SEM micrographs of norfloxacin-loaded NLCs at decreasing magnifications (A (100,000×), B (25,000×), C (13,000×), D (7,000×), E (4,000×), F (1000×).
The photographs depict nanoparticles that have a spherical shape and a smooth surface. No crystalline drug structure is seen, indicating complete encapsulation.

4.5 FTIR Spectroscopy

To determine the possible chemical interactions between the drug and formulation excipients, the molecular integrity of norfloxacin and its compatibility with

the lipid matrix were studied by FTIR spectroscopy. The spectra of pure norfloxacin, individual excipients (Precirol® ATO5, Tween 80, Labrafac® WL 1349, Transcutol® P), drug-free blank formulation (lipid matrix) and the optimized norfloxacin loaded NLCs were systematically compared in order to detect any chemical interaction which might affect the formulation stability or the drug activity as depicted in Fig. 4.4 [119].

Spectrum of pure norfloxacin showed its distinctive vibrational peaks, endorsing its structural identity and purity. A wide-ranging absorption band spanning 3200–3400 cm^{-1} was attributed to the O–H stretching of the carboxylic acid moiety and N–H stretching of the piperazinyl ring. Noticeable, sharp peaks in the middle of 1650 and 1700 cm^{-1} linked to the stretching vibrations of the two carbonyl groups: the ketone (C=O) and the carboxylic acid. Additional bands, including aromatic C=C stretches (1500–1600 cm^{-1}), C–F stretching (1200–1250 cm^{-1}), and C–N stretching (1300–1400 cm^{-1}), further corroborated its fluoroquinolone structure [120, 121].

The individual excipients exhibited their characteristic absorption profiles: Precirol® ATO5 showed strong aliphatic C–H stretching (2920, 2850 cm^{-1}) and ester C=O stretching (∼1735 cm^{-1}); Tween 80 displayed broad stretching of O–H (3500–3200 cm^{-1}), aliphatic C–H stretches, and ether C–O–C stretching (1100–1000 cm^{-1}); Labrafac® WL 1349 presented triglyceride-characteristic ester carbonyl (∼1740 cm^{-1}) and C–O stretching bands; and Transcutol® P exhibited O–H stretching (3500–3300 cm^{-1}) and prominent ether C–O–C stretching (1100–1050 cm^{-1}). The blank formulation without drug showed the absorption bands of its lipid and surfactant ingredients such as aliphatic C–H stretching (2920, 2850 cm-1), ester C=O stretching (1730-1740 cm-1) and C–O stretching (1000-1200 cm-1). No chemical interactions were observed between the selected excipients during the preparation process since no peaks assumed in the blank spectrum were unexpected and beyond the normal range of variation [122].

All the important absorption bands of pure norfloxacin were preserved in the optimized formulation containing norfloxacin, but with important and informative

changes. Importantly, no new peaks were detected and no peaks were lost when compared to the pure drug and blank formulation. This certainly precludes the development of the new covalent bonds and chemical compatibility of norfloxacin with all the formulation components has been confirmed.

The characteristic bands of the drug in the O–H/N–H stretching region (3400-3200 cm-1) and carbonyl region (1700-1650 cm-1), however, showed a significant increase in the degree of broadening and the decrease in the relative intensities with respect to the pure drug spectrum. This spectral change is not a sign of degradation but is a direct piece of evidence of physical encapsulation and intermolecular interactions.

The large broadening of the O–H/N–H band strongly suggests that these carboxylic acid and amine groups are involved in new, heterogeneous hydrogen bonding networks with the excipients, in particular with the ether oxygen of Transcutol® P and Tween 80 and the ester carbonyls of the lipids. The simultaneous widening of the drug's carbonyl bands and the unchanged narrow sharp peak of the ester carbonyl of the lipid matrix (1730–1740 cm^{-1}) suggests that the norfloxacin is molecularly dispersed in the lipid matrix. The molecules of the drug in this state are less free to vibrate than they are in the free state, and this causes peak broadening.

The characteristic aliphatic C–H stretches (2920, 2850 cm^{-1}) and the ester bands clearly depict the structural stability of the carrier itself. Norfloxacin is also chemically stable during the formulation process as there was no new peak in the chromatogram that could be attributed to drug-excipients covalent adducts or degradation products.

Thus, the FTIR data together show a stable formulation in which norfloxacin is physically entrapped and non-covalently bound (hydrogen bonding and van der Waals forces). This physical encapsulation that preserves the chemical integrity of the drug while altering its solid-state properties is a precondition for the crystalline-to-amorphous transition that was then verified by XRD and DSC analysis. The study of FTIR results along with other solid state characterization

techniques gives the strong evidence of the successful development of chemically compatible, physically stable NLC system with molecularly dispersed drug [123].

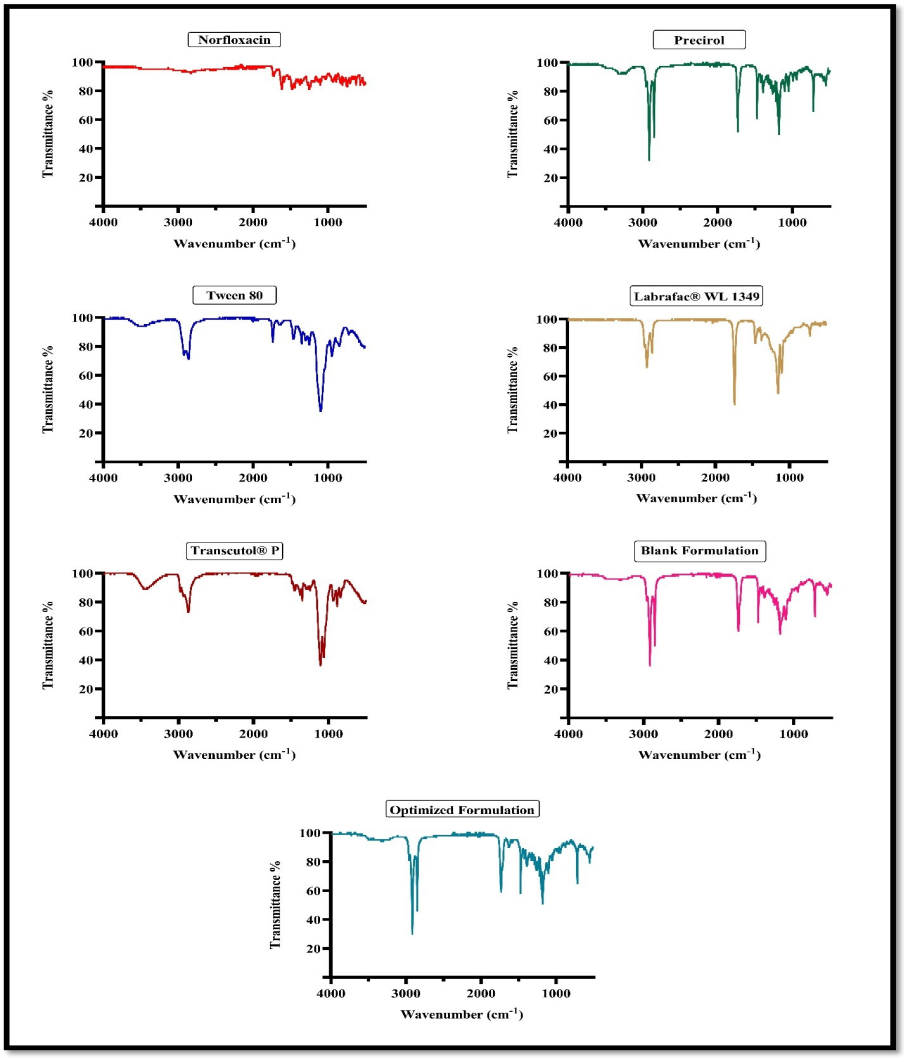

FIGURE 4.4: FTIR spectra of pure norfloxacin, Precirol® ATO5, Tween 80, Labrafac® WL 1349, Transcutol® P, blank formulation (lipid matrix without drug), and optimized norfloxacin-loaded NLC.

4.6 X-Ray Diffraction

To evaluate the crystalline properties, pure norfloxacin, pure Precirol® ATO5, blank formulation (lipid matrix without drug) and the optimized norfloxacin-loaded NLC formulation were analyzed by X-ray diffraction (XRD). The diffractograms shown in Figure 4.5 indicate that clear changes in structure occur after the drugs were incorporated into the lipid matrix.

The XRD pattern of pure norfloxacin shows sharp diffraction peaks with high intensities in the 2θ range of 15–30°, indicating its highly crystalline nature. The presence of well-defined reflections at 18.2°, 22.4°, 25.1° and 28.6° (2θ) suggests that the lattice of the solid state is well ordered, which is in agreement with previous reports on the solid state characteristics of fluoroquinolone antibiotics. These characteristic peaks can be used as fingerprints of the crystalline form of the drug and as a reference to investigate solid-state changes resulting from the formulation process [124].

Precirol® ATO5 showed two main diffraction peaks at the 19-23° (2θ) region in the XRD spectrum, which is the characteristic of the semi-crystalline and polymorphic type. This is a characteristic response of lipid excipients used in the preparation of nanostructured lipid carrier systems, where the presence of α, β and β polymorphic forms leads to lattice defects, which in turn increase the drug accommodation capacity of the matrix. The blank formulation (lipid matrix without drug) showed a diffraction pattern very similar to that of the pure Precirol®, indicating that the lipid matrix retained their crystalline characteristics during the formulation process, and that the addition of surfactants (Tween 80 and Poloxamer 188) and cosurfactant (Transcutol® P) did not significantly change the solid-state properties of the lipids [125].

The XRD diffractogram of the optimized formulation of NLCs loaded with norfloxacin, on the other hand, showed a significant decrease in intensity of the characteristic norfloxacin crystalline peaks with a significant increase in the peaks' broadening and in some areas, the complete disappearance of the norfloxacin peaks, which was a scientifically significant observation. The diffraction peaks of the major diffraction angles of norfloxacin were measured and compared to diffraction peaks of pure drug, the results showed that the integrated intensities of the diffraction peaks (at 22.4° and 25.1° 2θ) for the former was reduced by about 85-90% which indicated the profound reduction in the crystallinity of the drug following its incorporation in the lipid matrix. The remaining minor peaks in the formulation are due to the crystalline lipid matrix and not to crystalline drug as it can be seen when compared with the blank formulation pattern.

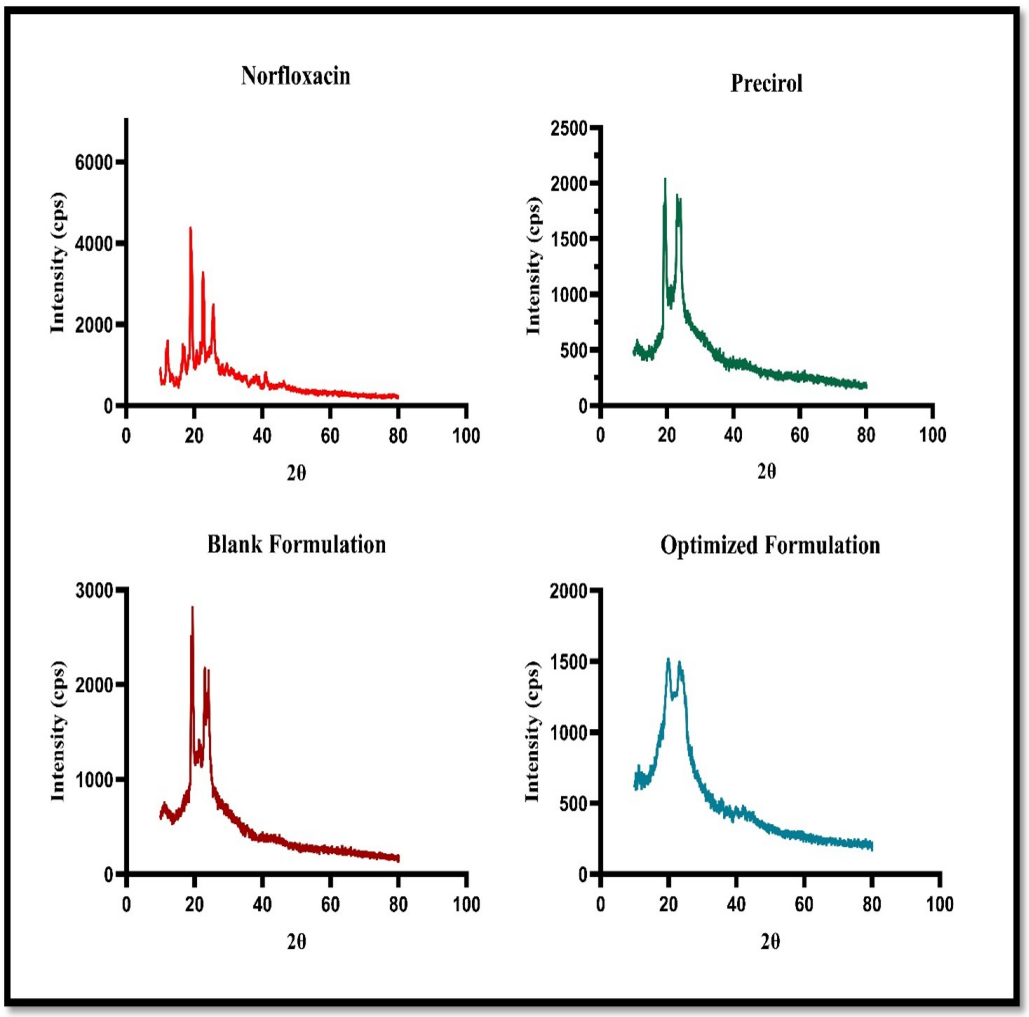

FIGURE 4.5: The XRD spectra of Pure Norfloxacin, pure Precirol, blank formulation and optimized Norfloxacin NLC formulation are shown.

The dramatic drop in crystallinity along with the broadness of the peaks clearly indicate the dispersion or complete amorphisation of a molecule at the molecular level in the NLC matrix. This amorphization has therapeutic relevance because of its direct impact on the apparent aqueous solubility and dissolution rate of this BCS Class IV compound by removing lattice energy barriers related to the dissolution of the crystalline drug [126, 127]. This "imperfect crystal" architecture is obtained by mixing the solid lipid (Precirol® ATO5) with the liquid lipid (Labrafac® WL1349), which provides the structural imperfections and cavities which accommodate the drug molecules in a molecularly dispersed state in the NLC system, thereby preventing recrystallization and maintaining the amorphous form during the formulation process [128].

4.7 Differential Scanning Calorimetry

Differential scanning calorimetry (DSC) was used to investigate the physical state of norfloxacin in the optimized NLC formulation and also to detect any possible thermal interaction between the drug and the ingredients of the lipid matrix. The thermograms shown in Figure 4.6 depict distinctive thermal events that can be correlated with the mechanism of solid-state changes that occur during incorporation of norfloxacin into the nanostructured lipid carrier [129].

The DSC thermogram of pure norfloxacin showed a single sharp endothermic melting peak around 220.0 ± 0.5°C (onset at 217.2°C; enthalpy $\Delta H = 145.8 \pm 2.3$ J/g), which is typical of a high degree of crystallinity in the anhydrous form. This melting transition is in good agreement with crystalline structure detected by XRD and is taken as a definitive thermal signature of the pure drug. The narrow peak width and high enthalpy value indicates that it is an ordered thermodynamically stable, crystalline structure. Pure Precirol® ATO5's thermogram revealed a broad endothermic peak at around 35–65°C, which is the temperature range for the melting of the lipid matrix. This broadness is well documented in glyceryl palmitostearate based lipids and is due to the melting of the lipids which is a complex mixture of mono-, di-, and triglycerides and the presence of multiple polymorphic forms (α, β, β) with different melting temperatures. The polymorphicity of Precirol® ATO5 is especially beneficial in the case of drug encapsulation because the coexistence of these polymorphs involves lattice defects that serve as extra cavities for the accommodation of drug molecules and increase the entrapment efficiency [21].

The drug free blank formulation (Precirol® ATO5 based lipid matrix containing the surfactants and co-surfactant) showed a similar wide endothermic curve, suggesting that the presence of Tween 80, Poloxamer 188, and Transcutol® P did not affect the intrinsic thermal behavior of the lipid matrix. No other thermal events are observable for the blank formulation which allows the conclusion that all excipients are chemically compatible and that no thermally induced interactions occur between excipients.

Interestingly, there was no endotherm peak of norfloxacin in the thermogram of the optimized norfloxacin-loaded NLC formulation. No thermal events corresponding to crystalline drug were detected, only the melting transition of the lipid part (centered at about 50–55°C). The norfloxacin melting endotherm is completely abolished, indicating that a significant solid-state change has occurred. It states that the crystalline drug is no longer present in its bulk crystalline state but in the amorphous state or molecularly dispersed state in the lipid matrix as a result of the formulation process [130]. The fact that none of the exothermic recrystallization events occur upon heating also indicates that the amorphous drug is physically stable in the lipid carrier over the temperature range studied. The lipid matrix itself is probably important in stabilizing the amorphous form of norfloxacin because of the polymorphic coexistence that creates the lattice defects. This physical stabilization is essential to obtain and maintain the improvement in solubility and dissolution rate which is the ultimate aim of formulation drug that is poorly water-soluble into NLC system [131].

The drug-loaded formulation's and blank formulation's DSC thermograms did not show any significant difference between the melting endotherm of the lipid melting peak (T peak blank = 52.7°C; T_peak loaded = 53.1°C; $\Delta T < 0.5$°C), suggesting that the incorporation of the drug did not affect the essential structure of the lipid matrix. Incorporation of the drug molecules into the lipid lattice is shown by the slight broadening of the lipid melting transition in the drug-loaded formulation ($\Delta T\_1/2$ of 8.2°C to 10.5°C), which is consistent with the increasing structural heterogeneity of the drug-lipid system and decreasing cooperative melting of the lipid matrix [132].

The DSC results are very complementary and are a direct complement to the FTIR and XRD data. Though FTIR showed that the drug's structure unaffected, and XRD confirmed the absence of long-range crystalline order, the drug's physical state was affected, and DSC revealed the complete disappearance of the drug crystallinity and the thermal stability of the amorphous state. The amorphization, which occurs during the formulation and is stabilized by the lipid matrix, is the basis for the promises of the system for enhanced biopharmaceutical performance.

A combination of spectroscopic and thermal data provides strong evidence of the successful incorporation of norfloxacin in a stable, nanostructured lipid carrier system with reduced crystallinity and uniform molecular dispersion [133].

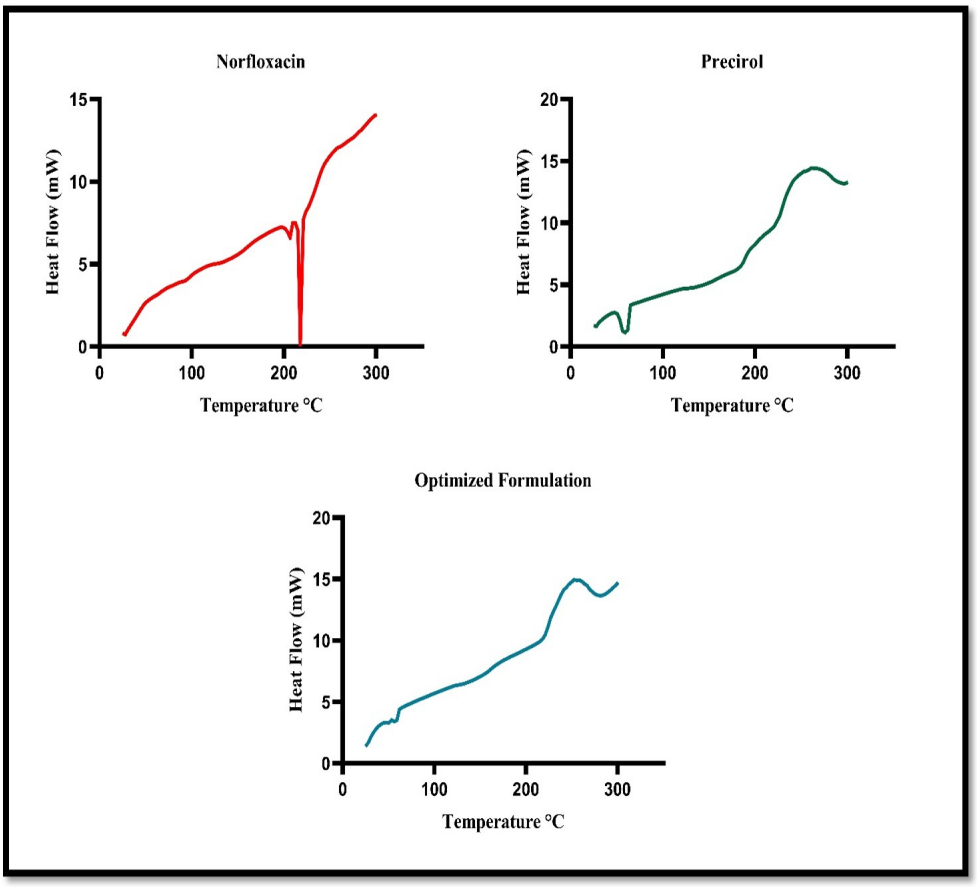

FIGURE 4.6: DSC showing thermograms of pure Norfloxacin, pure Precirol®, and optimized Norfloxacin-loaded in NLCs.

4.8 Physical Evaluation of NLC Carbopol 940 Gel

The optimized norfloxacin loaded NLC dispersion (F1) was then added to the Carbopol 940 hydrogel to prepare a semi-solid topical formulation (F1). Physical properties of the gel were successfully evaluated systematically to ensure its suitability for topical application on wound and the results are presented in Table 4.4.

The optimized F1 gel showed translucent to slightly opaque with pale yellow coloration which is due to the uniform dispersion of norfloxacin loaded NLC dispersion in the Carbopol 940 polymer matrix. Visual inspection on white and black background was performed to verify a homogeneous smooth gel, free of aggregates, grittiness, phase separation and entrapped air bubbles. This appearance indicates successful and stable incorporation of the NLC dispersion in the polymer network suggesting that the nanocarriers did not aggregate or precipitate during gelation. A homogeneous appearance is observed which shows successful and reproducible neutralization of the carboxyl groups of the Carbopol 940 polymer, a derivative of polyacrylic acid with crosslinked functionality, to form a structured gel network [134].

The pH of the F1 gel was determined as 6.21 ± 0.02 (mean ± SD, n = 3) which is inside the physiologically acceptable range for topical application into wounds (pH 5.5–7.0). This pH is advantageous because: (i) it is compatible with the pH of the wound microenvironment and did not cause any local irritation or change in the normals wound healing; (ii) it maintains the antibacterial activity of norfloxacin which is known to be active and stable at a pH range of 5.0–7.0; and (iii) it is within the pH range of unionized/zwitterionic form of norfloxacin which is known to improve the permeation of the membrane and antibacterial activity ($pK_{a1} \approx 6.35$, $pKa_2 \approx 8.80$). The pH was consistent throughout the three batches prepared independently (RSD$<$ 0.5%) which indicated the reproducibility of the neutralization process and the robustness of the gel system [48].

The F1 gel's viscosity was measured at various spindle speeds (0.5 to 100 rpm) by using Brookfield DV-II Pro viscometer (spindle S64). The apparent viscosity at 0.5 rpm was 12,900 ± 150 cP (mean ± SD, n = 3), which is thick and semi-solid to provide adequate retention on the wound surface and prevent the gel from running off when it is applied [135].

The rheological study indicated that the F1 gel is pseudoplastic (non-Newtonian) in nature as apparent viscosity decreased with increasing shear rate. This shear thinning effect has been observed in gels based on Carbopol 940 and is attributed

to the shearing out of the Carbopol polymer chains parallel to the flow direction and the breaking of intermolecular hydrogen bonding. The viscosity data were fitted to the power law model (= Kn), and the flow index (n) obtained was 0.55 ± 0.02 (mean ± SD, n = 3). This indicates that n < 1.0, confirming non-Newtonian pseudoplastic behavior, in agreement with the well documented rheological properties of the Carbopol 940 gels [136].

That is a clinically beneficial rheological profile for a number of reasons. Gels at rest (low shear rate) have the viscosity to keep the gel in contact with the wound site for extended periods without the drug being washed out with wound exudate, or rubbed off mechanically. In application (high shear rate), the gel flows easily at the mechanical shear rate applied during spreading; leading to smooth and even application without excessive spreading pressure, thus enhancing patient comfort and compliance. The pseudo-plastic properties enable the rapid recovery of viscosity once shearing forces removed after application, so that the gel stays semi-solid and protects the wound site. The NLC dispersion maintained the shear-thinning nature of Carbopol 940 polymer network without any disruption of the network during the evaluation period. This is in line with the reported results for the NLC-Carbopol gel formulations in the literature and suggests that the incorporation of lipid nanoparticles does not affect the rheological properties which are required in the case of topical application [137].

Spreadability of F1 gel was assessed by horizontal glass plate method (weighted glass plate method). A 1 g portion of the gel was accurately weighed and positioned on a pre-marked glass plate (1 cm diameter and used as a loading template to standardize the placement of the sample) and a second glass plate (50 g) was carefully placed on top. The increase in diameter was measured after 5 minutes, and the formula used to calculate spreadability was S = (M × L) / T, where M is the weight applied (50 g), L is the spread diameter (cm) following the weight application, and T is the weight application duration (s). The spreadability of the F1 gel was 6.6 ± 0.15 g·cm/s (mean ± SD, n = 3), and was excellent in terms of ease of spreading with minimal mechanical force. This is important for patient acceptance because it allows for even drug distribution, maximum penetration of

irregular wound surfaces, and minimal application discomfort. The spreadability value was in the optimum range reported for topical semi-solid formulation (5–8 g·cm/s) which indicates that the gel had the suitable consistency for easy and effective wound application [138].

Extrudability was evaluated by filling collapsible tubes with F1 gel and applying constant pressure to the tubes to expel 1 g of gel (g/cm^2). The extrudability of the F1 gel was found to be 17 ± 2 g (mean ± SD, n = 3), which was within the acceptable force range for extrusion that would allow for the practical use of the gel under clinical conditions for wound care and patient compliance. It is in the range of extrudability indicated for semi-solid topical formulations (15–20 g), demonstrating that the gel can be readily extruded from regular tubes without losing its structure [139].

The complete physical evaluation reveals that the norfloxacin NLC Carbopol 940 gel exhibits the desirable pharmaceutical quality parameters required for effective application on wound topically. The F1 gel demonstrated wound-compatible pH (6.21 ± 0.02), adequate shear-thinning viscosity (12,900 ± 150 cP at 0.5 rpm with flow index n = 0.55), satisfactory spreadability (6.6 ± 0.15 g·cm/s), and practical extrudability (17 ± 2 g). These outcomes along with the excellent physicochemical properties of the NLC dispersion, prove the successful development of stable and user-friendly formulation with immense scope for clinical translation in wound infection management.

TABLE 4.4: F1 Norfloxacin NLC Carbopol 940 Gel's Physicochemical and Rheological Evaluation

Parameters	**Results (Mean ± SD)**	**Acceptance Criteria**	**Interpretation**
Appearance	Translucent to slightly opaque, pale yellow, homogeneous	No phase separation, grittiness, or aggregates	Acceptable
pH	6.21 ± 0.02	5.5–7.0	Wound-compatible

Table 4.4 continued from previous page

Parameters	**Results (Mean ± SD)**	**Acceptance Criteria**	**Interpretation**
Viscosity (0.5 rpm)	12,900 ± 150 cP	10,000–15,000 cP	Adequate semi-solid consistency
Rheological behavior	Pseudoplastic (n = 0.55)	n <1.0 (non-Newtonian)	Shear-thinning, clinically favorable
Spreadability	6.6 ± 0.15 g·cm/s	5–8 g·cm/s	Excellent ease of application
Extrudability	17 ± 2 g	15–20 g	Acceptable for practical use
Drug Content	99.4 ± 1.3%	95–105%	Uniform drug distribution

All data are demonstrated as mean ± SD (n = 3). Drug content uniformity was consistent across three independently prepared batches (RSD < 1.5%)

4.9 *Ex Vivo* Skin Permeation Study

The skin permeation behavior of the optimized F1 NLC Carbopol 940 gel and plain norfloxacin gel was studied in an *ex vivo* skin permeation model for 24 h using excised rabbit ear lobe skin mounted vertically on static Franz diffusion cells (effective diffusion area 1.77 cm2) under two physiologically relevant receptor conditions (pH 5.5 simulating acidic microenvironment of infected skin surfaces and pH 7.4 representing deeper dermal tissue). Permeation was shown to be due to the passive diffusion of the drug through an intact stratum corneum, as skin barrier integrity was confirmed before each experiment using transepidermal electrical resistance (TEER > 1000 $\cdot cm^2$). Each donor compartment was given 1 g of the corresponding gel formulation (0.3% w/w norfloxacin; Cd = 3000 μg/mL), and it is several hundred times higher than theMIC_{90} of all target wound pathogens (*S. aureus* 1.0 μg/mL; *P. aeruginosa* 2.0 μg/mL; *E. coli* 0.12 μg/mL). To ensure

sink conditions were maintained, the concentration of the receptor drug was kept below 10% of the equilibrium solubility of norfloxacin throughout [140].

The cumulative permeation profiles for all the formulation-pH groups are shown in Fig. 4.7, and the parameters derived from these profiles are given in Table 4.5. The permeation was in the rank order as: F1 NLC gel 5.5 pH > F1 NLC gel 7.4 pH > plain gel 5.5 pH > plain gel 7.4 pH ($p<0.05$, two-way ANOVA with Tukey's post hoc test) for all time points.

The F1 NLC gel at pH 5.5 attained a Q24 of 179.76 ± 4.18 $\mu g/cm^2$, representing a 2.80-fold enhancement over the plain gel at pH 5.5 (64.18 ± 2.32 $\mu g/cm^2$), a 1.84-fold advantage over the F1 NLC gel at pH 7.4 (97.42 ± 2.78 $\mu g/cm^2$), and a 1.52-fold improvement over the plain gel at pH 7.4 (55.42 ± 2.18 $\mu g/cm^2$).These rank orders were observed as early as t = 0.5 h and were maintained during the 24 h period of testing, indicating that the permeation differentials are stable and dependent on the formulations and pH conditions.

The F1 NLC gel at pH 5.5 exhibited a significant early burst (19.32 ± 1.68 $\mu g/cm^2$ at 0.5 h), attributable to the surface-adsorbed drug fraction and enhanced drug partitioning into the stratum corneum facilitated by the nanometric carrier. Permeation then increased progressively to 119.86 ± 3.14 $\mu g/cm^2$ at 8 h before entering a near-plateau phase, with only a 1.1% increase between 20 h (177.83 ± 4.06 $\mu g/cm^2$) and 24 h (179.76 ± 4.18 $\mu g/cm^2$), indicating steady and sustained drug accumulation within the clinically relevant dosing period.

In contrast, the plain gel at pH 5.5 exhibited a steady linear release profile without an initial burst (8.24 ± 0.86 $\mu g/cm^2$ at 0.5 h; 64.18 ± 2.32 $\mu g/cm^2$ at 24 h). The plain gel at pH 7.4 yielded the lowest cumulative permeation (55.42 ± 2.18 $\mu g/cm^2$ at 24 h), which was 13.6% lower than the same gel at pH 5.5, highlighting the combined inhibitory effect of the conventional formulation and suboptimal pH.

These differences are further evident by steady-state permeation parameters (Table 4.5). The F1 NLC gel at pH 5.5 achieved a Jss of 7.16 ± 0.22 $\mu g/cm^2/h$ and Kp of 2.39 ± 0.07 × 10^{-3} cm/h, compared to 3.88 ± 0.16 $\mu g/cm^2/h$ and 1.29 ±

0.05×10^{-3} cm/h at pH 7.4. The plain gel yielded considerably lower flux values of 2.43 ± 0.14 μg/cm^2/h (pH 5.5) and 1.96 ± 0.11 μg/cm^2/h (pH 7.4), with corresponding Kp of 0.81 ± 0.05 and 0.65 ± 0.04 $\times 10^{-3}$ cm/h respectively. The NLC architecture conferred a 2.95-times flux enhancement under wound-relevant conditions and maintained a 1.60-times advantage even at physiological pH which was confirmed by an enhancement ratio of 0.81 (plain gel, pH 7.4), 1.60 (F1 NLC gel, pH 7.4), and 2.95 (F1 NLC gel, pH 5.5), with the plain gel (pH 5.5) as the reference (ER = 1.00). Of particular interest, the lag times of the F1 NLC gel were much shorter (0.2 ± 0.04 h at pH 5.5; 0.3 ± 0.05 h at pH 7.4) than those of the plain gel (0.8 ± 0.07 h and 1.1 ± 0.09 h, respectively), representing approximately 4-fold faster (pH 5.5) and 3.7-fold faster (pH 7.4) drug onset at the wound surface which is a critical attribute for early antibacterial action ($p < 0.05$).To quantify the intrinsic pH-responsiveness of the optimized NLC system, the pH-flux enhancement ratio (ERpH) was calculated as ERpH = Jss(pH 5.5) / Jss(pH 7.4). Using the values from Table 4.5, this yielded ERpH = 7.16 / 3.88 = 1.85, confirming that the NLC formulation preferentially drives norfloxacin permeation under the acidic condition's characteristic of infected wounds. The mechanistic basis for the observed ERpH of 1.85 is rooted in the ionization behavior of norfloxacin ($pK_{a1} = 6.35$, p$Ka_2 = 8.80$). At pH 5.5, the drug exists predominantly as a cationic species, which enhances its aqueous solubility and creates a steep concentration gradient that favors partitioning into the lipid-rich stratum corneum. Conversely, at pH 7.4—near its isoelectric point (∼7.4-7.5)—norfloxacin adopts a poorly soluble zwitterionic state, significantly reducing its thermodynamic activity and subsequent flux [141]. Despite this inherent pH-dependent solubility barrier, the F1 NLC gel at pH 7.4 still outperformed the plain gel at pH 5.5 (Jss: 3.88 vs. 2.43 μg/cm^2/h; ER: 1.60 vs. 1.00), confirming that the NLC architecture partially overcomes the drug's biopharmaceutical limitations through four synergistic mechanisms: (i) nanometric particle size (102 nm) maximizing contact area with the stratum corneum and enabling both intercellular and transappendageal penetration [142] ; (ii) Transcutol® P transiently fluidizing intercellular lipid lamellae, thereby reducing diffusional resistance of the viable epidermis [143]; (iii) Precirol ATO5 exerting an occlusive effect that increases skin hydration and improves

partitioning thermodynamics [144] ;and (iv) the Carbopol 940 matrix providing mucoadhesive prolongation of tissue contact time to sustain flux over the dosing interval [145].

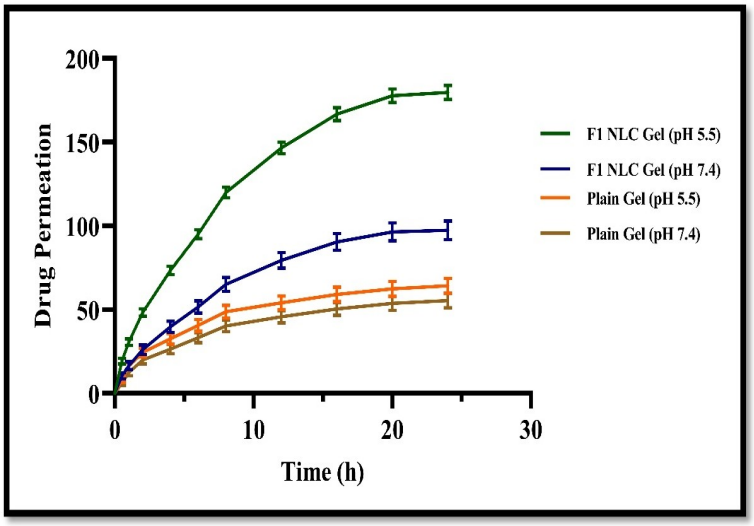

FIGURE 4.7: Drug permeation evaluation of NFX-NLC loaded gel and plain gel at both 5.5 and 7.4 pH

The translational implications of these findings are substantial. Based on Franz cell geometry (area = 1.77 cm^2; receptor volume = 20 mL), the F1 NLC gel at pH 5.5 generated an estimated receptor concentration of ∼15.91 μg/mL—approximately 16-fold and 8-fold higher than theMIC_{90} of *S. aureus* (1.0 μg/mL) and *P. aeruginosa* (2.0 μg/mL), respectively. In contrast, the plain gel at pH 5.5 yielded only ∼5.68 μg/mL, without the advantage of sustained release.

The permeation profile of the F1 NLC gel—maximizing delivery at the infected wound surface (pH 5.0–5.5) while inherently limiting permeation into deeper tissues (pH 7.4)—represents a pharmacokinetically favorable architecture that offers:

(i) targeted high-concentration delivery at the wound surface;

(ii) 24 h sustained permeation supporting once-daily application; and

(iii) a built-in constraint on systemic permeation. The calculated ERpH of 1.85 quantitatively validates this pH-triggered targeting mechanism [146, 147].

TABLE 4.5: Drug permeation parameters of F1 NLC Carbopol 940 gel on excised rabbit ear lobes skin at the two-receptor pH of medium (0.3% w/w norfloxacin; n = 3)

Parameter	**Formula**	**Plain Gel at pH 5.5**	**Plain Gel at pH 7.4**	**F1 NLC Gel at pH 5.5**	**F1 NLC Gel at pH 7.4**	**Significance**
Q24 (μg/cm^2)	Measured at t = 24 h	64.18 ± 2.32	55.42 ± 2.18	179.76 ± 4.18	97.42 ± 2.78	*
Jss (μg/cm^2/h)	Slope, t = 6–16 h	2.43 ± 0.14	1.96 ± 0.11	7.16 ± 0.22	3.88 ± 0.16	*
Tlag (h)	x-intercept, linear regression	0.8 ± 0.07	1.1 ± 0.09	0.2 ± 0.04	0.3 ± 0.05	*
ER	Jss (test) / Jss (Plain pH 5.5)	1 (Reference)	0.81	2.95	1.60	—
Kp ($\times 10^{-3}$ cm/h)	Jss / 3000 μg/mL	0.81 ± 0.05	0.65 ± 0.04	2.39 ± 0.07	1.29 ± 0.05	*

The value is statistically significant if F1 NLC Gel pH 5.5 is different from F1 NLC Gel pH 7.4. ($p < 0.001$), unpaired two-tailed Student's t-test; — means not applicable. Where * = $p < 0.05$, ** = $p < 0.01$, and ***= $p < 0.001$

4.10 Skin Irritation Test

The Draize skin irritation test was used to thoroughly investigate the dermal biocompatibility of the optimized norfloxacin NLC Carbopol 940 gel (F1) on nine

healthy adult New Zealand White rabbits (Oryctolagus cuniculus) [148]. The Research Ethics Committee (REC) of the Faculty of Pharmacy at Capital University of Science and Technology, Islamabad, accepted the study protocol (Approval Ref: REC/FOP/CUST/2025/08). Acclimatization of all animals was accomplished under standardized laboratory conditions (12 h light/dark cycle, 55 ± 5% RH, 22 ± 2°C) with ad libitum access to standard food and water during the entire study period.

The animals were divided into three groups randomly (n = 3 animals each): (i) Test group with optimized formulation of norfloxacin NLC Carbopol 940 gel; (ii) A 0.8% w/v sodium lauryl sulfate (SLS) solution, a known and recognized irritant, was applied to the positive control group; and (iii) Skin sites in the negative control group were left untreated and used as a baseline. Each rabbit's dorsal side was shaved with a special electric clipping machine 24 hours before the formulation was applied and prevented from any skin damage. A fixed area (about 6 cm^2) was marked on the back of each rabbit and an exact dose (0.1 g) of each test substance was spread evenly on the skin with a sterile polypropylene spatula and covered with an occlusion sheet to maintain contact for the 72 hours of observation

The clinical assessment of erythema and edema was done at 24, 48 and 72 hours after application by using the accepted Draize scale (0 = none; 1 = mild; 2 = moderate; 3 = severe). At 72 hours, the scores for erythema and edema were averaged for all animals in each group to obtain the Primary Irritation Index (PII). Based on OECD classification criteria: PII < 0.5 = non-irritant; PII 0.5–2.0 = slightly irritant; PII > 2.0 = moderately to severely irritant[149].

The F1 norfloxacin NLC gel test group showed good dermal biocompatibility during all the observations. There was no erythema or edema noted in any of the three animals at 24, 48 and 72 hours after treatment (Table 4.6). No erythema, edema, or behavioral evidence of irritation (scratching, licking, or restlessness) was observed at any time point, indicating that there was no dermal inflammatory response [150]. The calculated mean Primary Irritation Index (PII) for F1 NLC gel was 0.00 ± 0.00 thus the formulation is unmistakably non-irritant based on OECD

TG404 criteria (PII < 0.5). This classification is a confirmation that norfloxacin NLC Carbopol 940 gel does not cause any detectable inflammatory response when applied topically over intact skin and so it would be safe for repeated application on wounds.

On the other hand, the 0.8% SLS-treated positive control group continuously had notable erythema (2.33 ± 0.58) and mild to moderate edema (1.33 ± 0.58) at 24 hours, which increased and persisted through 48 hours (erythema 3.33 ± 0.58, edema 2.00 ± 0.00) and 72 hours (erythema 2.33 ± 0.58, edema 1.33 ± 0.58). The PII for the SLS-treated group exceeded 2.0, confirming moderate to severe irritant classification and validating the sensitivity of the experimental model.

The negative control (untreated) group showed no erythema or edema at any time point (PII = 0.00), confirming that the shaving and experimental procedures did not themselves induce irritation. Statistical analysis using unpaired two-tailed Student's t-test confirmed a significant difference between the F1 NLC gel and the positive control group at all-time points ($p < 0.001$), while no significant difference was detected between the F1 NLC gel and the negative control group ($p > 0.05$), confirming that the NLC gel does not elicit any detectable inflammatory response.

The favorable dermal safety profile of the norfloxacin NLC Carbopol 940 gel is attributable to the inherent biocompatibility of all excipients employed in the formulation. Precirol ATO5 and Labrafac WL1349 are GRAS (Generally Recognized as Safe)-classified lipid excipients with well-established non-toxic and non-immunogenic profiles in pharmaceutical and cosmetic formulations. Extensive toxicological evaluations have confirmed their lack of dermal irritation, sensitization, and systemic toxicity at concentrations typically employed in topical products [151]. Carbopol 940 is a widely approved pharmaceutical polymer with a long history of safe topical and mucosal application, having been extensively characterized for biocompatibility in numerous dermatological and wound care products [152]. In the optimized formulation, Tween 80 was used as a non-ionic surfactant at a 1.5% w/v concentration, is also similarly recognized as non-irritating at the concentration employed, as supported by its extensive use in parenteral, oral, and

topical pharmaceutical products with established safety profiles [153]. The absence of significant irritation confirms that NLC encapsulation does not introduce new inflammatory or cytotoxic properties, consistent with skin irritation findings reported for NLC–Carbopol gel systems in the literature [154].

The non-irritant classification of the F1 norfloxacin NLC gel, combined with its wound-compatible pH (6.21 ± 0.02), confirms that the formulation is safe for repeated topical application to wound surfaces without risk of local irritation or delayed wound healing as presented in Fig. 4.8.

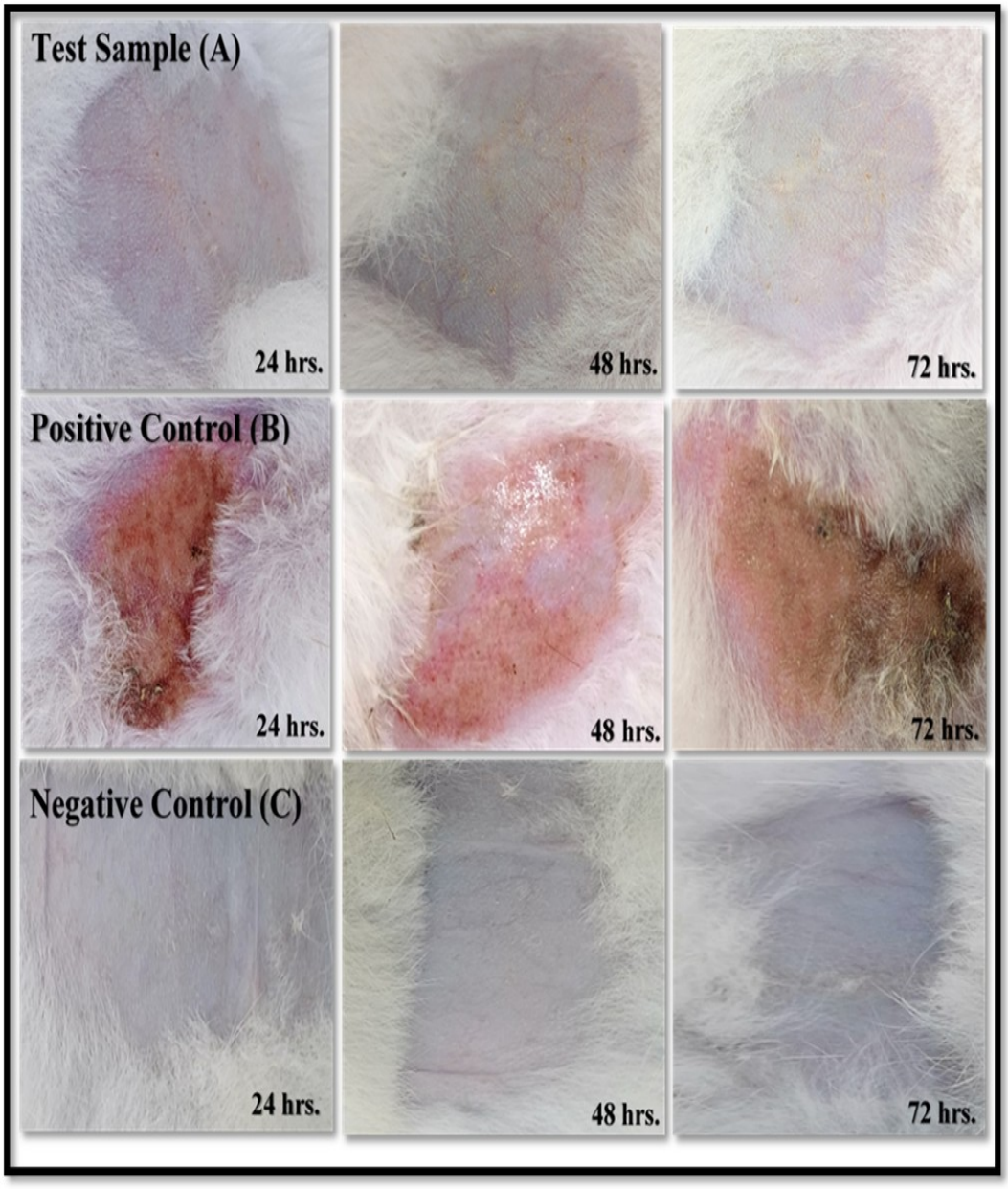

FIGURE 4.8: Test Sample (A), Positive Control (B), and Negative Control (C) showing results of skin irritation on rabbits.

Table 4.6: Skin Irritation Scores at 24 h, 48 h and 72 h in New Zealand White Rabbits

Total Groups	**Rabbit No.**	**Ery 24h**	**Ede 24h**	**Total 24h**	**Ery 48h**	**Ede 48h**	**Total 48h**	**Ery 72h**	**Ede 72h**	**Total 72h**
Test (F1 NLC Gel)	1	0	0	0	0	0	0	0	0	0
	2	0	0	0	0	0	0	0	0	0
	3	0	0	0	0	0	0	0	0	0
	Mean ± SD	0.00±0.00	0.00±0.00	0.00±0.00	0.00±0.00	0.00±0.00	0.00±0.00	0.00±0.00	0.00±0.00	0.00±0.00
Positive Control (SLS)	4	2	1	3	3	2	5	2	1	3
	5	2	1	3	3	2	5	2	1	3
	6	3	2	4	4	2	6	3	2	5
	Mean ± SD	2.33 ± 0.58	1.33 ± 0.58	3.33 ± 0.58	3.33 ± 0.58	2.00 ± 0.00	5.33 ± 0.58	2.33 ± 0.58	1.33 ± 0.58	3.67 ± 1.15
Negative Control	7	0	0	0	0	0	0	0	0	0
	8	0	0	0	0	0	0	0	0	0
	9	0	0	0	0	0	0	0	0	0
	Mean ± SD	0.00±0.00	0.00±0.00	0.00±0.00	0.00±0.00	0.00±0.00	0.00±0.00	0.00±0.00	0.00±0.00	0.00±0.00

The Primary Irritation Index (PII) was calculated as the arithmetic mean of erythema and edema scores across all three animals at 72 hours. For the test group, all scores were 0, yielding PII = 0.00 ± 0.00, unequivocally classifying the formulation as non-irritant according to OECD TG404 criteria (PII < 0.5). For the positive control (0.8% SLS), the mean erythema score was 2.33 ± 0.58 and mean edema score was 1.33 ± 0.58 at 72 hours, yielding a PII > 2.0, confirming moderate to severe irritant classification and validating the sensitivity of the experimental model. No erythema or edema was seen at any time point in the negative control (untreated) group, thus demonstrating that the shaving and experimental procedures alone were not enough to induce erythema or edema.

4.11 Stability Study

The F1 formulation remained clear and homogeneous with no physical changes like phase separation, precipitation, syneresis and colour change when stored in all three conditions at different time periods (0, 1, 2 & 3 months), indicating the physical integrity of the NLC – Carbopol matrix [155]. F1's starting pH was 6.21 ± 0.02. For every storage environment and duration, the pH values were consistently within the permissible pH range of ±0.5 units. A slight progressive decrease in pH has been observed under accelerated conditions (40°C/75% RH) to 6.12 ± 0.03 at 3 months, which may be due to some degree of hydrolytic degradation of the lipid excipients at higher temperatures, producing small amounts of free fatty acids [156].

Viscosity was found to be stable at both refrigerated and ambient temperature with percentage change maintained within the acceptable range of ±10% throughout the study. The viscosity gradually decreased (-%) under accelerated storage condition (40°C/75% RH) but did not exceed pre-specified limit of ±10% after 3 months of storage. This viscosity decrease with high temperature can be explained by a thermal relaxation of the Carbopol 940 polymer network and the decrease of

hydrogen bonding interactions under thermal stress, as reported for polyacrylate-based gels [157, 158].

TABLE 4.7: F1 Norfloxacin NLC Gel stability parameters Under ICH guidelines for three Months

Time (Months)	**Storage Condition**	**Appearance**	**pH ± SD**	**Viscosity (cP) ± SD**	**% Change in Viscosity**
0 (Initial)	Initial	Clear, homogeneous	6.21 ± 0.02	12,900 ± 120	—
1	4 °C	Clear, homogeneous	6.23 ± 0.03	12,810 ± 130	-0.70%
1	25 °C / 60% RH	Clear, homogeneous	6.20 ± 0.03	12,780 ± 140	-0.93%
1	40 °C / 75% RH	Clear, homogeneous	6.16 ± 0.03	12,710 ± 160	-1.47%
2	4 °C	Clear, homogeneous	6.22 ± 0.02	12,740 ± 150	-1.24%
2	25 °C / 60% RH	Clear, homogeneous	6.18 ± 0.02	12,710 ± 150	-1.47%
2	40 °C / 75% RH	Clear, homogeneous	6.14 ± 0.04	12,650 ± 175	-1.94%
3	4 °C	Clear, homogeneous	6.21 ± 0.03	12,685 ± 160	-1.67%
3	25 °C / 60% RH	Clear, homogeneous	6.16 ± 0.03	12,670 ± 160	-1.78%
3	40 °C / 75% RH	Clear, homogeneous	6.12 ± 0.03	12,640 ± 190	-2.02%

The formulation exhibited its pseudoplastic (shear-thinning) behavior under all

storage conditions, which indicated that the structure of the gel matrix was preserved and the dispersion of NLC in the polymer network was physically stable for a long period with no variation in the spreadability and therapeutic performance of the formulation [159].

All % change in viscosity values is calculated relative to the initial viscosity (12,900 ± 120 cP) at t = 0. All parameters remained within acceptable limits: no phase separation, precipitation, or color change observed; viscosity change ≤ ±10%; pH change ≤ ±0.5 units throughout. Data expressed as mean ± SD (n = 3). RH = relative humidity; ICH = International Council for Harmonization.

4.12 Antimicrobial Assay

The norfloxacin Carbopol 940 gel (positive control) and the NFX-NLC gel's antibacterial activity was tested according to the agar well diffusion method against four clinically relevant ATCC wound pathogens. No zone of inhibition (ZOI) was measured within the blank Carbopol gel, blank NLC gel and DMSO against any of the tested organisms at all doses, indicating that only the present antibacterial drug, Norfloxacin was responsible for the antibacterial effect and that the excipient matrix was microbiologically inert [160]. Results are reported in table 4.8 with interpretation. Applying the norfloxacin zone of inhibition thresholds (susceptible ≥ 17 mm, intermediate 13–16 mm, resistant ≤ 12 mm), the NFX-NLC gel rendered all four wound pathogens susceptible across all three tested doses (2.5 mg, 5 mg, and 10 mg). In contrast, the plain NFX Carbopol gel exhibited markedly inferior antibacterial activity, remaining within the resistant range (ZOI ≤ 12 mm) against *S. aureus* and *P. aeruginosa* at all three doses. Against *E. coli* and MRSA, resistant profiles were observed at 2.5 mg and 5 mg; at the highest dose (10 mg), the plain gel reached only the intermediate threshold (ZOI = 13 mm), consistent with the well-documented poor aqueous solubility of norfloxacin as a BCS Class IV drug, which severely limits free-drug bioavailability from conventional gel matrices. The susceptible ZOIs consistently achieved by the NFX-NLC gel against MRSA

(ATCC 43300) align with reports demonstrating that lipid nanoparticle encapsulation markedly enhances norfloxacin activity against resistant Gram-positive and Gram-negative pathogens, and confirm that the NLC platform overcomes the solubility-imposed bioavailability ceiling of plain norfloxacin gel [161].

This significantly enhanced antibacterial activity of the NLC gel could be attributed to various synergistic activities.

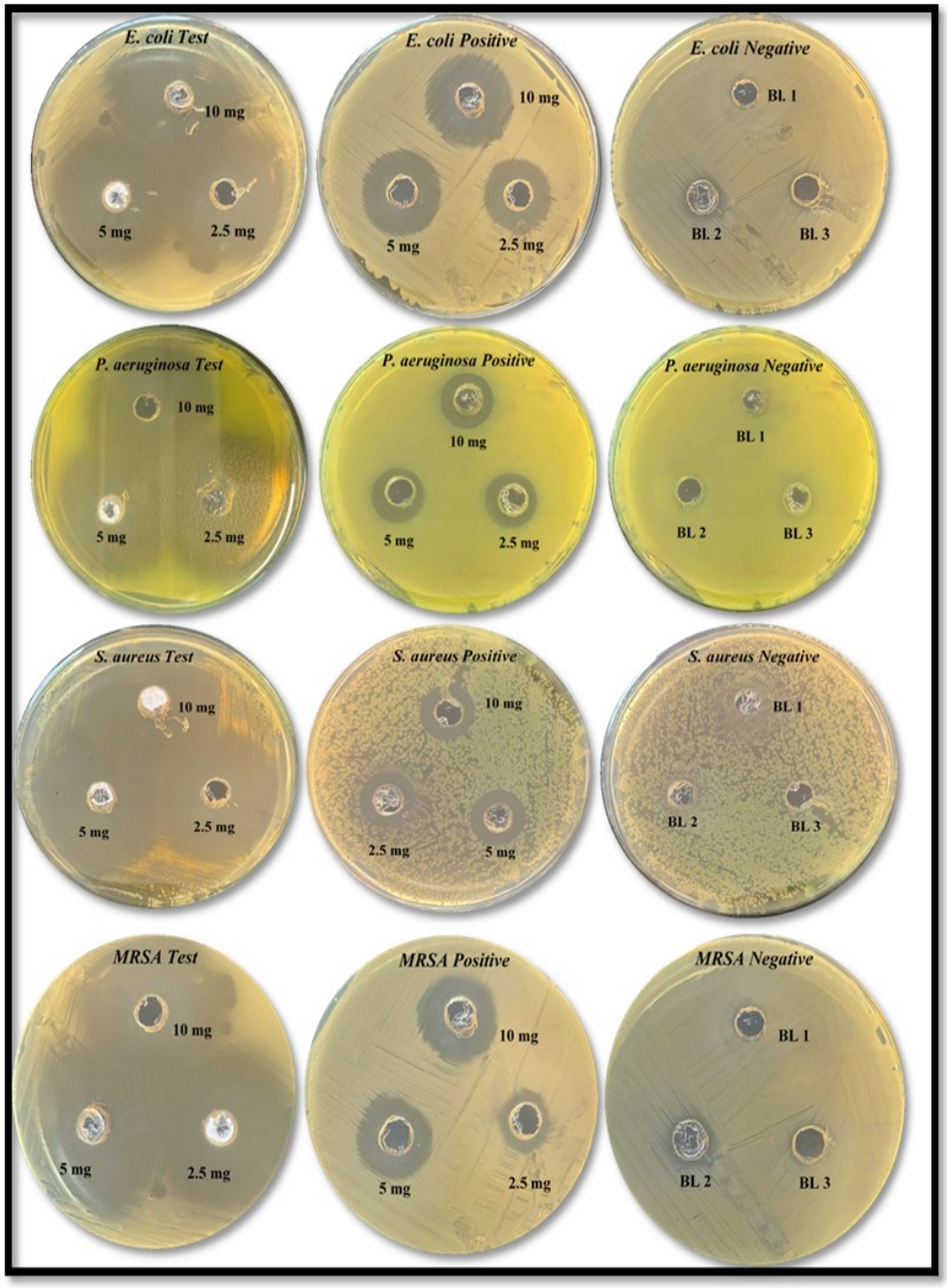

FIGURE 4.9: ZOI of *E. coli*, *P. aeruginosa*, S.aureus, and MRSA test, positive and negative

TABLE 4.8: Zones of Inhibition (mm) for NFX-NLC Gel, Plain NFX Gel, and Negative Controls Against Four Wound-Relevant Reference Organisms at Three Dose Levels, with Interpretation [162].

Test Organism	**Dose (mg)**	**NFX-NLC Gel ZOI (mm)**	**Plain NFX Gel ZOI (mm)**	**Negative Controls ZOI (mm)**	**Interpretation (NFX-NLC Gel)**
E. coli ATCC 25922 (Gram-negative)	2.5	22.0 ± 0.5	8.0 ± 0.3	No ZOI	S (Susceptible)
	5	23.0 ± 0.3	10.0 ± 0.4	No ZOI	S (Susceptible)
	10	24.0 ± 0.4	13.0 ± 0.5	No ZOI	S (Susceptible)
S. aureus ATCC 6538 (Gram-positive)	2.5	21.0 ± 0.3	3.0 ± 0.2	No ZOI	S (Susceptible)
	5	23.0 ± 0.4	5.0 ± 0.3	No ZOI	S (Susceptible)
	10	25.0 ± 0.5	6.0 ± 0.4	No ZOI	S (Susceptible)
P. aeruginosa ATCC 27853 (Gram-negative)	2.5	21.0 ± 0.4	3.0 ± 0.2	No ZOI	S (Susceptible)
	5	22.0 ± 0.3	4.0 ± 0.3	No ZOI	S (Susceptible)
	10	22.0 ± 0.5	6.0 ± 0.3	No ZOI	S (Susceptible)
MRSA ATCC 43300 (Gram-positive)	2.5	22.0 ± 0.4	9.0 ± 0.4	No ZOI	S (Susceptible)
	5	23.0 ± 0.3	11.0 ± 0.3	No ZOI	S (Susceptible)
	10	24.0 ± 0.4	13.0 ± 0.4	No ZOI	S (Susceptible)

Plain NFX gel (equivalent doses) served as positive control; blank Carbopol gel, blank NLC, and DMSO served as negative controls — no measurable ZOI recorded for any organism or dose. NFX = norfloxacin; NLC = nanostructured lipid carrier; ZOI = zone of inhibition; MRSA = methicillin-resistant *Staphylococcus aureus*; S = susceptible.

First, NLC encapsulation keeps norfloxacin in a molecularly dispersed, amorphous state (as confirmed by DSC and XRD) in a lipid core, which increases the apparent aqueous solubility and consequently leads to a higher diffusible free drug concentration at the zone perimeter than the crystalline drug dispersed in the Carbopol matrix of plain gel [163, 164]. Second, nanometric NLC particles (102 nm) move much more freely in the agar gel network as compared to drug in the entangled polyacrylate network of the Carbopol matrix, where the inherently limited aqueous solubility of this BCS Class IV drug reduces the effective inhibitory concentration gradient and diffusion area [165]. Third, the focused delivery to the bacterial membrane interface by concentrated delivery of lipid nanoparticles might further promote increased drug accumulation inside the cell, for example by increasing the partitioning of the drug into the membrane and, speculatively, by partially saturating efflux pump systems (NorA for *S. aureus*, and MexAB-OprM for *P. aeruginosa*), which would be worthy of targeted investigation in future efflux pump inhibition studies [166]. The clinical significance of this transition—from a uniformly resistant/intermediate antibacterial profile (plain gel) to a uniformly susceptible profile (NFX-NLC gel) against all four wound-relevant ATCC pathogens—represents the principal therapeutic value of the NFX-NLC Carbopol 940 gel platform for topical wound infection management [167, 168].

Chapter 5

Conclusion and Future Recommendations

5.1 Conclusion

This study successfully developed and characterized a norfloxacin-loaded nanostructured lipid carrier (NFX-NLC)-based Carbopol 940 gel as a novel topical platform for wound infection management.

The hot homogenization-ultrasonication technique produced well-defined NLC formulations, with the optimized formulation F1 achieving an optimal combination of particle size (102 nm), PDI (0.267), zeta potential (-37.7 mV), and encapsulation efficiency (94.95 ± 0.13%), parameters collectively indicative of a colloidally stable nanosystem with superior drug loading capacity.

The pH-dependent, sustained *in vitro* drug release following anomalous non-Fickian transport kinetics (Korsmeyer–Peppas $R^2 = 0.999$; $n = 0.654$) supports the clinical utility of the formulation in delivering norfloxacin at a higher flux at the wound surface pH (5.5) while maintaining sustained release at the physiological tissue pH (7.4).

FTIR spectroscopy, XRD, and DSC collectively confirmed the successful encapsulation of a chemically stable amorphous form of norfloxacin within the lipid matrix, which markedly enhanced the aqueous solubility and dissolution performance of this BCS Class IV drug. SEM imaging revealed a spherical, compact NLC architecture consistent with the favorable nanometric particle size distribution. The NFX-NLC Carbopol 940 gel demonstrated pseudoplastic rheological behavior, wound-compatible pH, and acceptable spreadability, properties conducive to uniform wound bed application. *Ex vivo* permeation studies confirmed significantly enhanced skin permeation flux compared to plain norfloxacin gel, with a permeation enhancement ratio of 2.95 at pH 5.5 and a pH-flux enhancement ratio of 1.85 between pH 5.5 and pH 7.4, attributed to the synergistic contribution of nanometric particle size, Transcutol P-mediated permeation enhancement, and Precirol ATO5-driven occlusion. Non-irritant classification (Primary Irritation Index = 0.00) was confirmed by skin irritation testing, and physicochemical integrity was validated through 3-month ICH-compliant stability studies conducted under refrigerated (4°C), ambient (25°C/60% RH), and accelerated (40°C/75% RH) conditions. Antibacterial evaluation by agar well diffusion demonstrated susceptible-range zones of inhibition against all four wound pathogens, *S. aureus* (ATCC 6538), MRSA (ATCC 43300), *E. coli* (ATCC 25922), and *P. aeruginosa* (ATCC 27853), at all three tested dose levels, with statistically superior performance over the plain norfloxacin gel. Collectively, these findings establish the NFX-NLC Carbopol 940 gel as a biocompatible, physicochemically stable, and antibacterially potent topical therapeutic platform with strong translational potential for the management of both Gram-positive and Gram-negative wound infections, including those involving resistant pathogens.

5.2 Future Recommendations

The findings of the present study open multiple promising avenues for further investigation, spanning preclinical validation, mechanistic studies, formulation refinement, and clinical translation.

The most immediate and critical next step is validation of antibacterial efficacy and wound healing promotion in well-established preclinical in vivo models. Excisional wound infection models in Sprague-Dawley rats or BALB/c mice using *S. aureus* (ATCC 6538), MRSA (ATCC 43300), *P. aeruginosa* (ATCC 27853), and *E. coli* (ATCC 25922) inoculation should be employed to evaluate bacterial burden reduction, wound contraction rate, re-epithelialization, and collagen deposition, with histopathological scoring as the primary endpoint. Comparative efficacy against marketed topical formulations (e.g., mupirocin 2% ointment, fusidic acid cream) should be included to establish clinical benchmarking.

Wound pathogens, particularly *P. aeruginosa* and MRSA, are predominantly encountered in biofilm rather than planktonic form within chronic wounds, and biofilm inherently confers 10–1000-fold greater antibiotic resistance than planktonic counterparts. Future studies should assess the anti-biofilm activity of the NFX-NLC gel using crystal violet biomass quantification, colony-forming unit enumeration from disrupted biofilms, and confocal laser scanning microscopy (CLSM) with LIVE/DEAD staining. Minimum biofilm eradication concentration (MBEC) should be determined and compared to that of plain norfloxacin gel to quantify the biofilm-disrupting advantage conferred by the NLC system.

While *ex vivo* permeation through porcine ear skin has confirmed enhanced flux, future work should employ human skin equivalents (e.g., EpiDerm™ or StrataTest® models) and confocal microscopy with fluorescently labeled NLCs to delineate the precise permeation pathway, whether follicular, transcellular, or intercellular, and to visualize NLC penetration depth within the stratum corneum and viable epidermis. Tape-stripping studies combined with HPLC drug quantification would further elucidate the depth-concentration profile within skin layers.

Although topical delivery is designed to minimize systemic absorption, quantification of residual systemic norfloxacin levels following topical application of the NFX-NLC gel should be conducted using LC-MS/MS in plasma and organ tissue samples from animal models, to confirm localized action and safety from systemic off-target effects.

Future formulation refinement could incorporate pH-responsive or protease-responsive lipid or polymer coatings on the NLC surface, enabling triggered drug release specifically in response to the elevated proteolytic activity or acidic microenvironment of infected wound beds. Smart NLC systems functionalized with hyaluronic acid, chitosan, or wound-responsive peptides could simultaneously promote wound healing and enhance targeting of drug release to the site of infection.

Given the increasing prevalence of multidrug-resistant wound pathogens, future studies should explore the incorporation of a second antibacterial agent, such as rifampicin or fosfomycin, within the NLC matrix alongside norfloxacin, and evaluate synergistic antibacterial activity using checkerboard assays and fractional inhibitory concentration (FIC) index calculation. The inclusion of silver nanoparticles or zinc oxide nanoparticles as co-encapsulated agents within the lipid matrix warrants investigation as a strategy to broaden coverage and overcome resistance mechanisms.

Transition from laboratory-scale to pilot-scale production using high-pressure homogenization or microfluidic processing should be explored to assess batch-to-batch reproducibility, process scalability, and compliance with Good Manufacturing Practice (GMP) requirements. Quality-by-Design (QbD) frameworks employing Design of Experiments (DoE) with expanded factor ranges should be applied to further delineate the design space and establish robust control strategies.

Following successful in vivo validation, a Phase I/II clinical pilot study in patients with chronic wounds or post-surgical wound infections, particularly those colonized with MRSA or *P. aeruginosa*, would provide definitive evidence of clinical safety, tolerability, patient compliance, and therapeutic efficacy necessary for regulatory submission and commercial development

Bibliography

[1] M. Rodrigues, N. Kosaric, C. A. Bonham, and G. C. Gurtner, "Wound healing: A cellular perspective," *Physiological Reviews*, vol. 99, no. 1, pp. 665–706, 2019.

[2] M. Singh, R. Yadav, A. Rehman, and P. R. Solanki, "Wound healing and management," in *Nanotechnological Aspects for Next-Generation Wound Management*, pp. 55–69, Elsevier, 2024.

[3] R. G. Frykberg and J. Banks, "Challenges in the treatment of chronic wounds," *Advances in Wound Care*, vol. 4, no. 9, pp. 560–582, 2015.

[4] C. K. Sen, "Human wounds and its burden: An updated compendium of estimates," *Advances in Wound Care*, vol. 8, no. 2, pp. 39–48, 2019.

[5] E. Jamil *et al.*, "Integrating clinical data into evidence-based practice: Institutional guideline development for diabetic foot infections," *Frontiers in Endocrinology*, vol. 17, p. 1752211, 2026.

[6] H. Sun *et al.*, "Idf diabetes atlas: Global, regional and country-level diabetes prevalence estimates for 2021 and projections for 2045," *Diabetes Research and Clinical Practice*, vol. 183, p. 109119, 2022.

[7] B. A. Lipsky and C. Hoey, "Topical antimicrobial therapy for treating chronic wounds," *Clinical Infectious Diseases*, vol. 49, no. 10, pp. 1541–1549, 2009.

[8] R. Serra *et al.*, "Chronic wound infections: The role of pseudomonas aeruginosa and staphylococcus aureus," *Expert Review of Anti-infective Therapy*, vol. 13, no. 5, pp. 605–613, 2015.

[9] N. A. Turner *et al.*, "Methicillin-resistant staphylococcus aureus: An overview of basic and clinical research," *Nature Reviews Microbiology*, vol. 17, no. 4, pp. 203–218, 2019.

[10] M. F. Moradali, S. Ghods, and B. H. A. Rehm, "Pseudomonas aeruginosa lifestyle: A paradigm for adaptation, survival, and persistence," *Frontiers in Cellular and Infection Microbiology*, vol. 7, p. 39, 2017.

[11] J. Pardeike, A. Hommoss, and R. H. Müller, "Lipid nanoparticles (sln, nlc) in cosmetic and pharmaceutical dermal products," *International Journal of Pharmaceutics*, vol. 366, no. 1–2, pp. 170–184, 2009.

[12] D. Simões, S. P. Miguel, M. P. Ribeiro, P. Coutinho, A. G. Mendonça, and I. J. Correia, "Recent advances on antimicrobial wound dressing: A review," *European Journal of Pharmaceutics and Biopharmaceutics*, vol. 127, pp. 130–141, 2018.

[13] S. Saghazadeh *et al.*, "Drug delivery systems and materials for wound healing applications," *Advanced Drug Delivery Reviews*, vol. 127, pp. 138–166, 2018.

[14] K. J. Aldred, R. J. Kerns, and N. Osheroff, "Mechanism of quinolone action and resistance," *Biochemistry*, vol. 53, no. 10, pp. 1565–1574, 2014.

[15] A. M. Emmerson and A. M. Jones, "The quinolones: Decades of development and use," *Journal of Antimicrobial Chemotherapy*, vol. 51, no. Suppl. 1, pp. 13–20, 2003.

[16] L. S. Redgrave, S. B. Sutton, M. A. Webber, and L. J. V. Piddock, "Fluoroquinolone resistance: Mechanisms, impact on bacteria, and role in evolutionary success," *Trends in Microbiology*, vol. 22, no. 8, pp. 438–445, 2014.

[17] G. L. Amidon, H. Lennernäs, V. P. Shah, and J. R. Crison, "A theoretical basis for a biopharmaceutic drug classification: The correlation of in

vitro drug product dissolution and in vivo bioavailability," *Pharmaceutical Research*, vol. 12, no. 3, pp. 413–420, 1995.

[18] D. L. Ross and C. M. Riley, "Aqueous solubilities of some variously substituted quinolone antimicrobials," *International Journal of Pharmaceutics*, vol. 63, no. 3, pp. 237–250, 1990.

[19] S. Lohan and M. Bhatia, "Amphotericin b-loaded nanostructured lipid carrier gel: Preparation and evaluation for enhanced skin permeation," *Biomedical and Pharmacology Journal*, vol. 18, no. 2, pp. 1559–1570, 2025.

[20] Y. Cheng *et al.*, "Preparation of norfloxacin-grafted chitosan antimicrobial sponge and its application in wound repair," *International Journal of Biological Macromolecules*, vol. 210, pp. 243–251, 2022.

[21] A. Beloqui, M. Solinís, A. Rodríguez-Gascón, A. J. Almeida, and V. Préat, "Nanostructured lipid carriers: Promising drug delivery systems for future clinics," *Nanomedicine: Nanotechnology, Biology and Medicine*, vol. 12, no. 1, pp. 143–161, 2016.

[22] A. Khosa, S. Reddi, and R. N. Saha, "Nanostructured lipid carriers for site-specific drug delivery," *Biomedicine & Pharmacotherapy*, vol. 103, pp. 598–613, 2018.

[23] R. H. Müller, M. Radtke, and S. A. Wissing, "Solid lipid nanoparticles (sln) and nanostructured lipid carriers (nlc) in cosmetic and dermatological preparations," *Advanced Drug Delivery Reviews*, vol. 54, pp. S131–S155, 2002.

[24] P. Ghasemiyeh and S. Mohammadi-Samani, "Solid lipid nanoparticles and nanostructured lipid carriers as novel drug delivery systems: Applications, advantages and disadvantages," *Research in Pharmaceutical Sciences*, vol. 13, no. 4, pp. 288–303, 2018.

[25] A. Gordillo-Galeano and C. E. Mora-Huertas, "Solid lipid nanoparticles and nanostructured lipid carriers: A review emphasizing on particle structure

and drug release," *European Journal of Pharmaceutics and Biopharmaceutics*, vol. 133, pp. 285–308, 2018.

[26] M. T. Islam, N. Rodriguez-Hornedo, S. Ciotti, and C. Ackermann, "Rheological characterization of topical carbomer gels neutralized to different ph," *Pharmaceutical Research*, vol. 21, no. 7, pp. 1192–1199, 2004.

[27] G. Bonacucina, M. Cespi, M. Misici-Falzi, and G. F. Palmieri, "Rheological, adhesive and release characterisation of semisolid carbopol/tetraglycol systems," *International Journal of Pharmaceutics*, vol. 307, no. 2, pp. 129–140, 2006.

[28] S. Dash, P. N. Murthy, L. Nath, and P. Chowdhury, "Kinetic modeling on drug release from controlled drug delivery systems," *Acta Poloniae Pharmaceutica*, vol. 67, no. 3, pp. 217–223, 2010.

[29] L. Gould *et al.*, "Chronic wound repair and healing in older adults: Current status and future research," *Wound Repair and Regeneration*, vol. 23, no. 1, pp. 1–13, 2015.

[30] S. L. Percival, S. M. McCarty, and B. Lipsky, "Biofilms and wounds: An overview of the evidence," *Advances in Wound Care*, vol. 4, no. 7, pp. 373–381, 2015.

[31] P. Bowler, B. Duerden, and D. G. Armstrong, "Wound microbiology and associated approaches to wound management," *Clinical Microbiology Reviews*, vol. 14, no. 2, pp. 244–269, 2001.

[32] H. Fael, R. Barbas, R. Prohens, C. Ràfols, and E. Fuguet, "Synthesis and characterization of a new norfloxacin/resorcinol cocrystal with enhanced solubility and dissolution profile," *Pharmaceutics*, vol. 14, no. 1, p. 49, 2021.

[33] National Center for Biotechnology Information, "Pubchem compound summary for cid 4539, norfloxacin," 2026. Accessed June 2026.

[34] P. Krzyszczyk, R. Schloss, A. Palmer, and F. Berthiaume, "The role of macrophages in acute and chronic wound healing and interventions to promote pro-wound healing phenotypes," *Frontiers in Physiology*, vol. 9, p. 419, 2018.

[35] S. Chen *et al.*, "Pseudomonas aeruginosa infection alters the macrophage phenotype switching process during wound healing in diabetic mice," *Cell Biology International*, vol. 42, no. 7, pp. 877–889, 2018.

[36] M. Li, Q. Hou, L. Zhong, Y. Zhao, and X. Fu, "Macrophage related chronic inflammation in non-healing wounds," *Frontiers in Immunology*, vol. 12, p. 681710, 2021.

[37] M. Ruffin and E. Brochiero, "Repair process impairment by pseudomonas aeruginosa in epithelial tissues: Major features and potential therapeutic avenues," *Frontiers in Cellular and Infection Microbiology*, vol. 9, p. 182, 2019.

[38] A. Schmidtchen, E. Holst, H. Tapper, and L. Björck, "Elastase-producing pseudomonas aeruginosa degrade plasma proteins and extracellular products of human skin and fibroblasts, and inhibit fibroblast growth," *Microbial Pathogenesis*, vol. 34, no. 1, pp. 47–55, 2003.

[39] T. J. Foster, "Surface proteins of staphylococcus aureus," *Microbiology Spectrum*, vol. 7, no. 4, 2019.

[40] S. Lindsay, A. Oates, and K. Bourdillon, "The detrimental impact of extracellular bacterial proteases on wound healing," *International Wound Journal*, vol. 14, no. 6, pp. 1237–1247, 2017.

[41] S. A. Eming, T. Krieg, and J. M. Davidson, "Inflammation in wound repair: Molecular and cellular mechanisms," *Journal of Investigative Dermatology*, vol. 127, no. 3, pp. 514–525, 2007.

[42] C. Tapeinos, M. Battaglini, and G. Ciofani, "Advances in the design of solid lipid nanoparticles and nanostructured lipid carriers for targeting brain diseases," *Journal of Controlled Release*, vol. 264, pp. 306–332, 2017.

[43] P. Jaiswal, B. Gidwani, and A. Vyas, "Nanostructured lipid carriers and their current application in targeted drug delivery," *Artificial Cells, Nanomedicine, and Biotechnology*, vol. 44, no. 1, pp. 27–40, 2016.

[44] F. Pinto, D. P. de Barros, and L. P. Fonseca, "Design of multifunctional nanostructured lipid carriers enriched with α-tocopherol using vegetable oils," *Industrial Crops and Products*, vol. 118, pp. 149–159, 2018.

[45] C.-L. Fang, S. A. Al-Suwayeh, and J.-Y. Fang, "Nanostructured lipid carriers (nlcs) for drug delivery and targeting," *Recent Patents on Nanotechnology*, vol. 7, no. 1, pp. 41–55, 2013.

[46] P. Costa and J. M. S. Lobo, "Modeling and comparison of dissolution profiles," *European Journal of Pharmaceutical Sciences*, vol. 13, no. 2, pp. 123–133, 2001.

[47] A. Zafar *et al.*, "Preparation of nlcs-based topical erythromycin gel: In vitro characterization and antibacterial assessment," *Gels*, vol. 8, no. 2, p. 116, 2022.

[48] M. Joshi and V. Patravale, "Nanostructured lipid carrier (nlc) based gel of celecoxib," *International Journal of Pharmaceutics*, vol. 346, no. 1–2, pp. 124–132, 2008.

[49] W. A. Mahdi, S. I. Bukhari, S. S. Imam, S. Alshehri, A. Zafar, and M. Yasir, "Formulation and optimization of butenafine-loaded topical nano lipid carrier-based gel: Characterization, irritation study, and anti-fungal activity," *Pharmaceutics*, vol. 13, no. 7, p. 1087, 2021.

[50] P. Shettigar, M. Koland, S. Sindhoor, and A. Prabhu, "Formulation and evaluation of clarithromycin loaded nanostructured lipid carriers for the treatment of acne," *Journal of Pharmaceutical Research International*, vol. 33, pp. 26–38, 2021.

[51] P. H. Joshi *et al.*, "Gatifloxacin loaded nano lipid carriers for the management of bacterial conjunctivitis," *Antibiotics*, vol. 12, no. 8, p. 1318, 2023.

[52] S. Lohan and M. Bhatia, "Amphotericin b-loaded nanostructured lipid carrier gel: Preparation and evaluation for enhanced skin permeation," *Biomedical and Pharmacology Journal*, vol. 18, no. 2, 2025.

[53] V. Dave, K. Kushwaha, R. B. Yadav, and U. Agrawal, "Hybrid nanoparticles for the topical delivery of norfloxacin for the effective treatment of bacterial infection produced after burn," *Journal of Microencapsulation*, vol. 34, no. 4, pp. 351–365, 2017.

[54] K. H. A. Mohammed, F. Rasslan, M. A. Abd El-Fattah, S. Shawky, O. M. Amin, and H. A. Eassa, "Treating burn infections with topical delivery of positively charged norfloxacin-loaded lipid-polymer hybrid nanoparticles," *Recent Advances in Drug Delivery and Formulation*, vol. 19, no. 2, pp. 142–155, 2025.

[55] A. M. Kamal El-Sagheir *et al.*, "Rational design, synthesis, molecular modeling, biological activity, and mechanism of action of polypharmacological norfloxacin hydroxamic acid derivatives," *RSC Medicinal Chemistry*, vol. 14, no. 12, pp. 2593–2610, 2023.

[56] S.-F. Ng, J. J. Rouse, F. D. Sanderson, V. Meidan, and G. M. Eccleston, "Validation of a static franz diffusion cell system for in vitro permeation studies," *AAPS PharmSciTech*, vol. 11, no. 3, pp. 1432–1441, 2010.

[57] S. Zsikó, E. Csányi, A. Kovács, M. Budai-Szűcs, A. Gácsi, and S. Berkó, "Methods to evaluate skin penetration in vitro," *Scientia Pharmaceutica*, vol. 87, no. 3, p. 19, 2019.

[58] International Council for Harmonisation of Technical Requirements for Pharmaceuticals for Human Use (ICH), "Ich guideline q1a(r2): Stability testing of new drug substances and products," 2003. Current Step 4.

[59] J. Hurler, A. Engesland, B. Poorahmary Kermany, and N. Škalko Basnet, "Improved texture analysis for hydrogel characterization: Gel cohesiveness, adhesiveness, and hardness," *Journal of Applied Polymer Science*, vol. 125, no. 1, pp. 180–188, 2012.

[60] Y. Wang *et al.*, "Preparation and stability study of norfloxacin-loaded solid lipid nanoparticle suspensions," *Colloids and Surfaces B: Biointerfaces*, vol. 98, pp. 105–111, 2012.

[61] M. Kravicz *et al.*, "Nanostructured lipid carrier formulation for delivering poorly water-soluble itf3756 hdac inhibitor," *Journal of Drug Delivery Science and Technology*, vol. 101, p. 106238, 2024.

[62] M. Cirri *et al.*, "Design, characterization and in vivo evaluation of nanostructured lipid carriers (nlc) as a new drug delivery system for hydrochlorothiazide oral administration in pediatric therapy," *Drug Delivery*, vol. 25, no. 1, pp. 1910–1921, 2018.

[63] Y. Rizikiyan, N. Sugihartini, and I. R. Rais, "Nanostructured lipid carrier (nlc) in topical preparations: A narrative review of components, manufacturing methods, characteristics and activities," *Jurnal Ilmu Kefarmasian Indonesia*, vol. 23, no. 1, pp. 138–156, 2025.

[64] Z. Dong, S. Xie, L. Zhu, Y. Wang, X. Wang, and W. Zhou, "Preparation and in vitro, in vivo evaluations of norfloxacin-loaded solid lipid nanoparticles for oral delivery," *Drug Delivery*, vol. 18, no. 6, pp. 441–450, 2011.

[65] C.-G. Coman *et al.*, "Chitosan-electrospun fibers encapsulating norfloxacin: The impact on the biochemical, oxidative and immunological profile in a rats burn model," *International Journal of Molecular Sciences*, vol. 25, no. 23, p. 12709, 2024.

[66] H. M. Eid, M. O. Mahmoud, H. M. Aboud, F. E. Ali, A. M. A. Ali, and A. A. Azouz, "Tunable nanospanlastics for 18α-glycyrrhetinic acid brain targeted delivery to manage cognitive deficits and misfolded protein aggregates in alzheimer's disease: In vitro optimization and in vivo pharmacodynamics assessment," *Journal of Drug Delivery Science and Technology*, vol. 116, p. 107959, 2026.

[67] E. Subroto, R. Andoyo, and R. Indiarto, "Solid lipid nanoparticles: Review of the current research on encapsulation and delivery systems for active and antioxidant compounds," *Antioxidants*, vol. 12, no. 3, p. 633, 2023.

[68] A. Rani *et al.*, "Nanostructured lipid carriers (nlc)-based topical formulation of hesperidin for effective treatment of psoriasis," *Pharmaceutics*, vol. 17, no. 4, p. 478, 2025.

[69] N. V. Shah, A. K. Seth, R. Balaraman, C. J. Aundhia, R. A. Maheshwari, and G. R. Parmar, "Nanostructured lipid carriers for oral bioavailability enhancement of raloxifene: Design and in vivo study," *Journal of Advanced Research*, vol. 7, no. 3, pp. 423–434, 2016.

[70] E. Binazir, B. Ghanbarzadeh, S. Hanifian, M. Gharekhani, H. S. Kafil, and P. M. Falcone, "Development and optimization of thyme–pennyroyal essential oils based active nanostructured lipid carrier (nlc) containing saffron extract with antioxidant and antimicrobial properties," *Food Bioscience*, vol. 61, p. 104992, 2024.

[71] Y.-C. Pyo, P. Tran, D.-H. Kim, and J.-S. Park, "Chitosan-coated nanostructured lipid carriers of fenofibrate with enhanced oral bioavailability and efficacy," *Colloids and Surfaces B: Biointerfaces*, vol. 196, p. 111331, 2020.

[72] F. Dehghani, N. Farhadian, V. M. Goyonlo, and O. Ahmadi, "A novel topical formulation of the leishmaniasis drug glucantime as a nanostructured lipid carrier-based hydrogel," *The American Journal of Tropical Medicine and Hygiene*, vol. 109, no. 2, pp. 301–309, 2023.

[73] H. Raza *et al.*, "In vitro and ex vivo evaluation of fluocinolone acetonide–acitretin-coloaded nanostructured lipid carriers for topical treatment of psoriasis," *Gels*, vol. 8, no. 11, p. 746, 2022.

[74] M. M. Wen, I. A. Abdelwahab, R. G. Aly, and S. A. El-Zahaby, "Nanophytogel against multi-drug resistant pseudomonas aeruginosa burn wound infection," *Drug Delivery*, vol. 28, no. 1, pp. 463–477, 2021.

[75] C. Upadhyay, D. Pathak, and M. Kulshreshtha, "Preparation and evaluation of different herbal gels synthesized from chinese medicinal plants as antimicrobial agents," *Pharmacological Research – Modern Chinese Medicine*, vol. 9, p. 100313, 2023.

[76] S. B. Wankhede, A. Prakash, B. Kumari, and S. S. Chitlange, "Simultaneous spectrophotometric estimation of norfloxacin and ornidazole in tablet dosage form," *Indian Journal of Pharmaceutical Sciences*, vol. 71, no. 3, pp. 325–328, 2009.

[77] V. Salve, R. Mishra, and T. Nandgude, "Development and optimization of a floating multiparticulate drug delivery system for norfloxacin," *Turkish Journal of Pharmaceutical Sciences*, vol. 16, no. 3, pp. 326–334, 2019.

[78] A. M. Al-Mahallawi, O. M. Khowessah, and R. A. Shoukri, "Nano-transfersomal ciprofloxacin loaded vesicles for non-invasive trans-tympanic ototopical delivery: In vitro optimization, ex vivo permeation studies, and in vivo assessment," *International Journal of Pharmaceutics*, vol. 472, no. 1–2, pp. 304–314, 2014.

[79] N. Okur, V. Yozgatli, and M. E. Okur, "In vitro–in vivo evaluation of tetrahydrozoline-loaded ocular in situ gels on rabbits for allergic conjunctivitis management," *Drug Development Research*, vol. 81, no. 6, pp. 716–727, 2020.

[80] S. Sindhoor and M. Koland, "Topical delivery of apremilast loaded nanostructured lipid carrier based hydrogel for psoriasis therapy," *Journal of Pharmaceutical Research International*, vol. 33, pp. 7–20, 2021.

[81] Organisation for Economic Co-operation and Development, *OECD Test No. 404: Acute Dermal Irritation/Corrosion*. Paris: OECD Publishing, 2015.

[82] C. Charmeau-Genevois, S. Sarang, M. Perea, C. Eadsforth, T. Austin, and P. Thomas, "A simplified index to quantify the irritation/corrosion potential of chemicals – part i: Skin," *Regulatory Toxicology and Pharmacology*, vol. 123, p. 104922, 2021.

[83] M. I. Siddique, H. Katas, M. C. I. M. Amin, S.-F. Ng, M. H. Zulfakar, and A. Jamil, "In vivo dermal pharmacokinetics, efficacy, and safety of skin targeting nanoparticles for corticosteroid treatment of atopic dermatitis," *International Journal of Pharmaceutics*, vol. 507, no. 1–2, pp. 72–82, 2016.

[84] B. Aldhubiab, R. M. Almuqbil, T. M. Shehata, W. E. Soliman, and H. S. Elsewedy, "Nanotechnological prospective for enhancing the antibacterial activity of mupirocin and cinnamon essential oil: A combination therapy," *Frontiers in Pharmacology*, vol. 15, p. 1468374, 2024.

[85] M. Balouiri, M. Sadiki, and S. K. Ibnsouda, "Methods for in vitro evaluating antimicrobial activity: A review," *Journal of Pharmaceutical Analysis*, vol. 6, no. 2, pp. 71–79, 2016.

[86] A. Khanna *et al.*, "Exploring norfloxacin analogs in combating antimicrobial resistance: Design, mechanistic insights and structure activity relationship," *Future Medicinal Chemistry*, vol. 17, no. 14, pp. 1739–1755, 2025.

[87] Y. Guo *et al.*, "Design and synthesis of new norfloxacin-1,3,4-oxadiazole hybrids as antibacterial agents against methicillin-resistant staphylococcus aureus (mrsa)," *European Journal of Pharmaceutical Sciences*, vol. 136, p. 104966, 2019.

[88] F. Tamjidi, M. Shahedi, J. Varshosaz, and A. Nasirpour, "Nanostructured lipid carriers (nlc): A potential delivery system for bioactive food molecules," *Innovative Food Science & Emerging Technologies*, vol. 19, pp. 29–43, 2013.

[89] M. Deaconu *et al.*, "Norfloxacin delivery systems based on mcm-type silica carriers designed for the treatment of severe infections," *Materials Chemistry and Physics*, vol. 238, p. 121886, 2019.

[90] A. Czajkowska-Kośnik, M. Szekalska, and K. Winnicka, "Nanostructured lipid carriers: A potential use for skin drug delivery systems," *Pharmacological Reports*, vol. 71, no. 1, pp. 156–166, 2019.

[91] M. N. Pereira *et al.*, "Nanostructured lipid carriers for hair follicle-targeted delivery of clindamycin and rifampicin to hidradenitis suppurativa treatment," *Colloids and Surfaces B: Biointerfaces*, vol. 197, p. 111448, 2021.

[92] R. H. Müller, U. Alexiev, P. Sinambela, and C. M. Keck, "Nanostructured lipid carriers (nlc): The second generation of solid lipid nanoparticles," in *Percutaneous Penetration Enhancers Chemical Methods in Penetration Enhancement: Nanocarriers*, pp. 161–185, Springer, 2016.

[93] T. Waghule *et al.*, "Voriconazole loaded nanostructured lipid carriers based topical delivery system: Qbd based designing, characterization, in vitro and ex vivo evaluation," *Journal of Drug Delivery Science and Technology*, vol. 52, pp. 303–315, 2019.

[94] S. A. Breda, A. F. Jimenez-Kairuz, R. H. Manzo, and M. E. Olivera, "Solubility behavior and biopharmaceutical classification of novel high-solubility ciprofloxacin and norfloxacin pharmaceutical derivatives," *International Journal of Pharmaceutics*, vol. 371, no. 1–2, pp. 106–113, 2009.

[95] S. A. Wissing and R. H. Müller, "The influence of solid lipid nanoparticles on skin hydration and viscoelasticity: An in vivo study," *European Journal of Pharmaceutics and Biopharmaceutics*, vol. 56, no. 1, pp. 67–72, 2003.

[96] C. Mendes, G. C. Meirelles, M. A. Silva, and G. Ponchel, "Intestinal permeability determinants of norfloxacin in ussing chamber model," *European Journal of Pharmaceutical Sciences*, vol. 121, pp. 236–242, 2018.

[97] S. Doktorovova, A. B. Kovačević, M. L. Garcia, and E. B. Souto, "Preclinical safety of solid lipid nanoparticles and nanostructured lipid carriers: Current evidence from in vitro and in vivo evaluation," *European Journal of Pharmaceutics and Biopharmaceutics*, vol. 108, pp. 235–252, 2016.

[98] M. L. Bruschi, *Strategies to Modify the Drug Release from Pharmaceutical Systems*. Woodhead Publishing, 2025.

[99] C. Varrica, M. Carvalheiro, C. Faria-Silva, C. Eleutério, G. Sandri, and S. Simões, "Topical allopurinol-loaded nanostructured lipid carriers: A novel approach for wound healing management," *Bioengineering*, vol. 8, no. 12, p. 192, 2021.

[100] K.-W. Wu *et al.*, "Primaquine loaded solid lipid nanoparticles (sln), nanostructured lipid carriers (nlc), and nanoemulsion (ne): Effect of lipid matrix and surfactant on drug entrapment, in vitro release, and ex vivo hemolysis," *AAPS PharmSciTech*, vol. 22, no. 7, p. 240, 2021.

[101] G. Zoubari, S. Staufenbiel, P. Volz, U. Alexiev, and R. Bodmeier, "Effect of drug solubility and lipid carrier on drug release from lipid nanoparticles for dermal delivery," *European Journal of Pharmaceutics and Biopharmaceutics*, vol. 110, pp. 39–46, 2017.

[102] W. Zhang, H. Meng, X. Zhou, Z. Zhang, and G. Zhu, "Effect of solid lipids on the properties of nanostructured lipid carriers: Particle size, thermal behavior and crystal structure," *Journal of Thermal Analysis and Calorimetry*, pp. 1–11, 2025.

[103] A. Boreham, P. Volz, D. Peters, C. M. Keck, and U. Alexiev, "Determination of nanostructures and drug distribution in lipid nanoparticles by single molecule microscopy," *European Journal of Pharmaceutics and Biopharmaceutics*, vol. 110, pp. 31–38, 2017.

[104] I. Lacatusu, N. Badea, A. Murariu, and A. Meghea, "The encapsulation effect of uv molecular absorbers into biocompatible lipid nanoparticles," *Nanoscale Research Letters*, vol. 6, no. 1, p. 73, 2011.

[105] V. M. Ghate, S. A. Lewis, P. Prabhu, A. Dubey, and N. Patel, "Nanostructured lipid carriers for the topical delivery of tretinoin," *European Journal of Pharmaceutics and Biopharmaceutics*, vol. 108, pp. 253–261, 2016.

[106] M. Sala, R. Diab, A. Elaissari, and H. Fessi, "Lipid nanocarriers as skin drug delivery systems: Properties, mechanisms of skin interactions and medical

applications," *International Journal of Pharmaceutics*, vol. 535, no. 1–2, pp. 1–17, 2018.

[107] V.-A. Duong, T.-T.-L. Nguyen, and H.-J. Maeng, "Preparation of solid lipid nanoparticles and nanostructured lipid carriers for drug delivery and the effects of preparation parameters of solvent injection method," *Molecules*, vol. 25, no. 20, p. 4781, 2020.

[108] J. Musakhanian, D. W. Osborne, and J.-D. Rodier, "Skin penetration and permeation properties of transcutol® in complex formulations," *AAPS PharmSciTech*, vol. 25, no. 7, p. 201, 2024.

[109] E. Ghasemian, A. Vatanara, A. Rouholamini Najafabadi, M. R. Rouini, K. Gilani, and M. Darabi, "Preparation, characterization and optimization of sildenafil citrate loaded plga nanoparticles by statistical factorial design," *DARU Journal of Pharmaceutical Sciences*, vol. 21, no. 1, p. 68, 2013.

[110] E. B. Souto *et al.*, "Sln and nlc for topical, dermal, and transdermal drug delivery," *Expert Opinion on Drug Delivery*, vol. 17, no. 3, pp. 357–377, 2020.

[111] S. Nene, S. Shah, N. Rangaraj, N. K. Mehra, P. K. Singh, and S. Srivastava, "Lipid based nanocarriers: A novel paradigm for topical antifungal therapy," *Journal of Drug Delivery Science and Technology*, vol. 62, p. 102397, 2021.

[112] S. Cavalcanti, C. Nunes, S. C. Lima, J. Soares-Sobrinho, and S. Reis, "Optimization of nanostructured lipid carriers for zidovudine delivery using a microwave-assisted production method," *European Journal of Pharmaceutical Sciences*, vol. 122, pp. 22–30, 2018.

[113] Y.-J. Huang and J. Zhang, "Synthesis and characterization of a series of norfloxacin-transition metal complexes," *Inorganica Chimica Acta*, vol. 501, p. 119244, 2020.

[114] A. G. Dias *et al.*, "Nanostructured lipid carriers containing norfloxacin and 2-aminothiophene derivative reduces fluoroquinolone resistance in multidrug-resistant staphylococcus aureus strains by efflux pump inhibition," *Pharmaceutics*, vol. 18, no. 2, 2026.

[115] N. Salahuddin, M. Abdelwahab, M. Gaber, and S. Elneanaey, "Synthesis and design of norfloxacin drug delivery system based on pla/tio$_2$ nanocomposites: Antibacterial and antitumor activities," *Materials Science and Engineering: C*, vol. 108, p. 110337, 2020.

[116] V. L. Beraldo-Araújo *et al.*, "Levofloxacin in nanostructured lipid carriers: Preformulation and critical process parameters for a highly incorporated formulation," *International Journal of Pharmaceutics*, vol. 626, p. 122193, 2022.

[117] N. Erdoğar, B. Gür, and D. Örgül, "Recent developments of novel nanotechnology-based drug delivery systems for dermal and transdermal applications," *European Journal of Pharmaceutical Sciences*, vol. 217, p. 107413, 2026.

[118] Y. Soleimanian, S. A. H. Goli, J. Varshosaz, and S. M. Sahafi, "Formulation and characterization of novel nanostructured lipid carriers made from beeswax, propolis wax and pomegranate seed oil," *Food Chemistry*, vol. 244, pp. 83–92, 2018.

[119] N. Abidi, "Introduction to ftir microspectroscopy," in *FTIR Microspectroscopy: Selected Emerging Applications*, pp. 1–12, Springer, 2022.

[120] M. Yang *et al.*, "Establishment of metrological traceability for fluoroquinolones measurement in monitoring plan of quality and safety for agroproduct in china," *Microchemical Journal*, vol. 177, p. 107315, 2022.

[121] P. O. Ferreira *et al.*, "Norfloxacin cocrystals: Mechanochemical synthesis and scale-up viability through solubility studies," *Journal of Pharmaceutical Sciences*, vol. 112, no. 8, pp. 2230–2239, 2023.

[122] E. M. Elshazly, M. G. Arafa, and S. A. Nour, "Development and optimization of moxifloxacin solid lipid nanoparticles via double emulsion organic solvent free technique applying box–behnken experimental design," *Scientific Reports*, 2025.

[123] R. Bibi, N. Ahmed, D. Khan, S. A. Khan, A. Muhammad, and H. Ullah, "Nlcs based in situ gelling systems for ocular delivery of drug cargo against bacterial conjunctivitis," *Journal of Drug Delivery Science and Technology*, p. 107677, 2025.

[124] W. D. G. Nunes *et al.*, "Thermal, spectroscopic and antimicrobial activity characterization of some norfloxacin complexes," *Journal of Thermal Analysis and Calorimetry*, vol. 132, no. 2, pp. 1077–1088, 2018.

[125] A. Singh, Y. R. Neupane, B. Mangla, and K. Kohli, "Nanostructured lipid carriers for oral bioavailability enhancement of exemestane: Formulation design, in vitro, ex vivo, and in vivo studies," *Journal of Pharmaceutical Sciences*, vol. 108, no. 10, pp. 3382–3395, 2019.

[126] P. Famta *et al.*, "Quality by design (qbd) commended exploration of bosutinib loaded lipid nanocarriers for food effect attenuation and bioavailability enhancement in breast cancer," *Journal of Drug Delivery Science and Technology*, vol. 90, p. 105180, 2023.

[127] S. Ahalwat and D. C. Bhatt, "Development of novel lipid matrix for improved sustained release effect of a hydrophilic drug via response surface methodology," *Journal of Drug Delivery Science and Technology*, vol. 67, p. 102993, 2022.

[128] G. I. Sakellari, I. Zafeiri, H. Batchelor, and F. Spyropoulos, "Formulation design, production and characterisation of solid lipid nanoparticles (sln) and nanostructured lipid carriers (nlc) for the encapsulation of a model hydrophobic active," *Food Hydrocolloids for Health*, vol. 1, p. 100024, 2021.

[129] Y. Deng *et al.*, "Norfloxacin co-amorphous salt systems: Effects of molecular descriptors on the formation and physical stability of co-amorphous systems," *Chemical Engineering Science*, vol. 253, p. 117549, 2022.

[130] D. Omari, A. Sallam, H. Al-Hmoud, and I. Rashid, "Modafinil–excipient compatibility study using differential scanning calorimetry," *Journal of Advanced Pharmaceutical Technology & Research*, vol. 14, no. 2, pp. 75–81, 2023.

[131] R. Chadha and S. Bhandari, "Drug–excipient compatibility screening—role of thermoanalytical and spectroscopic techniques," *Journal of Pharmaceutical and Biomedical Analysis*, vol. 87, pp. 82–97, 2014.

[132] H. Bunjes and T. Unruh, "Characterization of lipid nanoparticles by differential scanning calorimetry, x-ray and neutron scattering," *Advanced Drug Delivery Reviews*, vol. 59, no. 6, pp. 379–402, 2007.

[133] S.-Y. Lin, "Current and potential applications of simultaneous dsc-ftir microspectroscopy for pharmaceutical analysis," *Journal of Food and Drug Analysis*, vol. 29, no. 2, pp. 182–196, 2021.

[134] N. K. Garg, N. Tandel, S. K. Bhadada, and R. K. Tyagi, "Nanostructured lipid carrier–mediated transdermal delivery of aceclofenac hydrogel present an effective therapeutic approach for inflammatory diseases," *Frontiers in Pharmacology*, vol. 12, p. 713616, 2021.

[135] A. Z. M. Badruddoza, T. Yeoh, J. C. Shah, and T. Walsh, "Assessing and predicting physical stability of emulsion-based topical semisolid products: A review," *Journal of Pharmaceutical Sciences*, vol. 112, no. 7, pp. 1772–1793, 2023.

[136] T. Mezger, *The Rheology Handbook: For Users of Rotational and Oscillatory Rheometers*. European Coatings, 5 ed., 2020.

[137] A. Czajkowska-Kośnik, E. Szymańska, and K. Winnicka, "Nanostructured lipid carriers (nlc)-based gel formulations as etodolac delivery: From gel preparation to permeation study," *Molecules*, vol. 28, no. 1, p. 235, 2022.

[138] Y. T. Tan, K. K. Peh, and O. Al-Hanbali, "Effect of carbopol and polyvinylpyrrolidone on the mechanical, rheological, and release properties of bioadhesive polyethylene glycol gels," *AAPS PharmSciTech*, vol. 1, no. 3, p. 24, 2000.

[139] T. Abdullah and K. Al-Kinani, "Propranolol nanoemulgel: Preparation, in vitro and ex vivo characterization for a potential local hemangioma therapy," *Pharmacia*, vol. 71, no. 1, 2024.

[140] D. W. Osborne and J. Musakhanian, "Skin penetration and permeation properties of transcutol®: Neat or diluted mixtures," *AAPS PharmSciTech*, vol. 19, no. 8, pp. 3512–3533, 2018.

[141] H. A. Fathi, A. Allam, M. Elsabahy, G. Fetih, and M. El-Badry, "Nanostructured lipid carriers for improved oral delivery and prolonged antihyperlipidemic effect of simvastatin," *Colloids and Surfaces B: Biointerfaces*, vol. 162, pp. 236–245, 2018.

[142] M. B. Najm, M. Rawas-Qalaji, N. H. Assar, R. Yahia, R. El Hosary, and I. S. Ahmed, "Optimization, characterization and in vivo evaluation of mupirocin nanocrystals for topical administration," *European Journal of Pharmaceutical Sciences*, vol. 176, p. 106251, 2022.

[143] M. Sabzi, M. J. Afshari, M. Babaahmadi, and N. Shafagh, "ph-dependent swelling and antibiotic release from citric acid crosslinked poly(vinyl alcohol) (pva)/nano silver hydrogels," *Colloids and Surfaces B: Biointerfaces*, vol. 188, p. 110757, 2020.

[144] A. Alalaiwe, P.-W. Wang, P.-L. Lu, Y.-P. Chen, J.-Y. Fang, and S.-C. Yang, "Synergistic anti-mrsa activity of cationic nanostructured lipid carriers in combination with oxacillin for cutaneous application," *Frontiers in Microbiology*, vol. 9, p. 1493, 2018.

[145] F. Han *et al.*, "Nanostructured lipid carriers (nlc) based topical gel of flurbiprofen: Design, characterization and in vivo evaluation," *International Journal of Pharmaceutics*, vol. 439, no. 1–2, pp. 349–357, 2012.

[146] N. Ahmadi *et al.*, "Semi-solid dosage forms containing pranoprofen-loaded nlc as topical therapy for local inflammation: In vitro, ex vivo and in vivo evaluation," *Gels*, vol. 9, no. 6, p. 448, 2023.

[147] R. Calderon-Jacinto, P. Matricardi, V. Gueguen, G. Pavon-Djavid, E. Pauthe, and V. Rodriguez-Ruiz, "Dual nanostructured lipid carriers/hydrogel system for delivery of curcumin for topical skin applications," *Biomolecules*, vol. 12, no. 6, p. 780, 2022.

[148] J. P. Rooney *et al.*, "Analysis of variability in the rabbit skin irritation assay," *Regulatory Toxicology and Pharmacology*, vol. 122, p. 104920, 2021.

[149] S. Hussain *et al.*, "Itraconazole-loaded polycaprolactone nanoparticle gel for enhanced transdermal delivery: Development, characterization, and ex vivo evaluation," *International Journal of Nanomedicine*, pp. 15655–15681, 2025.

[150] A. B. Daniel *et al.*, "Retrospective evaluation of the oecd adopted in vitro skin irritation/corrosion tests for agrochemical formulations," *Regulatory Toxicology and Pharmacology*, p. 106122, 2026.

[151] E. Souto and R. H. Müller, "The use of sln® and nlc® as topical particulate carriers for imidazole antifungal agents," *Die Pharmazie*, vol. 61, no. 5, pp. 431–437, 2006.

[152] A. A. Date, M. D. Joshi, and V. B. Patravale, "Parasitic diseases: Liposomes and polymeric nanoparticles versus lipid nanoparticles," *Advanced Drug Delivery Reviews*, vol. 59, no. 6, pp. 505–521, 2007.

[153] A. R. Fernandes *et al.*, "Customized cationic nanoemulsions loading triamcinolone acetonide for corneal neovascularization secondary to inflammatory processes," *International Journal of Pharmaceutics*, vol. 623, p. 121938, 2022.

[154] M. Taheri, M. R. Arabestani, F. Kalhori, S. Soleimani Asl, M. Asgari, and S. M. Hosseini, "Antibiotics-encapsulated nanoparticles as an antimicrobial agent in the treatment of wound infection," *Frontiers in Immunology*, vol. 15, p. 1435151, 2024.

[155] U.S. Food and Drug Administration, "Ich q1a (r2): Stability testing of new drug substances and products," 2003. ICH Guideline.

[156] M. Mahapatra, S. Mohapatra, and G. K. Jena, "Nanostructured lipid carriers: A revolutionary approach in antifungal drug delivery," *Biomedical Materials & Devices*, vol. 4, no. 1, pp. 189–205, 2026.

[157] B. Singh, C. M. Day, S. Abdella, and S. Garg, "Alzheimer's disease current therapies, novel drug delivery systems and future directions for better disease management," *Journal of Controlled Release*, vol. 367, pp. 402–424, 2024.

[158] R. Hamed, A. Kamal, and A. Z. Alkilani, "Gelation and rheological characterization of carbopol® in simulated gastrointestinal fluid of variable chemical properties," *Pakistan Journal of Pharmaceutical Sciences*, vol. 33, no. 3, 2020.

[159] R. Hamed, T. Al Baraghthi, A. Z. Alkilani, and R. Abu-Huwaij, "Correlation between rheological properties and in vitro drug release from penetration enhancer-loaded carbopol® gels," *Journal of Pharmaceutical Innovation*, vol. 11, no. 4, pp. 339–351, 2016.

[160] A. van Belkum *et al.*, "Developmental roadmap for antimicrobial susceptibility testing systems," *Nature Reviews Microbiology*, vol. 17, no. 1, pp. 51–62, 2019.

[161] L. L. Wang, N. Battini, R. R. Y. Bheemanaboina, S. L. Zhang, and C. H. Zhou, "Design and synthesis of aminothiazolyl norfloxacin analogues as potential antimicrobial agents and their biological evaluation," *European Journal of Medicinal Chemistry*, vol. 167, pp. 105–123, 2019.

[162] Clinical and Laboratory Standards Institute, "Performance standards for antimicrobial susceptibility testing," 2011. CLSI document.

[163] P. Ganesan and D. Narayanasamy, "Lipid nanoparticles: Different preparation techniques, characterization, hurdles, and strategies for the production of solid lipid nanoparticles and nanostructured lipid carriers for oral drug delivery," *Sustainable Chemistry and Pharmacy*, vol. 6, pp. 37–56, 2017.

[164] J. M. V. Makabenta, A. Nabawy, C.-H. Li, S. Schmidt-Malan, R. Patel, and V. M. Rotello, "Nanomaterial-based therapeutics for antibiotic-resistant bacterial infections," *Nature Reviews Microbiology*, vol. 19, no. 1, pp. 23–36, 2021.

[165] M. A. B. Henostroza *et al.*, "Antibiotic-loaded lipid-based nanocarrier: A promising strategy to overcome bacterial infection," *International Journal of Pharmaceutics*, vol. 621, p. 121782, 2022.

[166] S. Dlamini *et al.*, "Enhancing activity and overcoming ciprofloxacin resistance via multifunctional nanostructured lipid carriers," *Journal of Drug Delivery Science and Technology*, vol. 108, p. 106933, 2025.

[167] Q. Pang, Z. Jiang, K. Wu, R. Hou, and Y. Zhu, "Nanomaterials-based wound dressing for advanced management of infected wound," *Antibiotics*, vol. 12, no. 2, p. 351, 2023.

[168] S. Hassanzadeh, S. Ganjloo, M. R. Pourmand, R. Mashhadi, and K. Ghazvini, "Epidemiology of efflux pumps genes mediating resistance among Staphylococcus aureus: A systematic review," *Microbial Pathogenesis*, vol. 139, p. 103850, 2020.